FACULTÉ DE PHARMACIE

UNIVERSITÉ LIBRE DE BRUXELLES

Development and Characterization of formulations for the nose-to-brain delivery of ghrelin and the management of cachexia

Thesis presented by Laurent SALADE

with a view to obtaining the PhD Degree in Biomedical and Pharmaceutical Sciences ("Docteur en Sciences Biomédicales et Pharmaceutiques")
Academic year 2018-2019

Supervisor: Professor Jonathan GOOLE

Co-supervisor: Professor Nathalie WAUTHOZ

Laboratoire de Pharmacie Galénique et Biopharmacie

Thesis jury:

Prof. Véronique MATHIEU (Université libre de Bruxelles, Secrétaire)
Prof. Karim AMIGHI (Université libre de Bruxelles, Président)
Prof. Sergio HASSID (Université libre de Bruxelles)
Prof. Anne DES RIEU (Université catholique de Louvain)
Jérôme LECHIEN (Université de Mons)

Je souhaiterais tout d'abord remercier le Professeur Karim Amighi, Directeur du Laboratoire de Pharmacie Galénique et Biopharmacie, pour m'avoir offert l'opportunité de réaliser mon doctorat dans ce Service. Service dans lequel règne une excellente ambiance de travail alliant à la fois la recherche universitaire et les diverses collaborations avec l'industrie pharmaceutique. Merci pour vos relectures pointilleuses, pour le partage de vos connaissances et vos suggestions lors des nombreuses réunions ainsi que pour votre disponibilité malgré un emploi du temps bien chargé.

Je tiens sincèrement à remercier mon Promoteur, le Professeur Jonathan Goole. Merci d'avoir été présent tout au long de ma thèse, de m'avoir aiguillé au fur et à mesure, d'avoir relu un nombre incalculable de fois mes travaux écrits et, enfin, merci à lui de m'avoir fait profiter de ses connaissances en formulation pharmaceutique. Durant ces 6 années, nous avons énormément interagit que ce soit dans le cadre de ma thèse, des congrès, des enseignements, ou autres. Je finis donc mon doctorat avec énormément de bons souvenirs en tête. Je ne pense pas me tromper en disant qu'une réelle amitié est née durant ces quelques années passées ensemble. Le tout se soldant par cette proposition que vous m'avez faite d'être le parrain de votre fille, ce qui me touche énormément.

J'adresse également mes remerciements à ma co-promotrice, le Professeur Nathalie Wauthoz. Merci pour sa patiente face à mes nombreuses questions (surtout en début de thèse), merci pour sa motivation et son optimisme lorsque le projet rencontrait certaines difficultés, merci aussi d'avoir partagé ses connaissances scientifiques avec moi. Son investissement, à la fois dans mon projet, mais également dans tous les projets qu'elle encadre m'a toujours énormément impressionné. En plus de cet aspect professionnel, nous partagions de nombreux points communs ce qui a toujours permis de travailler dans une ambiance agréable et conviviale.

Ce travail n'aurait pu être mené à bien sans votre aide et je me rends compte que j'ai bénéficié d'un encadrement absolument optimal du début jusqu'à la fin de ma thèse.

Mes remerciements vont aussi aux membres de mon comité d'accompagnement, les Professeurs Véronique Mathieu et Carine De Vriese. Merci à eux d'avoir été présents et d'avoir interagit sur les différents points abordés lors des réunions de suivi et merci donc d'avoir aidé le projet à évoluer au fil du temps.

Je remercie Marjorie Vermeersch, membre du CMMI, pour son expertise en microscopie électronique et pour les nombreuses images fournies.

Je remercie sincèrement Matthias Van Woensel de la KUL et Thomas Mathivet de l'INSERM pour leur aide et leurs connaissances en termes d'administration *nose-to-brain* et de microscopie par fluorescence, respectivement.

Merci à Magali Deleu, membre du LBMI, pour m'avoir appris l'utilisation de la titration calorimétrique isotherme ainsi que l'interprétation des résultats collectés.

Je remercie sincèrement les employés de la compagnie pharmaceutique « Aptar Pharma » : Bénédicte Grosjean, Ludovic Pointeau et Olivier Michelet. Merci d'avoir collaboré avec nous, de nous avoir fourni les dispositifs pour administration nasale et de nous avoir permis de réaliser de multiples expériences au sein de vos laboratoires.

Merci à Lionel Larbanoix, membre du CMMI, pour son aide et ses connaissances pointues en imagerie par fluorescence.

Merci à Maxime Paide (alias « Paidy ») et Nancy Van Aelst (alias « NVA ») pour nous avoir aidé à encadrer les travaux pratiques de Pharmacie Galénique pendant ces 6 années. Au total, pas moins d'un demi-millier d'étudiants seront passés par notre salle de laboratoire sans encombres et ce, toujours dans la bonne humeur.

Merci au Dr. Rémi Rosière (alias « Rosi ») pour la bonne ambiance dans le bureau, pour nos conversations plus ou moins scientifiques (en fonction des jours) et pour les super « after work » passés ensemble.

Merci à Philippe Gevenois (alias « PG ») pour tous ces repas de midi à la « Pizza » et pour ces congrès qui, pour certains d'entre eux, furent absolument mémorables.

Je remercie de manière plus générale l'entièreté du Service de Pharmacie Galénique et Biopharmacie pour la bonne ambiance qui règne dans ce service avec une équipe de travailleurs motivés et dynamiques mais qui sait aussi relâcher la « pression » quand il le faut pour profiter de bons moments tous ensemble.

Je remercie aussi du fond du cœur la famille Salade, famille de pharmaciens (à 75%), qui a toujours été là pour moi et qui s'est toujours intéressée à l'évolution de mon projet. Merci pour vos conseils, votre soutien, et pour tous ces moments agréables passés ensemble qui m'ont permis de me changer les idées quand il le fallait.

TABLE OF CONTENT

I. Abbreviations 8
II. Résumé 11
III. Summary 17
IV. INTRODUCTION 22
1. A challenging delivery 23
2. Anatomy of the nasal cavity 23
3. The nose-to-brain transport 27
3.1 Direct transfer: trigeminal nerve and olfactory pathways 28
3.2 Indirect transfer 31
3.3 Selection of the pathway of delivery 31
4. Nasal formulations 32
4.1 Liquid formulations 32
4.2 Powder formulations 34
4.3 Other formulations 35
5. Formulation strategies to enhance the nose-to-brain delivery 36
5.1 Enzymatic inhibitors 37
5.2 Mucoadhesive and mucopenetrating agents 38
5.3 Permeability enhancement 39
5.4 Lipid based systems 40
5.5 Cell penetrating peptide 41
5.6 Targeted interactions 41
5.7 Deposition in the olfactory region 42
6. Nasal devices 43
6.1 Liquid devices 43
6.2 Powder devices 47
6.3 Nose-to-brain devices 49
7. Potential applications of nose-to-brain delivery 51

7.1 Neurodegenerative diseases 51
7.2 Brain Cancers 53
7.3 Other pathologies 53
7.4 Nose-to-brain delivery of peptides and proteins 54
8. Cachexia and ghrelin 57
8.1 The cachectic syndrome 57
8.2 Classification of the cachexia severity 57
8.3 Epidemiology 59
8.4 Hormonal ethiology 59
8.5 Cachexia management with ghrelin 60
8.6 Nose-to-brain delivery of ghrelin for cachexia 63
8.7 Cachexia treatment with other drugs 64
9. Scientific strategy 66
9.1 Liposomes 66
9.2 Liposomes coated with chitosan 68
9.3 Final form of the formulation 69
V. Aims of the Work 70
VI. Experimental Part 73
1. Results Part I: Pre-formulation and development of a ghrelin-loaded liquid formulation for nose-to-brain delivery 74
1.1 Introduction 75
1.2 Materials and methods 77
1.3 Results and discussion 86
1.4 Conclusion 112
2. Results part II: Development of a dry-powder formulation for the nose-to-brain delivery of GHRL 114
2.1 Introduction 115
2.2 Materials and methods 116

2.3 Results and Discussion 126
2.4 conclusion 143
3. Results part III: *In vivo* characterization of chitosan-coated anionic liposome 145
3.1 Introduction 146
3.2 Materials and methods 147
3.3 Results and discussion 152
3.4 Conclusion 156
VII. Conclusion and Perspective 158
VIII. Bibliography 163
IX. Appendices 186

I. ABBREVIATIONS

AD	Alzheimer's disease
AgRP	Agouti related peptide
AL	Anionic liposomes
Empty-AL	Anionic liposomes without GHRL
BBB	Blood brain barrier
CAF	Caffein
CAL	Calcitonin
CASCO	Cachexia score
CES-1	Carboxylesterase-1
CFC	Chlorofluorocarbons
CL	Cationic liposomes
CMC	Critical micelle concentration
CNS	Central Nervous System
CPP	Cell penetrating peptide
CYP450	Cytochrome P450
DHDP	Dihexadecyl phosphate
DOTAP	1,2-dioleoyl-3-trimethylammonium-propane
DSPE-PEG 2000	1,2-distearoyl-sn-glycero-3-phosphoethanolamine-N-[carboxy(polyethylene glycol)-2000
EE	Encapsulation efficiency
EMA	European Medicines Agency
F405-GHRL	GHRL labelled with Alexa® Fluor 405
F800-GHRL	GHRL labelled with Dylight® 800
FDA	Food and Drug Administration
GHRL	Ghrelin
GHSR	Growth hormone secretagogue receptor
HBSS	Hank's balanced salt solution
HFA	Hydrofluoroalkanes
HTCC	N-[(2-hydroxy-3-trimethylammonium)propyl] chitosan chloride
HTCC-AL	HTCC-coated anionic liposomes
ITC	Isothermal titration calorimetry
LMWP	Large molecular weight protein
LUV	Large unilamellar vesicles
MEM NEAA's	Minimal essential medium nonessential amino acids
MLV	Multilamellar vesicles
NBD-cholesterol	25-[N-[(7-nitro-2-1,3-benzoxadiazol-4-yl) methyl]amino]-27-norcholesterol

NHS-fluorescein	N-hydroxysuccinimide fluorescein ester
NL	Neutral liposomes
PBS	Phosphate buffered saline
PD	Parkinson's disease
PDI	Polydispersity index
PEG	Polyethylene glycol
PLA	Polylactic acid
pMDI	Pressurized metered dose inhalers
SLN	Solid lipid nanoparticle

SUV	Small unilamellar vesicles
TEER	Transepithelial electrical resistance
TEM	Transmission electron microscopy
TFA	Trifluoroacetic acid
TGA	Thermogravimetric analysis
TJ	Tight junction
TRYP	Trypsin
UDS	Unit dose system
WGA	Wheat germ agglutinin

II. RÉSUMÉ

L'utilisation de la voie nasale dans le cadre d'un traitement thérapeutique est connue depuis de nombreuses années. Elle apparaît comme une voie d'administration simple à mettre œuvre pour le patient de par son aspect non invasif mais également par l'administration aisée pour le patient. De plus, elle convient aussi bien pour une administration chronique que pour une situation d'urgence lorsque le patient est inconscient. On peut notamment citer l'administration de benzodiazépines, tel que le midazolam, afin de maîtriser un épisode convulsif chez un patient.

Traditionnellement, l'administration intranasale était essentiellement utilisée afin de cibler une action locale (par exemple, le traitement d'un rhume avec un agent décongestionnant). Par la suite, son application pour une délivrance systémique (par exemple, le traitement de la migraine par administration de triptans) a été considérée de plus en plus fréquemment. Toutefois, la délivrance d'un agent thérapeutique dans les cavités nasales dans le but d'obtenir une activité systémique reste toujours limitée comparativement à d'autres voies telles que l'administration orale ou intraveineuse. En effet, même si la voie intraveineuse présente plusieurs limitations majeures, tel que son aspect invasif ou la douleur générée chez le patient, elle reste largement plus utilisée que la voie intranasale. Ceci s'explique, d'une part par les connaissances qui étaient jusqu'ici relativement limitées vis-à-vis de cette administration et, d'autre part, par l'utilisation d'anciens dispositifs médicaux qui ne permettaient pas un contrôle précis, en termes de dose délivrée et de taille de particules générées, lors de l'administration intranasale.

Par la suite, la voie intranasale s'est vue attribuée une troisième opportunité de délivrance, à savoir, le ciblage cérébral par la voie « *nose-to-brain* ». Cette fois, la cavité nasale a été considérée comme un point d'entrée pour accéder au système nerveux central. En effet, elle fournit un accès direct au cerveau tout en contournant la barrière hémato-encéphalique, obstacle majeur à la pénétration des agents thérapeutiques. Par ailleurs, le passage par la cavité nasale permettrait l'administration de molécules sensibles (par exemple, des biopharmaceutiques) en évitant une dégradation enzymatique trop importante.

Dans ce contexte, le traitement du syndrome cachectique a été sélectionné comme cible modèle justifiant une administration « nose-to-brain ». Il s'agit d'un syndrome caractérisé par une perte énergétique globale du patient qui résulte notamment d'une dénutrition, d'une perte de masse musculaire et d'un état inflammatoire généralisé chez celui-ci. Le syndrome cachectique est associé à des pathologies chroniques et

induit une aggravation du pronostique. Afin de traiter ce syndrome complexe et restaurer l'appétit chez ces patients, la ghréline (GHRL) a été choisie comme modèle de principe actif. La GHRL est une hormone peptidique qui présente, entre autres, un effet orexigène. Il s'agit donc d'une molécule biopharmaceutique qui a besoin d'atteindre ses récepteurs, localisés dans l'hypothalamus, afin d'exercer son effet thérapeutique.

Dans ce travail, l'objectif est de développer une formulation qui puisse protéger la GHRL lors de son administration tout en augmentation sa rémanence dans la cavité nasale afin d'être efficacement transférée vers le cerveau en favorisant sa diffusion au travers de l'épithélium nasal olfactif.

Dans un premier temps, la GHRL a été caractérisée, notamment en termes de stabilité par rapport à la température et au pH, mais également au niveau de sa charge électrostatique. Ces résultats nous ont aidés à sélectionner la meilleure stratégie de formulation mais également les conditions de stockage optimales. Une fois cette étape de préformulation finalisée, il a été décidé de travailler sur la mise au point d'une formulation liquide. La première formulation abordée consistait en des micelles composées de lipides possédant des groupements hydrophiles polyéthylène glycol « *DSPE-PEG (1,2-distearoyl-sn-glycero-3-phosphoethanolamine-N-[amino(polyethylene glycol)-2000] (ammonium salt)* ». Ce type de lipides pégylés avaient déjà montrés dans diverses études scientifiques des propriétés intéressantes dans le cadre d'une administration intranasale, notamment, en termes de mucopénétration. En adaptant légèrement le protocole trouvé dans la littérature, il a été possible d'obtenir des micelles caractérisées par un diamètre moyen adéquat (~15 nm). Les micelles produites ont également montré une bonne aptitude à encapsuler la GHRL avec un taux d'encapsulation de 98% m/m. Cependant, les micelles de DSPE-PEG n'ont pas permis d'augmenter la diffusion de la GHRL au travers une couche épithéliale. Cette étape étant primordiale afin d'obtenir des taux de GHRL satisfaisant au niveau cérébral, la formulation contenant les micelles de DSPE-PEG a été abandonnée.

Toujours dans l'esprit de vouloir associer des excipients lipidiques à un polymère plus hydrophile, une autre stratégie de formulation basée sur des liposomes enrobés de chitosans a été envisagée. Etant donné que la GHRL présente une charge positive à pH physiologique, des liposomes de charge négative ont été développés dans le but d'obtenir un taux d'encapsulation élevé. Tout d'abord, trois types de liposomes ont été

produits : anioniques, neutres et cationiques, l'objectif étant de montrer si l'apport d'une charge négative aux liposomes permettait d'augmenter le taux de GHRL encapsulée. En travaillant avec des liposomes anioniques, le taux d'encapsulation a pu être augmenté d'un peu plus de 46% par rapport au liposomes cationiques. Afin de voir si un lien existait entre la quantité de GHRL encapsulée dans les liposomes et la quantité de GHRL dégradée en présence d'enzyme, les trois types de liposomes ont été exposés à de la trypsine. Suite à l'exposition à l'enzyme, les liposomes anioniques ont montré une protection enzymatique 4 fois supérieure aux liposomes cationiques. Ces liposomes anioniques ont également démontré une protection de la GHRL en présence d'une carboxylestérase-1, une autre enzyme présentant un mécanisme de digestion différent de la trypsine. Par la suite, des tests par titration calorimétrique isotherme ont été réalisés afin de mieux comprendre les mécanismes d'interaction entre la GHRL et les liposomes anioniques. Cette technique a permis de constater que les interactions hydrophobes entre les deux composés étaient prédominantes. Jusqu'à ce stade du développement, les liposomes n'étaient pas associés aux chitosans. L'enrobage des liposomes anioniques par les chitosans a donc été réalisé et confirmé suite à une augmentation du diamètre (+48 nm) et de la charge (+6 mV) moyenne, mais aussi par modification morphologique des liposomes. Cet enrobage avec les chitosans avait pour but de conférer des propriétés de mucoadhésion à la formulation liposomale tout en augmentant la diffusion du peptide à travers l'épithélium olfactif. Ces effets ont été obtenus grâce à la charge positive des chitosans qui permet d'adhérer aux mucines mais aussi grâce à leur capacité d'ouvrir les jonctions serrées présentes au niveau de l'épithélium olfactif. Ces propriétés ont pu être confirmées en plaçant la formulation en présence de mucines solubles. L'enrobage de chitosan a permis d'augmenter la fixation des liposomes d'une vingtaine de pourcents par rapport à des non enrobés. De plus, la capacité des chitosans cationiques à assurer un rôle de promoteur d'absorption a été confirmé par des tests de perméabilités cellulaires. Une fois ces propriétés confirmées, la formulation a été introduites dans deux dispositifs destinées à l'administration de sprays nasaux liquides, à savoir : le dispositif VP3 d'Aptar Pharma et le dispositif SP270 de Nemera. La distribution de taille de la plume produite par chacun des aérosols a été évalué par diffraction laser. Les deux dispositifs ont été capables de générer un spray composé de gouttelettes supérieures à 10 µm, ce qui était le diamètre limite favorisant l'impaction au niveau de la zone olfactive plutôt que la diffusion vers des sections postérieures de l'arbre respiratoire.

Dans la seconde partie du travail, une formulation sous forme de poudre sèche a été produite par atomisation à partir de la forme liquide. L'objectif étant d'augmenter la stabilité de la GHRL lors du stockage et d'augmenter à la fois la rémanence et la pénétration du peptide au travers de l'épithélium nasal. Après optimisation, il a été possible de produire une poudre composée de particules supérieures à 10 µm, tout en conservant un rendement acceptable. Une faible humidité résiduelle a été confirmée par thermogravimétrie et la poudre a également montré une haute homogénéité au niveau de sa teneur en GHRL.

Ensuite, une étude comparative a été réalisée entre les formulations sèches et liquide pour comparer la stabilité de la GHRL lors du stockage à différentes température (4°C et 25°C), mais aussi leur capacité à fixer des mucines. Dans les deux cas, la poudre sèche a montré de meilleurs résultats. La poudre a ensuite été dispersée en phase aqueuse pour confirmer que les liposomes enrobés pouvaient être reconstitué en conservant leur distribution de taille adéquate (ex : absence d'agglomérats). Dans les limites de variabilités acceptables, les propriétés physicochimiques initiales des liposomes ont pu être conservées après reconstitution. De façon similaire à la formulation liquide, la poudre a ensuite été chargée dans un dispositif spécifiquement développé pour cibler la zone olfactive lors d'une administration intranasale. Le dispositif « UDS – Unit Dose System (Aptar Pharma) » a montré d'excellentes propriétés en termes de distribution de taille des particules dans l'aérosol mais aussi en termes de ciblage de la zone olfactive. Ce dernier aspect, fut étudié au moyen de « *Nasal cast* », c'est-à-dire une représentation en 3 dimensions des fosses nasales. Une fois l'aérosol généré dans cette cavité, il est alors possible de quantifier la quantité de GHRL déposée dans la zone olfactive. Dans ce cas-ci, la quantité déposée état de 52%, ce qui montre un ciblage efficace en tenant compte de la faible surface représentée par cet épithélium et de sa difficulté d'accès.

Pour finir, la formulation chargée avec de la GHRL fluorescente a été administrée par voie intranasale chez la souris. Cette dernière expérience a permis de montrer que la GHRL pouvait atteindre le cerveau après administration intranasale de la formulation et que cette dernière était indispensable pour permettre à ce transfert vers le cerveau de se faire. L'administration de ce type de biopharmaceutique par voie *nose-to-brain* avec cette formulation semble donc être une alternative intéressante à exploiter. Cependant, des études complémentaires permettant de quantifier plus précisément

cetransfert, de mieux définir sa cinétique et aussi d'évaluer l'efficacité du traitement devraient être réalisées.

III. SUMMARY

For many years, the nasal route of administration as part of a therapeutic treatment has been used. This route of administration is easy to implement, especially due to its non-invasiveness the ease of administration that it affords for the patient. In addition, it is suitable for chronic treatment as well as for an emergency situation when the patient is unconscious. For instance, the administration of benzodiazepines, such as midazolam, may be done to stop convulsions in a patient.

Traditionally, intranasal administration was mainly borrowed to target a local effect (e.g. treatment of a cold with a decongestant agent). Subsequently, its application for systemic delivery (e.g. treatment of migraine with triptans) was more and more frequently considered. However, the administration of a drug in the nasal cavities for systemic delivery still remains limited. Indeed, even if the intravenous route has several major limitations such as its invasiveness or the pain generated during administration, it remains more widely used than the intranasal route. This can be explained, on the one hand, by the knowledge that was relatively limited regarding the nasal delivery but also because of the unavailability of nasal devices allowing precise control of the nasal administration (i.e. accurate dose delivery, strong deposition in the nasal cavity, etc).

Subsequently, the intranasal route has led to a third therapeutic targeting, namely, the “nose-to-brain pathway”. In that case, the nasal cavity was considered as an opportunity to access the central nervous system (CNS). Indeed, the nose-to-brain delivery allows reaching the brain while bypassing the blood-brain barrier which is known to be a major obstacle to the diffusion of drugs in the CNS. Moreover, the passage through the nasal cavity would allow the administration of sensitive molecules (e.g. biopharmaceuticals) while avoiding excessive enzymatic degradation.

Therefore, the nose-to-brain pathway appears to be an attractive route for the delivery of unstable molecules, requiring an access to the brain to reach their site of action. In this context, the therapeutic target that has been selected was "cachexia". It is a complex metabolic syndrome associated with underlying illness and characterized by loss of muscle with or without loss of fat mass. It usually results in particular from undernutrition and a generalized inflammatory state in the patient. In order to treat this syndrome and to restore the appetite in these patients, the goal was to use ghrelin (GHRL) as a model drug. GHRL is a peptide hormone that exhibits, among other effects, an orexigenic action. This biopharmaceutical needs to reach its receptors, located in the hypothalamus, to exert its therapeutic effect.

In this study, the goal was to develop a formulation that was able to protect GHRL during its nasal administration, while increasing its residence time to promote its diffusion through the nasal olfactory epithelium.

In the first part of the project, GHRL was mainly characterized in terms of stability (e.g. temperature and pH), but also in terms of surface charge. These results allowed selecting the most suitable strategy of formulation as well as the optimal storage conditions. After these preformulation evaluations, it was decided to work on the development of a liquid formulation. The first formulation was based on micelles composed of lipids with polyethylene glycol "DSPE-PEG (1,2-distearoyl-sn-glycero-3-phosphoethanolamine-N- [amino (polyethylene glycol) -2000] (ammonium salt)" as hydrophilic group. This type of pegylated lipids have already shown, in many scientific studies, interesting properties in the context of intranasal administration, especially in terms of mucopenetration. With a slight adaptation of the protocol found in the literature, it was possible to obtain micelles of an adequate size (~15 nm). The micelles produced also showed good ability to encapsulate GHRL with an encapsulation rate of 98%, but micelles of DSPE-PEG failed to increase the GHRL diffusion through epithelial layer. This step is essential in order to obtain high GHRL levels in the brain. The formulation containing DSPE-PEG micelles has thus been abandoned.

Still in the goal of combining lipid excipients with hydrophilic polymer, another formulation strategy based on liposomes coated with chitosan has been considered. Since GHRL has a positive charge at physiological pH, anionic liposomes have been developed to get a high loading. Three types of liposomes have been produced: anionic, neutral and cationic. The objective was to evaluate the influence of the liposomes charge on GHRL encapsulation. By working with anionic liposomes, the loading could be 46% higher than that obtained from the cationic liposomes. In order to evaluate a potential relation between the amount of GHRL that was encapsulated in the liposomes and the amount of GHRL that could potentially be degraded in the presence of enzyme, the three types of liposomes were exposed to trypsin. Following enzyme exposure, anionic liposomes showed enzymatic protection 4 times higher than cationic liposomes. These anionic liposomes have also shown high GHRL protection in the presence of another enzyme with another mechanism of digestion, namely, carboxylesterase-1. Subsequently, isothermal titration calorimetry tests were performed to better understand the interaction mechanisms between GHRL and

anionic liposomes. This technique showed that hydrophobic interactions between both compounds were predominant.

The coating of anionic liposomes by chitosans was performed and confirmed by an increase of the mean diameter (+48 nm) and charge (+6 mV) as well as by the modification of the morphology of the liposomes. This coating of liposomes with chitosans was supposed to confer additional properties to the formulation such as mucoadhesion and permeation enhancement. These both effects can be obtained thanks to the positive charge of chitosans which allows adhering to the mucins of the mucus, on the one hand, and thanks to the opening of the epithelial tight junctions that enhances drug permeation, on the other hand. The chitosan coating allowed increasing the fixation of the liposomes to mucins by about twenty percent compared to uncoated liposomes. In addition, the "absorption promoter" effect of chitosans was confirmed on cells culture. Then, the formulation was introduced into two distinct nasal devices intended for the administration of liquid nasal sprays, namely, the VP3 device from Aptar Pharma and the SP270 device from Nemera. The aerosols produced by each device allowed generating droplets characterized by a mean diameter higher than 10µm, leading to potential satisfactory impaction onto the olfactory region instead of diffusion throughout posterior region of the nasal cavities.

In the second part of the work, a dry formulation was produced by spray-drying from the liquid dispersion of coated liposomes. The objective was to increase the stability of GHRL during storage as well as to enhance its remanence and diffusion through the olfactory epithelium. The optimized parameters allowed producing a powder characterized by a mean diameter higher than 10 µm with an acceptable yield. The powder produced exhibited a low residual moisture and showed good homogeneity in terms of GHRL content.

Then, a comparative study was carried out between the powder and the liquid formulation to compare the GHRL stability over time during storage at different temperatures (4°C and 25°C) but also their ability to fix mucins. In both cases, the dry powder showed better results The powder was also re-dispersed in aqueous phase to evaluate the ability of the liposomes to be reconstituted without modifying their physicochemical properties (e.g. size distribution, charges, stability). It was demonstrated that the majority of the initial properties could be preserved after reconstitution (i.e. rate of encapsulation). Similarly to the liquid formulation, the powder was loaded into a specific device developed for the nasal administration of powders

that allows targeting the olfactory region to optimize the nose-to-brain transfer. The device, "UDS - Unit Dose System " from Aptar Pharma, has shown excellent properties in terms of particle size distribution in the aerosol but also in terms of targeting the olfactory zone. The latest was studied by means of "nasal cast" that is a 3-printed model of artificial nasal cavities. After impaction in the different cavities of the cast, it was possible to quantify the amount of GHRL that was deposited in the olfactory zone. Using our optimized formulation in combination with the device developed by Aptar, it was shown that 52% of the powder was impacted onto the area corresponding to the olfactory region. Such data demonstrated the relative difficulty to target this section of the nasal cavities.

Finally, the formulation loaded with fluorescent GHRL was intranasally administered in mice. It was demonstrated that GHRL could reach the brain after intranasal administration of the formulation and that the formulation was essential to allow this transfer to the brain.

The administration of such biopharmaceutical by nose-to-brain with this formulation seems to be an interesting alternative to exploit. However, additional studies to quantify this transfer more precisely, to better define its kinetics and also to evaluate the efficacy of the treatment should be carried out.

IV.INTRODUCTION

1. A challenging delivery

In the body, the brain is surrounded by a protective layer, called the "blood-brain barrier" (BBB) which provides an effective barrier to the entry of external compounds. The BBB can therefore be considered as a real anatomical advantage. However, if we consider the brain in the optic of a treatment development, this barrier represents a major obstacle to the diffusion of effective treatments to the brain.

In this context, the nose-to-brain administration appears as a very interesting alternative because it would offer a direct access to the brain from the nasal cavity while bypassing the BBB. Moreover, the nasal administration does not involve any invasive step during administration which makes it more convenient than other conventional administrations such as the parenteral administration. It is also an attractive pathway for the brain delivery of large molecules and sensitive drugs such as biopharmaceuticals. Indeed, the nose-to-brain avoids hepatic first-pass effect and other gastro-intestinal degradations (e.g. gastric acid conditions).

This passage, even if it appears very attractive on paper, represents a real challenge. Indeed, the nose tends to eliminate the external contaminants from the nasal cavity and the residence time of the drug in the nose must therefore be increased. In addition, if drugs with high molecular weight are administered, their diffusion through the nasal barrier must be enhanced. These last two factors can be overcome thanks to an appropriate formulation development.

Finally, the amount of formulation deposited in the olfactory region of the nose should be maximized as it is the main place where the transfer to the brain takes place. This can be achieved by a suitable combination nasal device / aerosol generation.

These points thus represent the main challenges addressed in this thesis.

2. Anatomy of the nasal cavity

The human nasal cavity is characterized by a total surface of 180 cm^2, a volume of 15 mL associated to a length of 12 - 14 cm and a slightly acid environment (pH range = 5.5 - 6.5)[1,2]. Such large area is due to the presence of both microvilli and tortuous structures called « turbinates ». The nasal cavity is divided in two sections by a partition called « the *septum* ». Each section includes three distinct regions called : the vestibule, the respiratory mucosa and the olfactory mucosa (**Fig. 1**)[3].

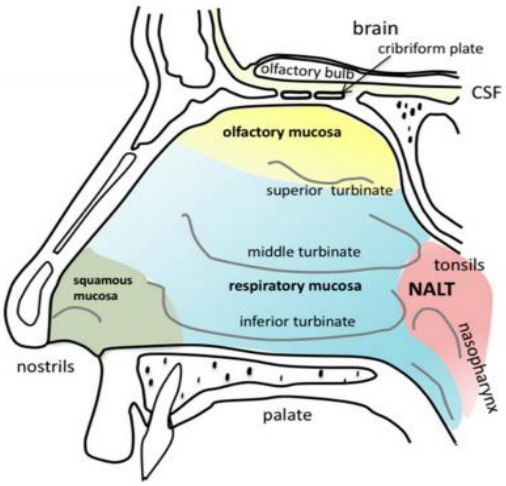

Figure 1. Anatomy of the human nasal cavity (NALT: Nasopharynx-associated lymphatic tissue) (reproduced with authorization)[4]

The human nose is responsible of three physiological functions, namely, breathing, olfaction and protection.

The nose ensures the warming of the external air which is made possible by the supply of arterial blood from the maxillary artery[5]. It also provides its hydration during breathing due to the presence of the respiratory mucosa that is spread over the majority of the nasal surface (80-90%) for a thickness of 0.3-5 mm[6,7]. Every day, the nose filtrates about 12,000 litres of air from the external environment[8].

The respiratory mucosa is constituted by three principal cell families. The *goblet cells*, which represents 5 – 15% of the total cell population, produce the nasal mucus. The *columnar cells* can be ciliated or not on their apical side. When ciliated, the cilia are 5–10 µm long and have a thickness of 250 nm[7]. They are beating towards the nasopharynx that is located at the back of the nasal cavity. All columnar cells have microvilli which contribute to the large surface of contact of the nasal cavity with the external environment. Finally, *basal cells* constitute the main continuous structure of the respiratory mucosa[9]. These cells are undifferentiated cells than can thus be considered as stem cells for generating other cell types.

The olfactory function is provided by the olfactory mucosa which is located in the upper part of the nose (**Fig. 1**), below the cribriform plate and behind the nostrils (7 cm)[10]. This olfactory region represents only a limited part of the total human nasal surface (10 cm^2)[11]. The area occupied by this mucosa is strongly species dependent. For instance, rats have a much more developed sense of smell thanks to the large surface

occupied by their olfactory mucosa (50% of the total surface versus < 10% in humans)[12]. Because of its isolated location in the nasal cavity but also due to the presence of a thin opening (1.5 mm) which restricts its access in the nasal cavity, the olfactory mucosa is a very well insulated area of the nose[10]. Its vascularization is ensured by branches of internal maxillary artery (mainly sphenopalatine) and also branches oh ophthalmic artery (anterior and posterior ethmoidal arteries). In the olfactory mucosa are described 4 types of cells, namely: the olfactory cells, the supporting cells or sustentacular cells, the basal cells and the glandular cells.

The *olfactory cells* characterized by long non-motile cilia which are not involved in the clearance of the mucus[10]. These cells are able to trap the olfactory molecules to transfer the signal to the olfactory bulb of the brain via their axons. The *supporting cells,* or *sustentacular cells,* are the most represented cells in the olfactory epithelium. They are involved in maintaining the ionic balance for allowing optimal olfaction and they also constitute a support for the olfactory epithelium[6,12]. The *basal cells* here have the same role as in the respiratory mucosa: they represent a stock of stem cells that can differentiate into other cell types (e.g. sustentacular cells or olfactory neurons cells)[12]. Finally, the *glandular cells* (integrated in Bowman's glands) are also represented and they are involved in the mucus production [13,14].

The olfactory mucosa consists of two main layers, namely: the olfactory epithelium and the *lamina propria* (**Fig. 2**). The *lamina propria*, the deepest layer of the olfactory mucosa, contains olfactory nerves fascicles and Bowman's glands.

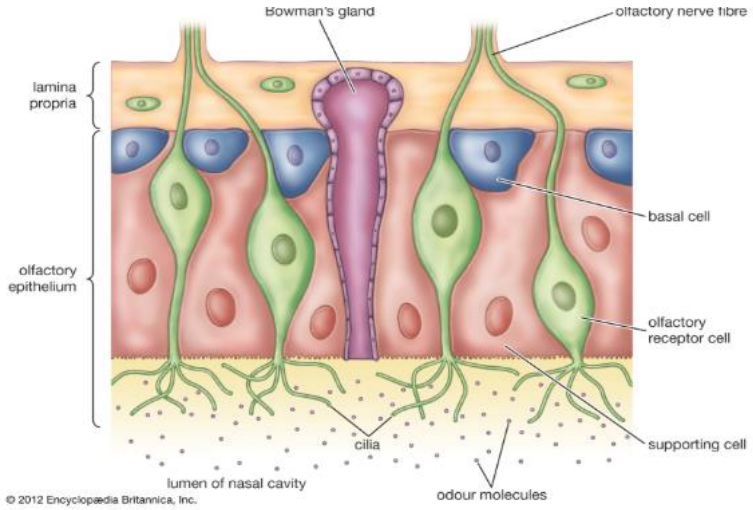

Figure 2. Structure of the human olfactory mucosa[15]

The presence of yellow pigments located in these Bowman's glands makes the olfactory mucosa easy to distinguish from the rest of the nose[16]. Bowman's glands

secrete a specific type of mucin that makes olfactory molecules more available to olfactory cells. Below the *lamina propria* is located the cribriform plate. It is a perforated bone through which the fibers of the olfactory nerves pass. This olfactory region allows a direct access to the CNS as it is the only place of the body where the brain has a direct physical connection to the external environment[17].

The nose is also one of the first protection of the organism against microorganisms and pollutants from the external environment. The nose is responsible of the filtration of the entering air involves a defense mechanism called the « muco-ciliary clearance » for cleaning the nose from undesired elements, once trapped in the mucus. The muco-ciliary clearance is a treadmill system that involves the synergic action of both cilia and mucus. Inhaled substances are first impacted on the nasal mucus and the latter is then swept by the cilia towards the rhinopharynx in order to be cleaned[18]. For instance, the nose is able stop 95% of particles that have a mean diameter from 15 µm[8]. The nasal mucus is composed of 95% of water, 2% of mucins (the major glycoprotein of the mucus), 1% of salts and 1% of various proteins (e.g. albumin, lysozymes) and 1% of lipids[19]. The mucus is displaced by the nasal cilia at a rate of 5 mm/min and it's turnover is about 15–20 min[20]. Nasal cilia from the respiratory mucosa have a length of about 2–4 µm[6] and cover about 15 to 20% of the total surface of the nasal cavity. Their synergic movement, oriented towards the nasopharynx, is performed with a beating frequency of 1000 beats per minute[17,21].

In addition to this physical defense mechanism, the nose has also its own metabolic system that is involved in the degradation of xenobiotics. For instance, CYP 450, a superfamily of mono-oxygenase, is well represented in the nasal mucosa[22]. There is also the presence of immunoglobulins (e.g. Ig-A and Ig-G) that are involved in the labelling and neutralization of antigens[23,24]. Lysozymes are also found in nasal secretions. They are lytic enzymes active in acidic conditions and responsible of the degradation of peptidoglycans, a major component of gram positive bacteria[25].

This defensive function appears to be essential to the body while any modification of its proper functioning may lead to various pathologies (e.g. chronic rhino-sinusitis)[26]. The administration of intranasal formulations containing excipients, such as mucoadhesive agents, may also have deleterious effects on the nasal clearance mechanism, potentially inducing a higher vulnerability of the organism against external pathogens.

In addition to the mucociliary clearance and its metabolic activity, intercellular connections between nasal epithelial cells which are called “tight junctions” are characterized by a specific permeability that will depend on the properties of the molecule. Tight junctions consist of a complex of various proteins which interact with each other but also with the membrane and the cytoskeleton[10]. It is known that molecules with diameter larger than 3.6 Å will diffuse in a very limited way while molecules larger than 15 Å will not be able to pass through[27]. In this context, it was suggested that the permeation of molecules with a molecular weight equal or larger than 1000 Da is very limited which justifies the use of absorption enhancers[28].

3. The nose-to-brain transport

A few decades ago, the nasal administration was limited to the local delivery of drugs. The main therapeutics administered were corticosteroids and antihistamines for the management of rhinosinusitis or nasal decongestants for cold[29]. It is the best choice for the treatment of nasal diseases as it provides a rapid onset of action while avoiding systemic side effects (thanks to the local delivery allowing better targeting). Many examples of nasal marketed products with local effects are already commercialized (e.g. Nasonex® (Schering-Plough, New Jersey, USA) containing mometasone or Beconase® (GlaxoSmithKline, Middlesex, UK) containing beclometasone). Next to local effects, the systemic delivery of molecules via the nasal cavity was exploited. Such therapeutics include analgesics (e.g. morphine), cardiovascular drugs (e.g. propanolol), hormones (e.g. progesterone, insulin, calcitonin), anti-inflammatory drugs (e.g. ketorolac), antimigraine drugs (triptans) and antiviral drugs (e.g. acyclovir)[29].

Moreover, the nasal cavity has also been considered as a potential immunization site for vaccines administration as it is the first site of the body to be exposed to inhaled antigens[30,31]. For instance, both preclinical and clinical studies have already emphasized satisfactory immune responses following the nasal administration of inactivated influenza vaccine[32,33]. The influenza vaccines Flumist® (brand name “Fluenz Tetra” in Europe) from AstraZeneca (Cambridge, UK) and Nasovac® from Serum Institute of India (Pune, India) have been approved by regulatory agencies in USA and India, in 2003 and 2010, respectively[34].

More recently, the nasal cavity has been considered as a gateway to access the brain. This new route of administration, called "nose-to-brain" delivery, offers many

advantages over other ways of delivery such as non-invasiveness and reduced first-pass effect. *In vivo* studies have already been focused on the nose-to-brain transfer of various drugs such as peptide hormones[35], opioïds[36], antiviral agents[37], antidepressants[38] and many others in order to better understand the route borrowed by such molecules.

Indeed, this route allows the transfer of a drug directly from the nose to the brain without having to cross over the blood-brain barrier (BBB) which is known to avoid the access of xenobiotics to the brain due to the presence of efflux pumps such as P-glycoproteins[39]. The diffusion of administered drugs from the nose to the brain can be done through the olfactory region (intra- or peri-neuronal) or through both olfactory and respiratory regions (thanks to the presence of trigeminal nerves[17]).

3.1 Direct transfer: trigeminal nerve and olfactory pathways

The trigeminal nerve innervates both olfactory mucosa and respiratory mucosa[17]. It makes the connection between the nasal mucosa, the pons and olfactory bulbs of the brain[17]. More precisely, trigeminal nerve accesses the brain through two distinct points of entry: 1) via the foramen near the cerebral pons and 2) via the cribriform plate of the ethmoid bone near the olfactory region (**Fig. 3**). Trigeminal nerve is one of the largest cranial nerve which is present in both sides of the head. Each trigeminal nerve is subdivided into three distinct branches, namely: the ophthalmic branch (V1), the maxillary branch (V2) and the mandibular branch (V3). The maxillary and ophthalmic branches are the most concerned by the nose-to-brain transfer as they have projections in the nasal cavity[5]. The transport of therapeutic molecules may be done intra- or peri-neuronally.

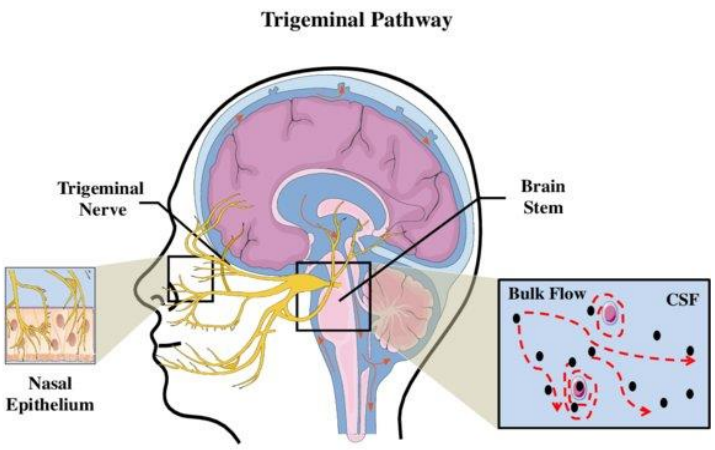

Figure 3. Illustration of the trigeminal pathway allowing a direct nose-to-brain transfer[40]

The first study that clearly highlighted the trigeminal route was performed by Thorne *et al.* in rats. The experiment involved the nasal administration of Insulin-Like Growth Factor labelled with radio iodine 125. After nasal administration, radioactivity was recovered in the following regions: trigeminal branches, olfactory bulb, the pons and the transfer was taking place along both olfactory and trigeminal nerves[35].

The olfactory pathway takes place via the olfactory neurons located onto the surface of the olfactory mucosa. These neurons may provide a direct access to the brain and, more precisely, to the olfactory bulb and the cerebrospinal fluid (**Fig. 4**)[41]. The axons are linked to the olfactory bulb by passing through the cribriform plate[12]. Similarly to the trigeminal pathway, the transport can be intraneuronal (slow transfer that can take a few hours) or perineuronal (fast transfer that can take a few minutes)[5].

For intraneuronal transport, an internalization of the drug is taking place by pinocytosis or endocytosis. The drug is then transferred by axonal transport to the olfactory bulb to be subsequently transported to other regions of the brain. The diameter of olfactory axons being limited in the range of 0.1 - 0.7 µm, entities to be transferred should not exceed a mean diameter of 0.7 µm[42]. For the extraneuronal transport, the drug crosses the olfactory epithelium and is thus transferred to the brain passing by the perineuronal space. The transport across the olfactory epithelium involves transcellular (mainly through sustentacular cells)[17] or paracellular mechanisms[10].

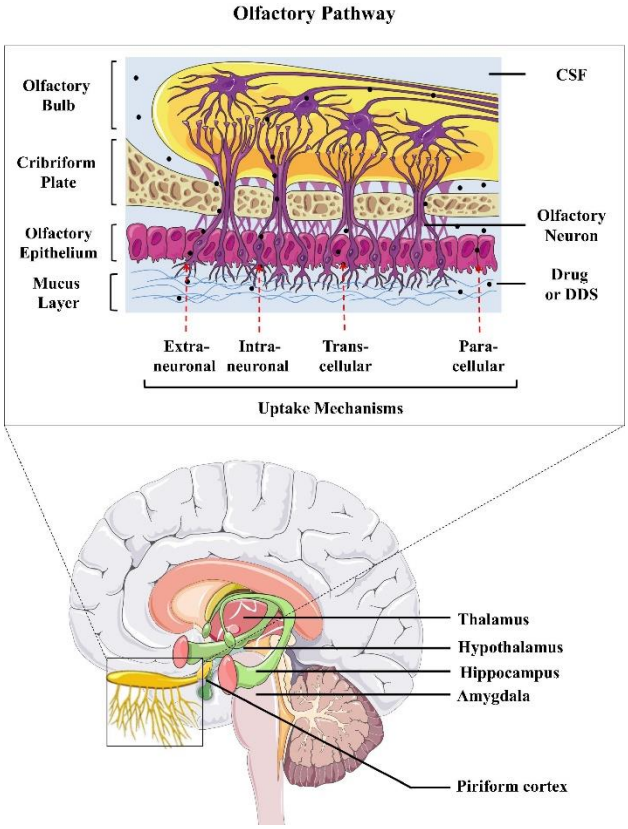

Figure 4. Illustration of the olfactory pathway with the different uptake mechanisms[40] The transcellular transport rather concerns lipophilic molecules (e.g. naloxone, buprenorphine, testosterone and propranolol)[43] with a diffusion rate that is correlated to its lipophilicity[17]. The drug is then captured by the cerebrospinal fluid or the CNS.

When the drug diffuses through the paracellular pathway, it has to diffuse through the tight junctions of the olfactory epithelium between sustentacular cells and olfactory neurons[17]. This access is mainly limited by the molecular weight of drugs (that will directly influence the diffusion rate) and concerns rather hydrophilic molecules (e.g. metoprolol)[43]. Such transport is thus positively influenced by excipients that have the ability to open the tight junctions (e.g. chitosan)[44]. It was already observed in rat models that high molecular weight and protein drugs can borrow such epithelial transfer (e.g. insulin, nerve growth factor, vasoactive intestinal peptide)[45–47]. The intraneuronal transfer has been reported as being much slower than the extraneuronal transport[48]. The potential transfer of a drug via both pathways (intra- and extraneuronal) is still possible but difficult to predict.

3.2 Indirect transfer

In addition to direct transfer, the access to the brain can also be performed due to the high vascularization of the respiratory mucosa. The main limitation of this transport is that it does not allow bypassing the BBB[49]. Indeed, the presence of both tight junctions and efflux pumps make it an efficient barrier for accessing the brain. This systemic route concerns rather lipophilic molecules of low molecular weight which pass transcellularly[10]. On the other side, hydrophilic drugs (e.g. peptides and proteins) that borrow paracellular passages are characterized by a lower bioavailability that is directly linked to their molecular weight[50].

Therefore, this pathway involves the passage through the BBB while associating the high metabolism (renal and hepatic). There is also a lack of selectivity with respect to the targeted organ with potential higher risks of side effects[5].

It is also important to notice alternatives to nose-to-brain delivery allow reaching the brain while circumventing the BBB (e.g. intracerebral administration). However, such techniques are strongly invasive and represent an important risk of toxic effect as they make the brain more accessible for potential microorganisms[49].

3.3 Selection of the pathway of delivery

A defined drug can diffuse through a specific nose-to-brain pathway depending on multiple parameters such as the drug properties (e.g. polarity) and the formulation intrinsic properties (e.g. particles size or absorption enhancers)[50,51]. Despite the difficulty to predict the road followed by a molecule, it is well described that intra-neuronal and intracellular routes via the olfactory epithelium are not the priority access roads[52]. Indeed, many drugs were recovered in the brain a few minutes after nasal administration which is rather suggesting the predominance of an extracellular transport via the olfactory mucosa[52]. Indeed, it is known that the extracellular transports provide a faster transport to the brain than intracellular and axonal pathways.

The physico-chemical properties of the drug being hardly difficult to adapt, a relevant way to select a pathway or, more precisely, to avoid an undesired one, is the targeted delivery in specific nasal anatomic sites through the formulation.

4. Nasal formulations

4.1 Liquid formulations

Liquid nasal formulations include aqueous solutions, suspensions (commonly encountered with corticosteroids) and micro- or nanoemulsions[53]. Usually, the volume of solution/suspension which may be delivered is in the range25-150 µL and is limited to a maximal volume of 200 µL[54]. The nasal delivery of larger amount of liquid was correlated to high formulation losses by flowing towards the back of the nasal cavity[55].

The major disadvantages of liquid formulations are a fast elimination from the nasal cavity due to a rapid clearance, the need of preservatives (which can potentially be toxic for the nasal mucosa) for a long-term storage and the necessity to deliver large volumes to reach the therapeutic concentrations. In addition, the liquid formulation can be problematic for the administration of biopharmaceuticals because of their important instability in liquid phase[56]. However, medicines that are extemporaneously reconstituted are now developed with under powder-state formulation in which a defined volume of solvent is added when the patient has to use the therapeutic. Such formulations allows avoiding the use of preservatives in the formulation and early drug degradations in the aqueous phase[57].

In contrast, liquid formulations are very suitable for the treatment of chronical pathologies where dryness of the nasal mucosa is a part of the symptoms[58]. To formulate nasal liquid dosage forms, some conventional excipients classes are frequently used:

- pH adjuster / buffer: the pH selected for the formulation can potentially influence both drug dissolution/absorption, drug stability and nasal mucosa integrity. For a defined pH and depending on the administered drug, the molecule can be ionized or unionized. For an optimal permeation through the nasal mucosa, the drug should ideally be in a unionized form. Additionally, the nasal cavity is characterized by a pH ranged from 4.5 to 6.5 and any deviation out of this range may involve deleterious effects. Indeed, too acidic conditions imply an acceleration of the mucociliary clearance, whereas basic conditions may cause the inactivation of lysozymes. Lysozymes play an essential role in the defense against microorganisms and their inactivation results in an increased vulnerability of the nasal cavity against pathogens[54].

- Solubilizers: The use of solvents and co-solvents provide an increase of the drug solubility which may lead to a higher bioavailability. However, care must be taken with the amounts of co-solvents added. Indeed, co-solvents may strongly influence the tonicity of the formulation and make it incompatible with *in vivo* administration. Among the main solvent families that are used, the following can be cited: alcohol, glycols or glycerides. Co-solvents can eventually be replaced by surfactants or cyclodextrins[59,60].

- Preservatives: many nasal liquid formulations can potentially be contaminated by microbiological agents due to the presence of water and the repeated contacts between the nasal device and the nasal mucosa. Therefore, it is required to ensure the microbiological stability of the treatment throughout its period of use. This explains why preservatives are often added. Among the compounds that are frequently found in nasal liquid formulations, parabens, benzoic alcohol, benzalkonium chloride, EDTA and phenyl ethyl alcohol may be listed[60].

- Antioxidants: for molecules that are subject to oxidation, the addition of antioxidants may be needed. Classical agents are the following: sodium bisulfite, sodium metabisulfite, tocopherol and butylated hydroxytoluene[60].

- Humectants: In some very specific conditions (e.g. nasal chronic diseases), the hydration of the nasal mucosa can be affected. It may be valuable to deliver agents that will help restore this state of hydration. These agents are called humectants (e.g. glycerol, sorbitol and mannitol).

- Gelling / thickening agent: such kind of agents can provide extended residence time of the formulation in the nasal cavity (e.g. sodium carboxymethyl cellulose, hydroxypropyl cellulose). By reducing the rate at which the formulation is cleaned from the nasal cavity, the drug has more time to diffuse through the nasal mucosa.

- Other excipients: There is a variety of other excipients that can enhance the drug absorption through the nasal mucosa. They are part of a more pushed formulation development. Among them, penetration enhancers, mucoadhesive agents or enzyme inhibitors may be found.

Actually, nasal liquid pharmaceuticals are still predominant on the nasal market with powder forms that still remain less frequent[56].

4.2 Powder formulations

The development of a nasal powder rather than a liquid formulation can provide some benefits such as a higher drug stability during storage of the dosage form or the avoidance of both preservatives and cold conditions for shipping and storage[61]. This makes even more sense when the administration of protein or peptide is envisaged[56]. Powders also make possible to administer larger amounts of drug[62]. Moreover, permeation in the nasal cavity was found to be increased with the use of dry formulation [63–65]. This point was confirmed by Tanaka *et al.* when comparing the dissolution of a drug between oral and nasal administrations[62]*.* They highlighted the fact that nasal administration involves the dissolution in a very small volume of liquid (nasal fluid). This very limited volume of dissolution created a highly drug concentrated medium that is correlated to a high diffusion rate.

In addition, powders are characterized by a prolonged residence time in the nasal cavity in comparison to liquids which offers more opportunity for the drug to be transferred through the nasal mucosa[66]. Regarding excipient, the composition is usually very simple and it was also reported that some kinds of absorption enhancers (e.g. chitosan derivatives) offered a higher transmucosal bioavailability when delivered as powder[67]. However, nasal powders can still be marketed with the active drug alone or with excipients. For example, Rhinocort® Turbuhaler® from AstraZeneca only contains budesonide powder without any additional carrier or absorption enhancer. In contrast, Teijin Puvlizer Rhinocort® contains beclomethasone dipropionate dispersed in a mixture of hydroxypropylcellulose carrier particles and lubricants (stearate magnesium and stearic acid)[68].

On the other hand, the development of a dry-powder formulation presents additional issues such as the production of a powder with reproducible and homogeneous drug content and particle size characteristics. Other powder-specific parameters such as density, residual moisture and electrostatic charges can strongly influence and modify the physical behavior of the final formulation. Nevertheless, even if liquid formulations still represent the majority of nasal medicines, studies conducting the development of nasal powders are increasing in number[68–70]. Up to now, most nasal powders that are available in the market contain corticosteroids for rhinitis management. Some example of nasal marketed products containing corticosteroids can be cited, namely: Rhinocort® turbuhaler® (AstraZeneca, London, UK) containing budesonide, in Europe, or Teijin

Rhinocort® (Teijin, Tokyo, Japan) loaded with beclomethasone dipropionate and Erizas® (Nippon Shnyaku, Kyoto, Japan) loaded with dexamethasone cipecilate, in Japan. These local nasal powders are intended to the treatment of seasonal allergic, perennial and vasomotor rhinitis but also for the treatment of nasal polyps. Considering the entire nasal market with powders, an example of marketed product with systemic passage can also be described: "Onzetra Xsail®" that was out-licensed from Optinose AS (Oslo, Norway) to Avanir Pharmaceuticals Inc. (Aliso Viejo, CA, USA). The nasal medicine is loaded with sumatriptan for the treatment of migraine. It has been approved in 2016 by the FDA[71].

Unfortunately, the number of studies considering the development of nasal powders for the delivery of biopharmaceuticals still remains limited[72,73]. Indeed, the nasal delivery of a peptide in the powder form would provide lower drug degradation during storage, higher diffusion through the mucosa and reduced enzymatic degradation (due to the higher drug concentration on the mucosa and the subsequent activity saturation of local enzymes).

4.3 Other formulations

A third alternative when developing nasal dosage forms may be the use of semi-solid formulation which may include gels, creams and ointments. A very particular system which is based on "*in situ*" gelling formulations was widely studied for nasal administration. Such system is characterized by an initial low viscosity that permits an easy application by spraying or dripping in the nose. Once in the nasal cavity, the viscosity of the formulation increased thanks to a phase transition which allows prolonging the residence time onto the mucosa. Such formulation strategy makes possible to improve the bioavailability of an administered drug while reducing the doses administered, which results in an increase of the patient safety[74]. The mechanisms that induce the swelling of the polymer are based on triggering factors that are specific of the physiological environment of the nose[75]. Three main categories of *in situ* gelling polymers can be found, namely, the pH dependent polymers (e.g. carbopol), the temperature dependent polymers (e.g. poloxamer 407 or xyloglucans) and, finally, the ionic dependent polymers (e.g. gellan gum)[76,77]. For instance, such formulations were evaluated for the nasal administration of lamotrigine, loratadine or sodium cromoglycate with promising results[78–80].

5. Formulation strategies to enhance the nose-to-brain delivery

Regardless of the targeted administration (local, systemic, nose-to-brain), the efficacy of the nasal treatment will depend on 4 parameters: the physicochemical properties of the drug (e.g. the molecular weight); the characteristics of the formulation (e.g. the viscosity); physiological factors of the nasal cavity (e.g. enzymatic activity) and the specifications of the device (e.g. shape of the nozzle).

Nasal permeation may be increased with the addition of absorption enhancers (**Tab. 1**). Such absorption enhancers may be co-administered with the drug or administered as nanoparticles which combines both drug and excipients (e.g. polymer-coated nanoparticles)[81]. It must be noticed that such strategies may also be used to increase the permeation of nasal therapeutics for systemic transfer and are therefore not limited to nose-to-brain applications.

Table 1. Main categories of absorption enhancers used for nasal drug delivery (adapted from Merkus et al. and Swatantra et al., 2011)[60,82]

Categories	Examples	Mechanisms
Surfactants	Sodium laurylsulfate (anionic) Polysorbate (non-ionic).	Modification of the epithelial permeability
Bile salts	Sodium glycodeoxycholate Sodium glycocholate	Tight junctions opening, modification of the membrane permeability, mucolytic effect
Cyclodextrins	α, β, γ cyclodextrins	Interaction with the nasal membrane and opening of the tight junctions
Fatty acids	Oleic acid Lauric acid	Disruption of the membrane, solubilisation of the phospholipids
Cationic compounds	Poly-L-arginine	Electrostatic interaction with anionic residues present on mucosa surface

Cationic polymers	Chitosans	Electrostatic interaction with anionic residues and opening of the tight junctions
Bioadhesive compounds	Carbopol Starch	Diminution of the nasal clearance, opening of the tight junctions
Fusidates	Sodium taurodihydrofusidate	Solubilization of the mucus, formation of micelles
Co-polymer block	Poloxamer	Decrease of the mucus viscosity, opening of the tight junctions and interactions with lipid membrane

Next to permeation enhancers, other excipients are commonly used to improve the efficacy of nasal treatments.

5.1 Enzymatic inhibitors

Even through nasal delivery avoids the hepatic first-pass effect, various enzyme families are found in the nasal cavity. Indeed, the presence of peptidase, protease, phase I and phase II enzymes has been reported and their presence may interfere with the delivery of numerous therapeutics. For instance, it has been reported that the activity of CYP 450 in the olfactory epithelium was even higher than in the liver[22]. Therefore, the incorporation of enzyme inhibitors in nasal formulations may be advisable. Different enzyme inhibitors were tested for nasal application such as peptidase inhibitors (e.g. bestatin and comostate amylase) and trypsin inhibitors (e.g. aprotinin and leupeptin)[83]. The concomitant nasal administration of salmon calcitonin with comostate amylase, aprotinin or leupeptin induced hypocalcaemia in rats[84,85].

5.2 Mucoadhesive and mucopenetrating agents

The mucociliary clearance is represented throughout the nose but some particularities can be observed between the different nasal regions. Indeed, although the olfactory mucosa is characterized by the presence of static cilia, the cleaning mechanism is still effective but rather works on basis of the gravity and the sustained production of mucus from the Bowman's glands[86]. Therefore, the use of mucoadhesive agents may be justified and needed to extend the drug residence time in the olfactory region of the nose.

In this context, numerous studies have been carried out to ascertain the utility of using mucoadhesive agents to maximize the nose-to-brain transfer. In order to illustrate this aspect, it has been shown that a combination of pectin and chitosan can reduce the olfactory clearance[87]. Moreover, the use of a combination chitosan / hydroxypropyl β-cyclodextrins in solution provided a higher diffusion of buspirone towards the brain in comparison with a non-adhesive solution[87,88]. The use of mucoadhesive excipients appears as an effective tool to maximize the transfer to the brain.

Special attention should be paid to chitosan and its derivatives, which represent one of the most commonly used category of mucoadhesive agents in nasal formulations. Chitosans are biocompatible derivatives obtained by deacetylation of chitin. The mucoadhesion takes place via an electrostatic interaction between the cationic polymer with its amino groups and the anionic charges of sialic acid residues present at the surface of mucins in the nasal mucus[89]. In addition to this mucoadhesion, chitosans present absorption enhancer properties as they can open the epithelial tight junctions which results in an easier diffusion of the drug through the paracellular pathway[90].

There are numerous chitosan derivatives which may be selected according to the desired pharmaceutical application. Indeed, chitosan can be obtained in a very wide range of deacetylation degrees (40 - 98%) and molecular weights, namely: low molecular weight < 50 kDa, medium molecular weight 50 - 150 kDa or large molecular weights > 150 kDa[91]. Conventional chitosans (**Fig. 5**) are insoluble at neutral or basic pH while acidic conditions allow the protonation of its amino groups (pKa 6.3) and its solubilization. Moreover, chitosan derivatives have been subject to a multitude of

chemical modifications to modulate their properties. For instance, N-trimethyl chitosan allows the solubilisation of the polymer at physiological pH[92].

For nose-to-brain delivery, chitosans have been formulated in a multitude of therapeutic preparations (e.g. solutions[87], suspensions[93], *in situ* gel[94], micro-emulsion[95], nanoparticles[96] and microspheres[97]). When polystyrene nanoparticles were coated with chitosan, it was shown that chitosan provided stronger interaction with the porcine olfactory mucosa in comparison with uncoated nanoparticles. It was also concluded that, by increasing the cationic charge of the polymer, the mucus retention time was prolonged[98].

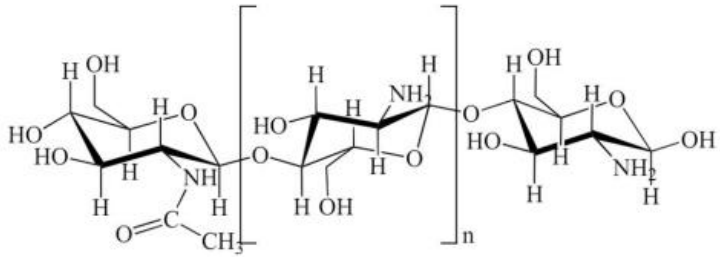

Figure 5. Chemical structure of conventional chitosans with N-acetyl-glucosamine and D-glucosamine units[99]

If particle adhesion is an essential condition, diffusion of the therapeutic molecule through the mucus may be a limiting factor for passage to the brain. Indeed, the mucus can act as a kind of barrier and it is described as a double-mechanism filter[100]. The first mechanism works like a sieve that prevents too large molecules to diffuse. The second mechanism is based on interactions with the particle surface and will let them diffuse according to their charge and polarity. It is generally observed that by developing small nanocarriers coated with a neutral polymer such as polyethylene glycol, it is possible to increase the diffusion through the mucus[81]. The explanation of the mucopenetration would come from the combination of small entities (i.e. nanoparticles), that easily diffuse, with a polymer, that prevents any interactions with the mucus.

5.3 Permeability enhancement

For achieving an efficient nose-to-brain delivery, the nasal epithelium can sometimes be a limiting step to the diffusion of therapeutic molecules. Permeation enhancers can

increase the diffusion of a drug by various mechanisms involving an alteration of the epithelium integrity or by increasing the mucus fluidity (**Tab. 1**).

For instance, a group of absorption enhancers works by opening the epithelium tight junctions that thus make the diffusion easier. The use of such excipient is very relevant for increasing the diffusion of molecules that borrow a paracellular transport. In this group are found, among others, chitosans and the amphiphilic Poloxamer® 188 (a block co-polymer with a low molecular weight consisted of hydrophobic polyoxypropylene oxide linked with hydrophilic polyethylene oxide chains). Poloxamer® 188 has been widely studied in nose-to-brain delivery. Its enhancing effect (**Tab. 1**)was attributed to its elastic behaviour, its ability to decrease the mucus viscosity and its capacity of altering both epithelial lipid membrane and tight junctions[101,102].

Some excipients belonging to this family have already been mentioned in other categories as they present multiple properties (e.g. chitosan).

5.4 Lipid based systems

In 2009, the very first experiments that assessed the nose-to-brain delivery of a protein with a lipid-based nanosystem was performed by Migliore *et al*.[103] This was the starting point for the delivery of other biopharmaceuticals through the nose-to-brain pathway with lipid-based systems. The use of lipid-based systems may be useful when working with hydrophobic drugs at high concentrations or for improving their diffusion through the nasal barrier[104]. The following lipid-based systems have been already described: microemulsion, solid lipid nanoparticles (SLN) and liposomes.

It was shown that the brain diffusion of tacrine for Alzheimer treatment was higher in both mucoadhesive and non-mucoadhesive microemulsions than after nasal administration of a tacrine solution[105].

The nose-to-brain delivery of risperidone loaded in SLN was also investigated for the management of psychotic disorders[106]. It was observed that the nasal delivery of SLN provided higher risperidone levels in mice brains compared to intravenous administration of the same formulation.

Liposomal suspensions were also shown to improve the diffusion of anti-schizophrenic agents in the brain after nasal administration in mice[107].

It is also possible to confer extra mucoadhesive / absorption enhancing properties to the formulation by associating lipid-based systems with other excipients. For instance, by working with anionic lipids, it is possible to combine them with cationic excipients to get modular physicochemical properties of the final dosage form[108].

5.5 Cell penetrating peptide

When the diffusion of a drug has to be increased, there are other possibilities than the use of conventional absorption enhancers. Indeed, very promising results have been collected following the nasal delivery of formulations loaded with cell penetrating peptides (CPPs). CPPs work by enhancing the uptake of the drug administered thanks to their ability to enter the cells[109]. Generally, CPP's are about 5–40 amino acids residues long and can be obtained either in a synthetic or natural manner (e.g. natural viral proteins)[110]. CPPs increase the drug diffusion by inducing a translocation in the cell membrane. The pathway borrowed (energy dependent or independent) will depend on the nature of the drug, the nature of the CPP and the family of cells to be crossed. CPPs were shown to diffuse through a panel of physiological barriers found in the retina, the neurons, the skin, the intestine and the brain[111]. Three distinct families of CPPs have been described with cationic, hydrophobic and amphipathic CPP.

Among them, the low molecular weight protamine (LMWP) is an example of CPP that was assessed for the nose-to-brain delivery of nanoparticles[112]. LMWP was coupled to PEG-PLA nanoparticles for the delivery of coumarin-6 in rats. Higher levels of coumarin-6 were recovered in the brain after nasal administration when the nanoparticles were grafted with LMWP. Another study demonstrated that higher levels of different proteins (bovine serum albumin, peroxidase and β-galactosidase) could be achieved in the brain following a nasal administration thanks to the conjugation with LMWP[111]. Therefore, it is proven that, by adding LMWP in nose-to-brain formulations, higher drug levels can be reached in the brain.

5.6 Targeted interactions

Another strategy for optimizing a nasal formulation is the use of excipients which have particular affinities for a biological compound that is well-represented in the nose. For instance, lectins are proteins isolated from plants (e.g. tomatoes or wheat germ) that

have affinities for glycan. These sugar groups are present on the surface of biological tissues such as the olfactory mucosa of the nose. The combination of a drug with lectins allows improving the targeting of the olfactory area for a potential nose-to-brain transfer.

Among all the lectins available, wheat germ agglutinin (WGA) have been deeply assessed for nose-to-brain delivery[17]. This lectin has a propensity to bind both sialic acid and glucosamine residues which are strongly represented in the nasal mucosa. Therefore, the co-administration of WGA with various molecules (e.g. coumarin, vasoactive intestinal peptide) allowed achieving higher concentrations in the olfactory bulb, cerebrum and cerebellum in rats[113–115]. It was also highlighted that WGA coupled to horseradish peroxidase could fix sensory olfactory cells of the nasal mucosa[116,117].

Other lectins have also been investigated for the nose-to-brain pathway, namely, the *solanum tuberosum* lectin, the *Ulex europeus* agglutinin and the odorranalectin[81]. Among them, odorranalectin was described to be less immunogenic derivative than other lectins[118]. For instance, this compound was studied for the treatment of Parkinson's disease by nose-to-brain delivery. In the form of nanoparticles as well as in combination with a PEG-PLA mixture, they were able to deliver high concentrations of urocortin peptide in the brain.

5.7 Deposition in the olfactory region

Even if a formulation has been optimally developed, the amount of drug deposited in the olfactory region should be maximized to increase its transport to the brain. The administration of charged particles maybe associated with an electric field to better guide the particles for the nose-to-brain transfer. Using this method, it was possible to reduce the drug losses in the anterior part of the nose while increasing the deposition in the olfactory mucosa[119].

The optimization of the *in vivo* impaction of a powdered formulation may be also achieved through specific *in vitro* evaluation. Artificial nasal cavities called “nasal casts” were used to evaluate the vestibular intubation (releasing the particles in a precise point of the vestibule), the deep intubation (the nozzle of the nebulizer is placed below the olfactory mucosa) and the electric guidance deposition (enhancing the deposition of charged particles in the olfactory region by applying an external electric

force). The electric guidance resulted in 16% v/v of deposition in the olfactory region while deep intubation provided only 1% v/v of deposition[120].

It is also possible to deposit more formulation in the olfactory zone thanks to the use of specific devices. Recently, the number of devices dedicated to the nose-to-brain delivery has increased due to the growing interest.

6. Nasal devices

Even if both the formulation strategy as well as its properties are predominant for the nasal delivery, the choice of the medical device is also very crucial. The device selected will drastically impact the efficacy of the nasal treatment by changing the amounts of drug deposited in the nasal cavity or by delivering more accurate doses, for example. It is thus essential to perform characterization tests with the combination "formulation + device" in order to work on the final therapeutic product. Indeed, some formulation properties can be modified once loaded in the nasal device. For example, the aerosol size distribution can differ from the size distribution of the raw formulation (e.g. if agglomeration issues appear once loaded in the device). As a proper choice of the device was particularly important in our work, it was decided to describe the different technologies available to allow a better understanding of the choice of the devices selected to perform our in vitro evaluation of both dry and liquid formulations.

6.1 Liquid devices

Liquid formulations represent the great majority of the pharmaceuticals dosage forms available for nasal administration. For the nasal delivery of liquid formulations, the following devices are available: droplets dispensers, rhinyle catheters or tubes, multi-doses metered-dose pump sprays, single or duo-dose spray devices and pressurized systems[53].

Droplets dispenser

This is one of the most traditional and old device used in the nasal field (**Fig. 6**). Droplets dispensers are available as unit or multi-doses systems. They present the advantage of having a low cost production and an easy manufacturing protocol. However, they present a lot of limitations in terms of microbiological contamination and dose reproductibility[58].

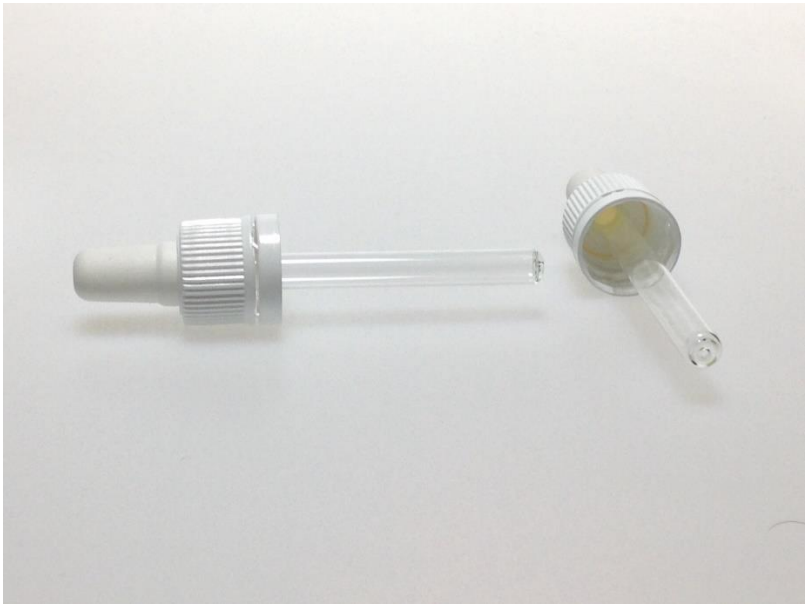

Figure 6. Example of nasal droplet dispenser (www.gravis.fr)

These devices are preferably replaced by new pressurized systems or mechanical spray pumps. Nowadays, droplets devices are limited to the local delivery of drugs such as corticosteroids. The nasal drop form with single-doses delivery systems still remains the best choice for the treatment of certain local pathologies such as nasal polyps where high deposition in the middle meatus is needed[121,122].

Rhinyle catheters and tubes

This device category is rather used for experimental studies (e.g. preclinical experimentations) and is not widely represented in the nasal market[123]. However, the example of desmopressin can still be cited as it is delivered with such device during its commercialization[124]. The configuration of the device is made with a tip connected to the nasal cavity while the other extremity is connected to the patient's mouth. The patient has to blow through the tube in order to propel the formulation in the nose.

Metered spray pumps

This category represents the most common devices present in the nasal market since a few decades (**Fig. 7**). They allow the delivery of a defined volume of liquid comprised in the range 25 - 200 µL. At the beginning of their use, these devices required a “prim” step to initiate the device. However, they may lead to some variabilities during the administration. Indeed, many parameters such as the actuation force or the shape of the nozzle may strongly impact the size distribution in the aerosol or the shape of the

plume[125]. Metered-dose spray pumps usually require the addition of preservatives but this disadvantage has been overcome thanks to the development of innovative devices that have ensured microbiological stability without adding preservatives. An example of such devices is the “Advanced Preservative Free” system developed by Aptar Pharma and based on a combination of a filtration membrane and a seal (www.aptar.com).

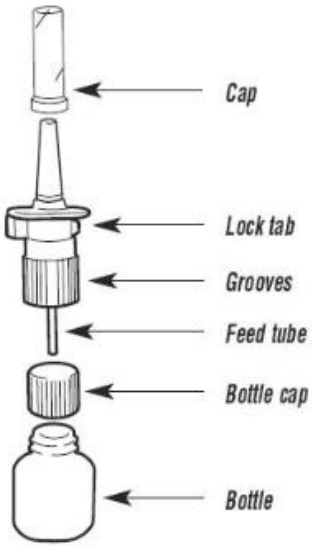

Figure 7. Illustration of the metered spray pump used for the delivery of salmon calcitonin in the product Fortical®

Single or duo-dose spray devices

Sometimes, nasal administration requires the delivery of more accurate doses of drug (e.g. drugs with narrow therapeutic index). In contrast to metered-dose spray pumps which are rather designed for chronic treatments, single or duo-dose spray devices are more relevant when the drug administered is very expensive[53].

Figure 8. FluMist®, quadrivalent nasal spray flu vaccine from AstraZeneca (www.flumistquadrivalent.com)

For instance, when the spray devices are used for the delivery of nasal vaccines (**Fig. 8**) like the influenza vaccine "FluMist®" (www.flumist.com)[126].

Pressurized systems

Previously, the pressurized metered dose inhalers (pMDI, **Fig. 9**) were loaded with chlorofluorocarbons (CFC) as propellants for the aerosol generation. Gradually, these CFC's have been removed and changed for hydrofluoroalkanes (HFA) due to their ecological side effects on the ozone layer. Additionally, CFC involved dryness of the nasal mucosa as well as unpleasant cold effect for the patient during the administration. Another drawback is the very high velocity of the droplets at the exit of the device.

Figure 9. Illustration of the pMDI nasal technology from 3M company (www.3m.com)

These major disadvantages were solved by changing CFC for HFA[127,128]. pMDI also present a few advantages such as their limited size and their easy transport as well as the selection of the dose delivered and isolation plus protection of the content[129].

6.2 Powder devices

For the nasal delivery of powders, three categories can be described:

Nasal inhalers

Inhaler devices are based on the breath actuation by the patient. The powder is contained in a blister or in a capsule in a similar way to dry-powder inhalers for lung delivery (**Fig. 10**). Before the administration, the blister or capsule is pierced and the patient inhales the powder which is aerosolized and deposited in the nose. Administration is similar to the lung delivery with dry powder inhalers excepted that inhalation is performed through the nose instead of the mouth.

Figure 10. Illustration of the nasal inhaler "Turbuhaler®" (on the left) used for the delivery of "Rhinocort®" (AstraZeneca) and Rhinocort® products with powder and liquid devices (metered spray pumps) for the nasal delivery (on the right).

Such devices were developed by companies such as Astra Zeneca (http://www.astrazeneca.com). They adapted the "Rhinocort Turbuhaler®", initially intended to lung delivery, for the nasal delivery of budesonide for the treatment of nasal polyps.

Nasal powder sprayers

The aerosol is produced following the generation of a positive pressure in a compressible compartment included in the device. When the positive pressure is released, the aerosol is generated and the powder is expelled outside of the device. Several devices from various companies (e.g. the Unit-Dose System "UDS" from Aptar Pharma, www.pharma.aptar.com, **Fig. 11**) are based on this principle and consist of an air-loaded compartment sealed with a membrane. The compartment is then

compressed and the membrane pierced. Finally, the pressure allows the production of the aerosol[53]. The UDS device is designed to deliver precise amounts of powder but also liquids. Once used by the patient, it can be discarded as it is a disposable device. This device has a system of ball / valve that prevents contamination from outside air[123].

Figure 11. Unit-Dose System (UDS) from Aptar Pharma (www.aptar.pharma.com)

Nasal insufflators

The basic principle of this device involves a connection between the mouth (the mouthpiece) and the nose (the nosepiece). When the patient expires in the device, the powder is expelled from the insufflator towards the nasal cavity through the nosepiece. During expiration, there is a displacement of the soft palate which involves the isolation of the nasal cavity from the rest of the respiratory tract. This particularity avoids the loss of significant amounts of powder in the lower respiratory tract (e.g. in the lungs)[53]. A device based on this operation has for example been developed and optimized by Optinose® (www.optinose.com) with their "Breath powdered Bi-directional™ technology" (**Fig. 12**).

Figure 12. Bi-directional nasal delivery system from Optinose® (www.optinose.com)

The nasal delivery of sumatriptan by using the bi-directionnal™ technology and in the form of a dry-powder (AVP-825) was compared to its nasal delivery by using a conventional liquid spray and in the form of a liquid[130]. The clinical study reported, among others, the sumatriptan plasma concentration during 4 hours. It can be concluded (**Fig. 13**) that by using the powder-state form combined with this technology, both faster and higher absorption of the drug were achieved.

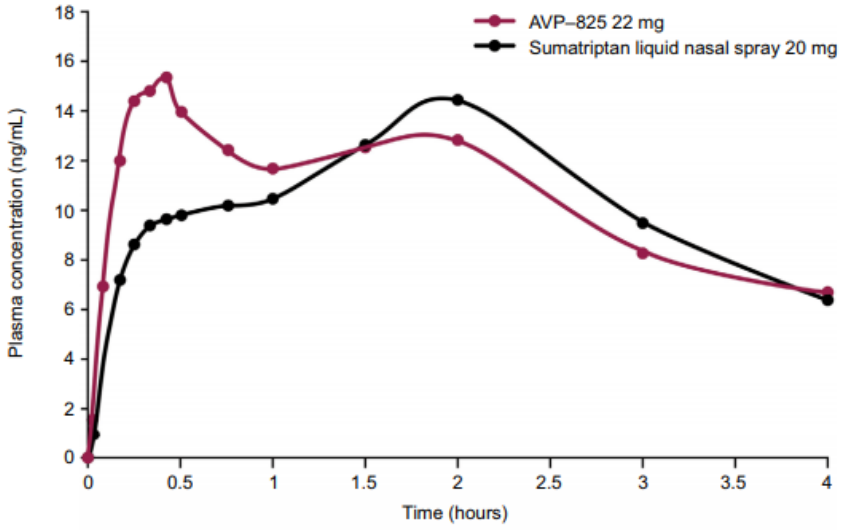

Figure 13. Comparison of sumatriptan plasma concentration-time profile during 4 hours between the powder loaded in the breath-powdered device compared to a conventional liquid spray (n =20)[131]

6.3 Nose-to-brain devices

As previously discussed, the deposition site of the drug in the nasal cavity is one of the main factors affecting the effectiveness of a nose-to-brain delivery. In addition to the

inherent design of each device, the deposition, which should be oriented towards very specific and different areas of the nasal cavity, is greatly dependent on the orientation of the plume.

Conventional pump spray will rather orientate the deposition in the anterior part of the nose (nasal valve and vestibule)[104,132,133]. A device that generates a thinner plume will usually rather deposit in the turbinates[134]. For instance, using a conventional metered dose spray-pump, it was shown that only 2.5% v/v of formulation were deposited in the olfactory region[135]. Some researchers showed that, with classical droplet dispensers, it is even possible to deposit satisfactory amounts of drug in the olfactory region[87]. Obviously, these observations were collected from studies that characterized their formulation of interest and the aerosol properties can still vary depending on the formulation characteristics.

A first example of device dedicated to nose-to-brain delivery is the Vianase® device (**Fig. 14**) from Kurve Technology™ (Kurve Technology Inc., Lynnwood, WA, USA). It combines an electronic atomizer associated to a vortex. This device is developed for liquid formulations and allows a precise control of the size of the droplets generated in the aerosol. In clinical studies, this device provided improvements in conditions for Alzheimer's patients after a nose-to-brain delivery[136].

Figure 14. Vianase® device from Kurve Technology™ (www.kurvetech.com)

The nasal device developed by Optinose® (Optinose US Inc., Yardley, PA, USA) previously described in the paragraph "Nasal Insufflators" was also assessed for its ability to target the olfactory region. An experimental study compared the deposition of labelled lactose with either the Opt-powder device or with a conventional pump-spray

(Rexam SP270, Rexam Pharma, France). It appeared that, with the Opt-powder system, 18% v/v was deposited in the upper part of the nose in contrast to only 2.4% v/v with the conventional liquid pump-spray[135].

Another system providing similar advantages has been proposed by SipNose (SipNose Ltd. Yokneam, Israel).

Impel NeuroPharma (Impel NeuroPharma Inc., Seattle, WA, USA) also developed a nose-to-brain device which works with the “Precision Olfactory Deposition™” (POD) technology. The device implies a propellant gas (HFA) to generate the aerosol. It was suited for the nasal administration of both powder and liquid formulations. A deposition of 45% v/v in the upper part of the nose could be achieved with the POD technology[137].

The UDS devices previously described from Aptar Pharma (Aptar Pharma Inc., Le Vaudreuil, France) was also presented to be able to target the nose-to-brain pathway. High deposition (52% v/v) was obtained in nasal casts when a powder formulation was delivered from the UDS device[138].

7. Potential applications of nose-to-brain delivery

7.1 Neurodegenerative diseases

Among the various existing pathologies, neurodegenerative diseases remain the ideal target for nose-to-brain medicines[139]. Indeed, the treatment of such pathologies requires chronical administrations that are easier to implement from the nose-to-brain delivery due to its non-invasiveness and its direct access to the brain. Therefore, it provides benefits in terms of efficiency and compliance.

Alzheimer’s disease (AD)

AD is a widespread cause of dementia that is characterized by the presence of amyloid plaques, cognitive dysfunctions, the loss of cortical neurons and, finally, neurofibrillary nodes[140]. Up to now, currently therapeutic agents used to treat this pathology are acetylcholinesterase inhibitors or glutamate neurotransmission blockers. These molecules are mostly delivered orally, which limits their access to the brain because of the blood-brain barrier[141]. Unfortunately, these therapeutics only provide limited

improvements. Such failure explains the need of finding new drugs as well as novel routes of administration[142].

In this context, the nose-to-brain delivery of R-flurbiprofen (R-FP) in mice has provided very interesting data[143]. The levels of R-FP recovered in the brain after the nasal administration of R-FP loaded in albumin nanoparticles (301.2 ± 36.3 ng/mL, t = 0.5h, n = 4) were higher than after oral administration of the R-FP solution (117.0 ± 23.9 ng/mL, t = 0.5h, n = 4). In addition, the protection afforded to the cellular mitochondria was also enhanced after nasal administration.

Insulin is another drug that was deeply studied for its beneficial effects on the memory and, flowingly, as a potential treatment for AD. The resistance to insulin, the decrease of the gene expression for insulin receptor and the decrease in circulating insulin levels in the brain may explain the beneficial effects obtained in patients with AD after insulin administration[144,145]. A study focused on intranasal administration of insulin in patients with mild to moderate AD during 4 months has brought improvements in regards to their cognitive capacities[145]. Another study has assessed the improvement of the cognitive capacities in 24 patients with early AD. Patients received either the placebo or insulin by nasal administration. Patients who experimented nose-to-brain delivery have shown better attention and verbal memory[146]. Another study involving 36 patients with AD has also highlighted memory improvement after nasal insulin delivery in comparison with the placebo[147].
Obviously, these therapeutic effects may be attributed to both nose-to-brain but also systemic passages. This is why various strategies have been discussed to better target the nose-to-brain transfer such as the association with cell-penetrating peptides[148].

Parkinson's disease (PD)

This degenerative pathology is characterized by a destruction of dopaminergic neurons located in the *substantia nigra*[149]. Among the various drugs nasally delivered for PD management, bromocryptin is a first relevant example. A pre-clinical experimentation compared the diffusion of bromocryptin loaded-nanoparticles in chitosan after either nasal or intravenous delivery in mice. The high concentration of bromocryptin recovered in the brain after 0.5 hour was attributed to the nose-to-brain transfer[150]. The nose-to-brain transfer also involved a significant increase in dopamine brain levels.

Other therapeutics have also been proposed for the management of PD by the nasal route : ropirinol[151], rasagilin[152] and pramipexol[153].

7.2 Brain Cancers

The nose-to-brain delivery also represents a great opportunity for the treatment of brain cancers. Previously, the treatment of such cancers involved the use of highly invasive administration procedures such as the “convection-enhanced delivery” which delivers anticancer agents directly to the tumour via catheters through the skull[154]. Moreover, the use of non-selective drugs involved toxicity against healthy brain tissues and, subsequently, led to neural damages. Nowadays, research deeply focuses on the development of more targeted treatments involving non-invasive administration[154].

Among the different types of brain cancers, malignant glioma is the most frequent. Among the different glioma, the glioblastoma is the most aggressive form and is correlated to a survival rate below 5% over 5-years[155]. Taking this into consideration, glioblastoma has been the target of many scientific studies developing nose-to-brain treatments[156]. For instance, nasal delivery of GRN 163, a telomerase inhibitor, provided an increase of the median survival in rats from 35 days to 75.5 days[154]. Nose-to-brain delivery of siRNA targeting the Galectin-1, an overexpressed protein in glioblastoma, was evaluated by another research group with promising findings[156]. By using the siRNA complexed nanoparticles, they could decrease the expression of Galectin-1 in both human and murine glioblastoma cells. Moreover, they reduced by 50% the Galectin-1 expression in tumour bearing mice. The combination nose-to-brain / tumour targeting could provide a promising treatment for brain cancers.

7.3 Other pathologies

Obviously, nose-to-brain application is not only limited to neurodegenerative diseases or brain cancers. Indeed, a multitude of other pathologies could also be targeted like depression, migraine or schizophrenia[157].

For instance, the management of depression by nose-to-brain delivery of duloxetin was assessed. Such delivery provided better improvements in depressed rats compared to the oral route of administration[158].

Other studies have considered the nose-to-brain delivery of triptans to treat headache. Triptans work by inducing the contraction of cerebral arteria which, subsequently, allows achieving a better distribution of the blood in the brain. Many nasal medicines containing triptans are already commercialized such as Imitrex® (GSK, Brentford, UK) which is a first relevant example of commercialized sumatriptan-loaded nasal spray. However, such marketed product does not focus on a direct nose-to-brain transfer and rather uses a systemic pathway in order to reach the CNS. Subsequently, new formulations have been developed in order to provide a nose-to-brain transfer to sumatriptan (e.g. micellar nanocarriers)[157]. Other tripans such as zolmitriptan loaded-microemulsion could be efficiently delivered in the brain of rats[159]. It was concluded that higher diffusion of zolmitriptan into the brain following nasal administration resulted from the contribution of both systemic and direct transfers.

Schizophrenia may also be a relevant pathology to be treated from nose-to-brain delivery. Preclinical studies have been already conducted in mice. It was shown that it was possible to reach concentrations 6 - 8 times higher compared to the intravenous administration of paliperidone[160]. In this study, they also evaluated the "direct transfer percentage (DTP)" by making a ratio between areas under the curve (AUC) in the brain and in the blood following either nasal or intravenous administration. The DTP thus represents the amount of paliperidone directly transferred from the nose to the brain. This percentage was 68.82 ± 6.0% following the nasal administration of the microemulsion containing paliperidone.

Among these pathologies, the cachexia syndrome can also be considered as a new potential therapeutic target for a nose-to-brain treatment.

7.4 Nose-to-brain delivery of peptides and proteins

The first study that focused on the delivery of a protein directly from the nose to the brain was performed in 1995 by Thorne et al[161]. This was the first study quantitatively describing the nose-to-brain transport of a protein. In 2002, a very interesting work was published by Born *et al*.[162]. They proved that three peptides (vasopressin, melanocortin and insulin) nasally administered in human patients could reach the cerebrospinal fluid without passing by the bloodstream. Even if intranasal delivery of such biotherapeutics provided higher bioavailability in the brain compared to other routes of administration (e.g. intravenous, oral), the drug levels in the brain remain limited when administered

without addition of excipient (< 1%)[45]. Indeed, peptides and proteins are complex molecules characterized by a high molecular weight associated with a certain hydrophilicity that makes their delivery quite challenging in terms of both stability and diffusion through the biological membranes. Indeed, it is commonly accepted that a drug having a molecular weight greater than 1000 Da will have difficulties to pass through the nasal mucosa and, therefore, requires the use of absorption enhancers[163]. Once the drug diffusion increased, the drug should also be protected against enzymes from the olfactory mucosa (e.g. CYP-450, esterase, transferase)[164,165]. The development of nose-to-brain formulations should be focused on preventing both issues.

Among the various biomolecules evaluated for nose-to-brain application, one of the most studied was insulin (that was briefly discussed in the paragraph "1.6.1. Neurodegenerative Diseases"). At the very beginning, the nose-to-brain administration of insulin was used to increase insulin peripheral sensitivity which was a result of its effect in the brain[166]. Then, a second application for AD was considered due to its therapeutic effects on the memory recovery[148,167].

The majority of peptide drugs that were, or are, concerned by clinical studies for their nose-to-brain application are listed in (**Tab. 2)**.

Table 2. Peptide drugs concerned by clinical studies for their nose-to-brain application[40]

Peptide drugs	Therapeutic targets	Clinical phase
Insulin	- Alzheimer's disease - Obesity - Parkinson's disease - Schizophrenia - Major depressive disorder	Phase I → IV
Oxytocin	- Cognitive and behaviour disorders - Autism Spectrum disorder - Post-traumatic stress disorder - Sexual dysfunction	Phase I → IV

	- Schizophrenia - Pain management	
Arginin-vasopressin	- Cognitive and behaviour disorders - Pro-social effects	Phase I
Melanocortin (4–1 0)	- Obesity	Phase I → II
Cholecystokinin	- Obesity - Alzheimer's disease - Cognitive and behaviour disorders	Phase I → II
NAP neuropeptide	- Alzheimer's disease - Schizophrenia	Phase I → II
Hypocretin-I (orexin A)	- Obesity - Alzheimer's disease - Parkinson's disease - Narcolepsy	Phase I
Hexarelin	- Growth hormone deficiency	Phase I
Neuropeptide Y	- Obesity	Phase I
Insulin-like growth factor-I	- Diabetes - Obesity	Phase I

It must still be noticed that, even if nose-to-brain transfers are reported, it is usually a contribution of multiple pathways that allow a drug to access the brain (i.e. systemic, olfactory and trigeminal). This is one of the major obstacles in the development of a clinical study; experimenters experiencing great difficulty in distinguishing the different transport routes borrowed by a drug. Therefore, the development of a therapeutic that would selectively use a direct nose-to-brain transport would theoretically be impossible.

8. Cachexia and ghrelin

8.1 The cachectic syndrome

Cachexia can be defined as “a complex metabolic syndrome associated with underlying illness and characterized by loss of muscle with or without loss of fat mass” [168]. The prominent clinical feature of cachexia is weight loss in adults (corrected for fluid retention) or growth failure in children (excluding endocrine disorders). Anorexia, inflammation, insulin resistance, and increased muscle protein breakdown are frequently associated with cachexia[169]. The most frequent cachexia-associated pathologies are: chronic obstructive pulmonary disease, heart failure, cancers, kidney pathologies and rheumatoid arthritis[170].

Cachexia results from a general metabolic disorder with an imbalance between food intake and energy consumption. The inflammatory state would be favoured by a dysregulation in inflammatory cytokines[171]. These cytokines could also have leptin-like activity on the appetite which results in an appetite decrease[172]. These cytokines would also involve the blockage of hormonal signalling pathways such as the axis involving both neuropeptide Y and GHRL[173]. The levels of specific inflammatory cytokines (e.g. C-reactive protein and interleukin-6) are even measured and serve to establish the severity of the syndrome in the patient[174]. Patients where the cachectic syndrome is found often see their prognosis worsened.

8.2 Classification of the cachexia severity

In order to classify the severity of the cachectic syndrome, many methods of classifications have been described[175]. Each of them considers different criteria to establish the state of progress of the syndrome. Most of the classifications have been set up for cancer cachexia. The cachexia staging is not only interesting to establish the severity of the syndrome; it also facilitates the orientation of the treatment.

A first classification method describes three different stages: pre-cachexia, cachexia and refractory cachexia[175]. The pre-cachexia stage is characterized by preliminary clinical signs which precede a significant weight loss. Pre-cachexia is defined by a weight loss ≤ 5%, anorexia and metabolic modifications. Depending on the evolution

of the underlying pathology with respect to the treatment (e.g. response to chemotherapeutics), the stage of the syndrome may progress to the next stage: cachexia. The cachectic stage may be established if one of the following criteria is encountered: loss of stable body weight > 5% during the last 6 months or a body mass index < 20 Kg/m² and a weight loss > 2% or sarcopenia and weight loss > 2%. The third stage, refractory cachexia, is usually encountered with aggressive cancers and where there is a lack of response to chemotherapeutics[175]. This stage is defined by a low performance status of the patient coupled to a life expectancy lower than 3 months.

Another classification was proposed for cachexia; the latter is called CAchexia SCOre (CASCO) and is based on a numerical system[174]. The score generated is comprised between 0 and 100 and four different states of cachexia can be attributed depending on the score obtained: mild cachexia (0 - 25), moderate cachexia (26 - 50), severe cachexia (51 - 75) and terminal phase (76 - 100). The score is calculated using 5 tools: loss of body mass / composition changes, inflammation / metabolic disorders / immunosuppression, physical performance, anorexia and quality of life (**Fig. 15**).

It can be seen that the loss of body mass represents 40% of the total distribution which shows its predominant role. Inflammation is also involved and the levels of both C-reaction protein and interleukin-6 can be increased in cachectic patients. Among the different metabolic disturbances, the patients may have anaemia or lower levels of albumin. These data may be evaluated and included in the CASCO score calculation. Moreover, the physical performances being directly linked to the muscle performance, it is a useful tool to assess the loss of muscle mass in cachexia. The syndrome also includes a loss of both appetite and food intake that are correlated to anorexia that is directly linked to the quality of life.

All these parameters are therefore interrelated and must be integrated separately in this complex calculation to produce a final value that will help to guide the treatment.

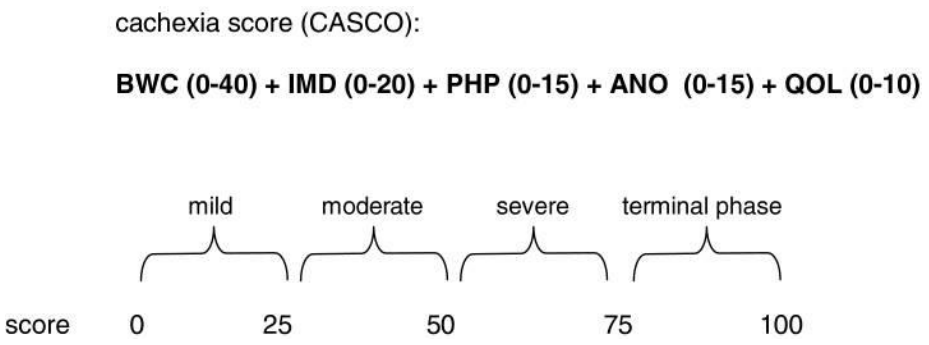

Figure 15. CASCO staging system with the 5 tools: BWC body weight loss and composition, IMD inflammation/metabolic disturbances/immunosuppression, PHP physical performance, ANO anorexia, QOL quality of life[174]

8.3 Epidemiology

The prevalence of cachexia is strongly dependent of the pathology/ies that is/are associated to the syndrome. For end-stage chronic heart failure, the prevalence is 5 – 15 % while the prevalence for advanced cancers is 80%[170]. For instance, in patients with pancreatic cancer, cachexia would be responsible for 50 - 80 % of the deaths[176]. About the mortality, cachexia would be responsible of 10 - 15 % of deaths per year for Chronic obstructive pulmonary disease (COPD), 20 - 30 % per year for heart failure - kidney diseases and 80% for cancers[170]. Cachexia is often responsible for the aggravation of treatment-related side effects.

8.4 Hormonal ethiology

Among the multiple factors causing cachexia, there is a disturbance of the hormonal axis regulating appetite (**Fig. 16**). The latter is located in the arcuate area of the hypothalamus. In this complex hormonal balance, leptin, a peptide hormone that plays a crucial role in the regulation of appetite was found. Leptin acts via the CNS and induces a decrease of appetite as well as an augmentation of the energy consumption by the body[177,178]. Leptin activates a signalling path that involves other downstream hypothalamic neurotransmitters. In case of body mass loss and when the body is functioning properly, the levels of leptin decrease and the hormonal signalling path that has the opposite effect - the stimulation of food intake - is stimulated.

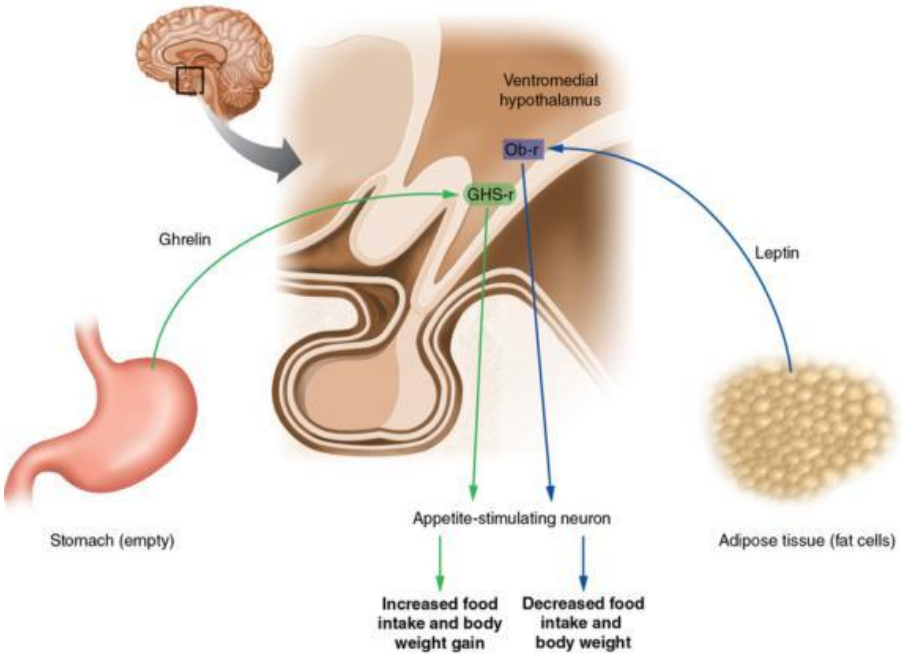

Figure 16. Hormonal regulation of food intake with GHRL increasing and leptin decreasing effects (GHS-r: GHRL receptor; Ob-r: obesity receptor), www.humankinetics.com

This orexigenic hormonal chain involves, among others, the neuropeptide Y, GHRL and other neuropeptides[173]. The cachectic state will result, in part, from a disruption of this hormonal balance between both appetite regulating systems. For instance, it appeared that in rats bearing tumours, the circulating levels of GHRL where lower in comparison with healthy rats and some kind of GHRL resistance could even be observed[179]. The experimentation could highlight some improvements in terms of anorexia – cachexia state after GHRL administration while the administration of a GHRL antagonist induced a worsened evolution of these animals.

8.5 Cachexia management with ghrelin

Up to now, the most suitable therapeutic approach for cachexia management is to adopt a multifactorial scheme of treatment. This involves dietary advice, the treatment of the inflammatory state, re-stimulation of the patient's appetite, and of course, the treatment of the underlying pathology. To stimulate the appetite in critically ill patients, the administration of GHRL would be an attractive option as it plays a major role in the orexigenic hormone system[180].

Regarding its chemical structure, it is composed of 28 amino acids on which is grafted a fatty acid chain of octanoic acid type[181]. This fatty acid group is added on the “Ser-3” residue and it is essential for the GHRL binding to its receptors (**Fig. 17**). The octanoic acid is post-transcriptionally added by a specific enzyme which is called GHRL -O-acyl transferase “GOAT”.

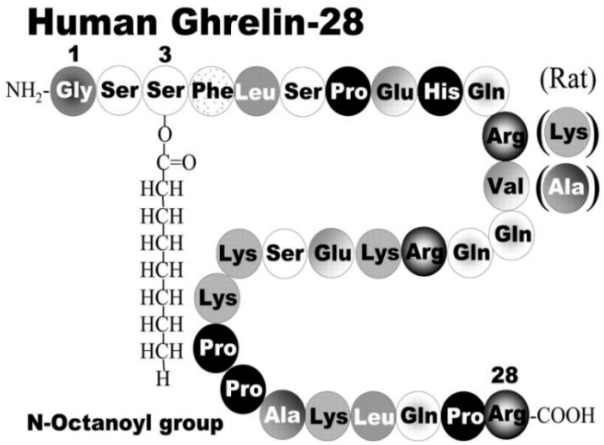

Figure 17. Amino acid sequence of human octanoylated GHRL and rat GHRL sequence with modifications on residues 11 and 12 octanoylated GHRL [182]

GHRL is the first and only peptide hormone described in the body with this particular fatty acid group[183]. In the body, GHRL can be found in two circulating forms: the octanoylated or acylated form which is the biologically active form and the desoctanoylated or desacylated form which is the stable and predominant form of circulating GHRL.

The main secretory organ of the peptide is the stomach but other organs also contribute to its production such as lungs or colon[184,185]. The secretion of GHRL is characterized by infradian cycle with higher plasmatic peaks before each meal (**Fig. 18**)[186]. A treatment involving GHRL administration should mimic the circadian rhythm and, therefore, should be based on a chronic administration.

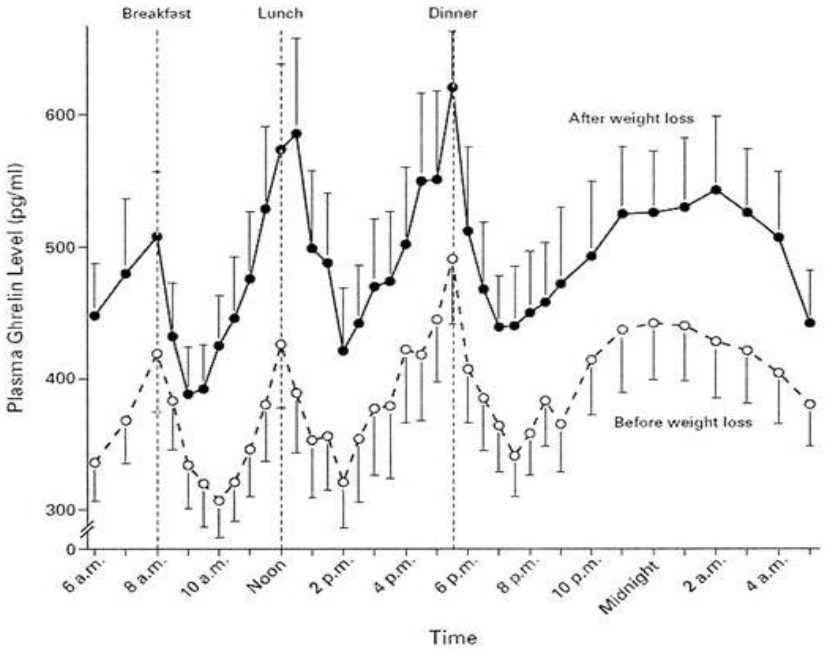

Figure 18. Mean (± standard error) 24-h plasma GHRL profiles in 13 obese subjects before and after diet-induced weight loss. Breakfast, lunch, and dinner were provided at the times indicated[187]

To promote its physiological activity in the body, GHRL needs to fix its specific receptors, the Growth Hormone Secretagogue receptors (GHSR-1a)[188].

GHSR-1 comprises 7 transmembrane units and is coupled to G-protein. It is important to notice that the structure of this receptor is conserved between species which allows certain correlations between the data collected from pre-clinical studies on animals (e.g. mice, rats) and those from humans. Following the binding of GHRL to the GHSR-1, there is a release of neuropeptide Y and Agouti-related peptide (AgRP) which have both appetite stimulating effects[189].

Therefore, GHRL administration in cachectic patients could potentially help to restore their appetite. Moreover, GHRL also possesses anti-inflammatory activity which makes its administration even more interesting. Thanks to its various physiological activities that could be beneficial for the treatment of cachexia, GHRL has been extensively studied in both animals and humans. It was shown that external delivery of GHRL, such as after intravenous administration, increased the food intake in healthy patients[190]. The usual GHRL doses intravenously administered in humans for cachexia management were in the range 2 – 8 µg/Kg once a day[191]. However, from this initial

dose, a non-negligible percentage of the peptide was rapidly metabolized in the plasma which drastically limited its effectiveness after parenteral administration[190].

8.6 Nose-to-brain delivery of ghrelin for cachexia

Considering its potential therapeutic activity as well as its physicochemical properties, the nose-to-brain delivery of GHRL could be an optimal strategy to treat cachexia.

Indeed, GHRL is a very sensitive peptide, especially in its acylated form. The acylated form has a plasmatic half life time in human of about 9 - 13 min with a degradation predominantly assumed by plasmatic butyrylcholinesterase[190,192]. This degradation being very fast, it is essential to select a route of administration with a limited metabolism (e.g. nose-to-brain pathway). However, due to the presence of enzymes in the nasal cavities, protection should be afforded to properly administer GHRL.

The second advantage of the nose-to-brain delivery of GHRL is related to the localization of the GHSR-1a receptors which are mainly localized in the arcuate nucleus of the hypothalamus. GHRL must therefore access the brain, diffuse towards the hypothalamus to fix its receptors and thus exercise its physiological activity. However, such transfer does not take place spontaneously in an efficient manner which implies to maximize the amount of drug deposited in the olfactory area while promoting the diffusion through the mucosa and, at least, increasing the contact time between the drug and the nasal mucosa.

The third benefit provided by nose-to-brain delivery of GHRL is its non-invasiveness. The objective of the treatment regimen adopted with this peptide is to recreate the daily secretion peaks found in the healthy individual (i.e. secretion before each meal) which thus requires repeated administrations. The administration should be repeated several times during the day and for several days which is quite cumbersome for an invasive administration. The nose-to-brain pathway offers an obvious increase of the patient compliance.

8.7 Cachexia treatment with other drugs

The first group of therapeutic agents acts on the stimulation of the appetite and include progesterone analogues (e.g. megestrol acetate or medroxyprogesterone) corticosteroids and cannabinoids (e.g. Delta-9-tetrahydrocannabinol) (**Tab. 3**). The second group acts by inhibiting inflammatory cytokines like TNF-α or interleukin-6[193]. This group includes, among other, ω-3 fatty acids (e.g. eicosapentaenoic acid) and thalidomide.

The last class is composed by anabolic agents that are used to enhance the muscle anabolism (e.g. fluoxymesterone or megestrol acetate).

Clinical studies have shown that the best results were usually provided with a combination of multiple pharmacological agents that have different and complementary modes of action[193].

Table 3. Summary of the main therapeutic agents used for the management of cachexia (adapted from Aoyagi et al., 2015)[194]

Name	Class	Physiological effect	Mechanism
Megestrol acetate	Derivative of progesterone	Stimulation of appetite and improvement of the nutritional status	Possible release of neuropeptide Y
Medroxyprogesterone	Derivative of progesterone	Stimulation of appetite and improvement of the nutritional status	Decrease of serotonin and inflammatory cytokines levels (Il-1, Il-6 and TNF- α)
Delta-9-tetrahydrocannabinol	Cannabinoid	Increase of the food intake and body mass	Possible activation of endorphin receptors. Inhibition of prostaglandins and Il-1
Melanocortin antagonist	Adenocorticotrop hormone antagonist	Prevention of anorexia and lean body mass losses	Neuropeptide Y alteration or melanocortin-4

			receptor antagonism
Thalidomide	Immunomodulatory	Limit weight and body mass losses	Decreases TNF-α, pro-inflammatory cytokines, nuclear factor kappa B, cyclooxygenase 2, angiogenesis
Etanercept	Immunomodulatory	Diminution of the fatigue, improves adjuvant therapy adherence	Diminish effect of TNF
Eicosapentaenoic acid	Lipid	Mixed, increase of body weight and appetite	Diminution of the inflammatory cytokines levels
Corticosteroid	Immunomodulatory	Augmentation of appetite	Various
Formoterol	Beta-2 agonist	/	Protein and muscle degradation antagonism
Erythropietin	Glycoproteic hormone	Increase of both metabolic and sportive capacity of patients	Diminution of Il-6 levels
ACE inhibitors	Heart medication	Reduction of muscle mass losses	Diminution of TNF-α levels
B-blockers	Heart medication	Preservation of the body weight, muscle and lean body mass	Akt phosphorylation

Among the various molecules tested for cachexia, anamorelin seems to be one of the most promising drugs. Anamorelin (development code name ONO-7643) is a non-peptide, orally active, selective agonist of GHRL receptors[195,196]. Anamorelin is under development by the Swiss pharmaceutical group Helsinn Healthcare SA (Lugano, Switzerland) for its application against cachexia in patients with non-small cell lung cancer (NSCLC). In 2016, they published the data collected from phase III studies with

improvements in mean body mass, body weight and appetite[195].

In May 2017, and despite these promising results obtained, the European Medicines Agency (EMA) refused twice to authorize the marketing of anamorelin. Indeed, Helsinn Healthcare SA asked for a second examination of the demand but the EMA finally concluded that the benefit - risk balance was not satisfactory (https://www.ema.europa.eu).

The data on the safety of the drug were not exhaustive enough and some parameters monitored in the patients (e.g. the hand grip strength) did not show an improvement considered sufficient.

9. Scientific strategy

9.1 Liposomes

Liposome is a widely exploited nanodelivery system that does not only improve the effectiveness of the treatment but it also helps to minimize the toxicity of certain therapeutics. Many products containing liposomes have already been marketed such as Ambisome® (Nexstar Pharmaceuticals Inc.) which contains amphotericin B-loaded liposomes for the treatment of fungal infections by intravenous administration[197]. Liposomes are characterized by a particular structure that combines an aqueous core surrounded by a lipid bilayer (**Fig. 19**). This bilayer may be composed of various lipids which may be pegylated or charged. Such characteristic allows the administration of either hydrophilic molecules, which will be encapsulated in the aqueous core, or hydrophobic molecules, which will be included in the lipid bilayer.

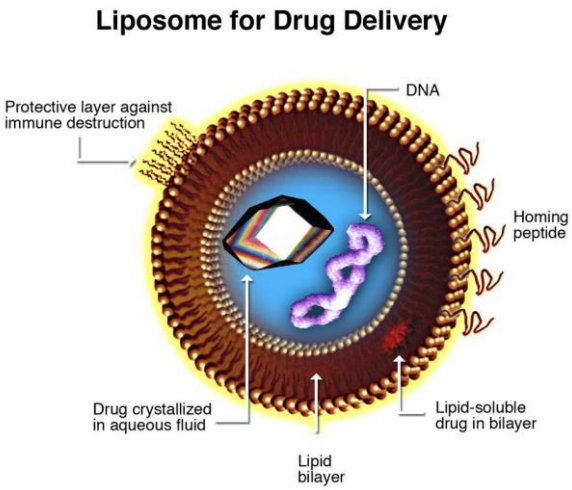

Figure 19. Liposome structure with some examples of ligands associated to their encapsulation site in liposomes according to their polarity[198]

Liposomes can be prepared in various ways, but the best-known protocol is probably the rehydration of a thin lipid film also called the “Bangham method”[199]. The lipid mixture, mostly composed of phospholipids, is dissolved in an organic phase which is then removed by evaporation. This results in a lipid film on which a well-defined aqueous medium is dropped off. A stirring step is carried out which makes it possible to disperse the lipids in the form of liposomes in the aqueous medium. This step is often performed at a temperature above the lipid transition temperature because the lipids are more flexible.

The liposomes produced with this method are called “multilamellar vesicles” (MLV) as they measure about 1 - 5 µm and they comprise several lipid bilayers. Two other categories of liposomes exist with smaller sizes and only one lipid bilayer. Unilamellar liposomes with a size in the range 100 - 250 nm are classified in the “large unilamellar vesicle” (LUV) group while liposomes measuring 50 - 100 nm are named “small unilamellar vesicles” (SUV)[199].

From the initially produced MLV with the Bangham method, it is still possible to switch to LUV or SUV by conducting an additional step of sonication or extrusion. It is even possible to obtain nano-sized liposomes.

Depending on the expected application for liposomes, the investigator may select phospholipids among a multitude of compounds available. For instance, PEGylated liposomes may increase the residence time of an encapsulated drug in the systemic

circulation while the use of phospholipids with a specific charge may enhance the yield of the encapsulation[200].

Liposomes were thus chosen as the starting point for the formulation strategy in this work. This choice was made because liposomes already shown enhancement in both diffusion and protection of peptide hormones (e.g. calcitonin or insulin) once delivered in the nose[201,202]. The choice was made on a mixture of lipids containing among other dihexadecyl phosphate (DHDP). The presence of phosphate groups in this lipid allowed conferring a negative resultant charge to the liposomes. These anionic liposomes should provide an effective encapsulation of GHRL which is positively charged. The positive charge of the peptide is attributed to the presence of cationic amino acids (**Fig. 17**) in the sequence, namely: 4 lysines, 2 arginines and 1 histidine.

Theoretically, anionic liposomes should afford both protection and penetration enhancement. However, a major parameter in nasal delivery is the mucoadhesion that helps increasing the residence time by fighting against the mucociliary clearance and, thus, enhance the drug diffusion. Moreover, the mucopenetration is another aspect that should be considered in order to strengthen the treatment efficacy. It was previously reported that the nasal delivery of nanoparticles coated with various polymer were able to improve the drug diffusion through the mucus[81]. It was thus decided to associate a mucoadhesive polymer to the liposomes by developing chitosan-coated liposomes.

9.2 Liposomes coated with chitosan

Among the various excipients that are available for the coating of liposomes, the choice was made on chitosan. As previously explained (paragraphs 1.4.2 and 1.4.3), the use of chitosans in the nasal field has been widely explored due to their very attractive properties such as biocompatibility, mucoadhesion and penetration enhancement. Indeed, they have the ability to adhere to the nasal mucosa thanks to the interaction between their positive amino groups and the sialic residues of nasal mucins. Moreover, their propensity to transiently open the epithelial tight junctions allows increasing the drug diffusion through the nasal epithelium[203].

Among the multiple chitosan types and derivatives existing, it was decided to work with N-[(2-hydroxy-3-trimethylammonium)propyl] chitosan chloride (HTCC). This trimethylated derivative offers the advantage of being soluble at physiological pH.

The coating of liposomes by HTCC takes place by an electrostatic interaction between cationic chitosans and anionic liposomes. The assembly of these two excipients thus makes it possible to produce a formulation which has the potential of being mucoadhesive, absorption enhancer and protector against enzymatic degradation.

9.3 Final form of the formulation

Firstly, the formulation will be developed as a liquid colloidal suspension. However, the liquid-state form presents a lower stability for the drug and, especially, for biopharmaceuticals like peptide hormones. This is the reason why, once the final liquid formulation obtained, the study will focus on the production of the powder-state formulation from the liquid formulation. The goal with the powder state is to achieve a higher drug stability coupled with a higher adhesion to the mucosa and a greater concentration gradient[204,205].

The mucoadhesive powder produced will be loaded in nasal devices specifically designed to maximize the amount of powder deposited in the olfactory region. This would allow the delivery of accurate doses of drug with an efficient nose-to-brain transfer.

V. AIMS OF THE WORK

Cachexia affects about 9 million people worldwide, regardless of the underlying pathology[206]. In addition to this alarming number, it is estimated that 50 - 80% of cancer patients are affected by this syndrome and 20% of the deaths in such patients could be attributed to cachexia[207].

Therefore, the development of a treatment for cachexia appears to be primordial. However, the management of the syndrome requires a multifactorial approach and, potentially, the administration of several therapeutic agents. Ideally, the treatment should not be too cumbersome since the patient is already receiving a treatment for his underlying pathology.
The nose-to-brain delivery of GHRL could meet many criterions required for such treatment. Indeed, GHRL may provide beneficial effects on appetite as well as on inflammatory state. Intranasal administration being non-invasive and quite simple to implement, may be considered as an ideal route of administration.

The objective of this work was to develop an effective formulation for the nose-to-brain delivery of GHRL. Such effectiveness included enzymatic protection, mucosal adhesion, enhanced epithelial penetration and, finally, high peptide stability during storage. It was also necessary to reach the deposition of a significant amount of drug on the olfactory mucosa. Finally, it has to be shown that the peptide should efficiently reach the brain following a nasal administration.

The first part of the study focused on both the pre-formulation studies and the liquid formulation development. The pre-formulation part focused on GHRL characterization and the evaluation of its physicochemical properties. By performing a detailed characterization of the drug (e.g. stability evaluation, charge measurements, etc.), it should have been easier to formulate the drug. This part of the project also included the selection of the formulation strategy for the liquid-state formulation. GHRL being a cationic peptide on which a fatty acid group is grafted; the formulation strategy could involve ionic and/or hydrophobic interactions between the drug and the excipients. A first strategy involving pegylated phospholipids was envisaged. This first strategy was complemented with a second and alternative strategy involving coated liposomes was considered. This second liquid formulation system was based on anionic liposomes coated with cationic chitosan. Numerous characterization methods have been used to demonstrate the interest of these formulations in the context of intranasal administration, namely: exposure to enzymatic digestion, adhesion to mucins, permeation through epithelial layer and finally, evaluation of aerosol properties for

nasal delivery. Once the data collected for liquid formulations, the project continued with the production of a dry powder formulation.

The second step of the project was thus the development and the evaluation of a dry powder formulation. The purpose was to get higher drug stability during storage, stronger adhesion to the mucosa and increased drug diffusion through the nasal barrier. Therefore, the liquid formulation previously developed was spray-dried with the aim of combining a high yield of production with a suitable particle size that allowed intranasal deposition. Physicochemical properties of this dry formulation were compared to those of the liquid formulation to highlight the benefits provided by the powdered state formulation. The objective was also to achieve a large deposition in the olfactory region of the nose by using a nasal device specifically designed to target this anatomical region.

In the third part of the manuscript, *in vivo* evaluations have been performed with the liquid formulation. The aim was to confirm that GHRL could reach the brain after intranasal administration of the formulation as well as to compare its diffusion with raw GHRL.

VI.EXPERIMENTAL PART

1. Results Part I: Pre-formulation and development of a ghrelin-loaded liquid formulation for nose-to-brain delivery

1.1 Introduction

To our knowledge, only a few studies has been focussed on the development of GHRL-based formulations[208]. The intravenous route, which is rather cumbersome for chronic administration,[209] is currently the most exploited for GHRL administration[210] while the intranasal delivery is very rarely considered. However, a first study recently published has been focused on the nasal administration of a vaccine containing GHRL-antigen for the management of obesity[211]. Other studies focused on chemical modifications of the peptide chain or on the use of GHS-R agonists (e.g. anamorelin) to get a better bioavailability and/or stability compared to physiological GHRL[212,213]. Therefore, the development of a formulation containing GHRL for nose-to-brain delivery would be a real innovation that could lead to a new therapeutic alternative for patients with cancer cachexia.

Especially when considering the administration of biotherapeutics, formulation appears to be essential (e.g. to protect the drug from enzymatic degradation). However, due to the lack of stability usually encountered with biotherapeutics, their formulation appears to be challenging. Therefore, before carrying out the formulation development, pre-formulation studies need to be performed to characterize the physicochemical properties of the peptide. For instance, the stability of the drug under various conditions (i.e. specific pH's and temperatures) should be evaluated.

Then, a formulation strategy had to be selected on basis of the GHRL properties but also and especially according to the properties required to obtain an effective nasal drug. Among them the main ones are: the mucoadhesion to increase the persistence of the formulation in the nasal cavity, the increase of the transnasal permeability of the drug and, finally, the protection of the peptide with respect to the enzymatic digestions[60]. At first, it was decided to develop a liquid formulation in order to easily screen various excipients and, subsequently, select the most promising ones. On the basis of this liquid formulation, we can subsequently adapt it or use it as a basis for the production of a nasal powder, for example. The formulation envisaged have all involved the use of lipid based excipients. The presence of the fatty acid chain on GHRL's peptide core could be a good way to promote interactions with such excipients and thus to obtain a satisfactory drug loading in the formulation. Another selection

criterion for excipients was their prior use in the context of nasal formulation development. Indeed, the goal was to work with excipients that already exhibited good compatibility with the nasal mucosa. This way, it is possible to move quickly towards more advanced development stages. Two relevant examples can be given with pegylated phospholipids and chitosans that have been both widely assessed for nasal delivery with encouraging findings[214,215].

Therefore, the first formulation that was developed in this work involved the use of pegylated phospholipids (DPSE-PEG 2000) and the incorporation of GHRL into DPSE-PEG micelles. These PEG-grafted lipids have a propensity to self-assemble once put in aqueous medium which results in the production of liposomes, bicelles or micelles depending on the lipids mixture used, for example[216]. The development of such polymeric micelles was considered to enhance the mucopenetration of the drug in the nasal mucus[81].

The second type of formulation was based on the development of anionic liposomes (AL) coated with chitosan derivatives. Liposomes have been considerably evaluated for nasal delivery especially due to their biocompatibility and their ability to entrap a wide variety of drugs[217]. Liposomes were combined to chitosan which provides both mucoadhesive and permeation enhancing properties to the formulation. It is produced by deacetylation of chitin which results in a polymer chain constituted by glucosamine and N-acetylglucosamine residues attached by β (1→4) glycosidic linkages[218]. Both formulations were characterized in terms of entrapment efficiency, Zeta potential, size distribution and permeation through Calu-3 cell layers.

Based on the first evaluations, the characterization of liposomal formulation was more deeply investigated as it appeared to be the most promising strategy.

The following properties were evaluated:

- The influence of the liposomes charge on the ability of the formulation to entrap GHRL and to protect it against the activity of nasal enzymes;

- The capacity of the formulation to fix mucins as it is considered as a relevant indicator of its ability to prolong the residence time in the nasal cavity;

- The comprehension of the interaction mechanisms involved in the formulation between excipients and GHRL;

- The influence of the formulation on the drug diffusion through a model of epithelial tissue (Calu-3 monolayer);

- The characterization (i.e. droplet size distribution) of the aerosols generated from two nasal devices loaded with the liquid formulation and their comparison

A part of these results are published in the following article: “Salade, L. *et al.* Development of coated liposomes loaded with ghrelin for nose-to-brain delivery for the treatment of cachexia. *Int. J. Nanomedicine* **12,** (2017).

1.2 Materials and methods

1.2.1 Materials

Synthetic human octanoylated (1–28 amino-acid sequence, purity 98%) GHRL was purchased from Scipeptide (Shanghai, China). Acetonitrile, methanol, trifluoroacetic acid (TFA), dichloromethane (all solvents high-performance liquid chromatography [HPLC] grade), dihexadecyl phosphate (DHDP; purity 98%), human isoform B carboxylesterase 1 (Ces1; activity ≥ 500 units/mg protein), cholesterol (purity ≥ 99%) and mucin type 1S were obtained from Sigma-Aldrich (St Louis, MO, USA). Minimal essential medium nonessential amino acids (MEM NEAAs), gentamicin 50 mg/mL, sodium pyruvate 100 mM, heat-inactivated FBS, l-glutamine 200 mM, 0.25% trypsin (Tryp)–EDTA phenol red, Hank’s balanced salt solution (HBSS) and penicillin–streptomycin were obtained from Thermo Fisher Scientific (Waltham, MA, USA). 1,2-distearoyl-*sn*-glycero-3-phosphoethanolamine-N-[carboxy(polyethylene glycol)-2000 (DSPE-PEG 2000), soybean phosphatidylcholine (Lipoid S100) and 1,2-dioleoyl-3-trimethylammonium-propane (DOTAP; chloride salt) were purchased from Lipoid GmbH (Ludwigshafen, Germany). N-([2-hydroxy-3-trimethylammonium] propyl) chitosan chloride (HTCC) with 92 kDa molecular weight, deacetylation of 80%, and substitution of 33% was purchased from KitoZyme (Herstal, Belgium).

1.2.2 Evaluation of GHRL stability

GHRL (1 mg/mL) solutions in PBS pH 7.4 (PureLab system; Elga LabWater, High Wycombe, UK) were exposed to the following temperatures: 4°C, 25°C, 37°C, and 60°C. The effects of different pH levels were also studied (i.e. 3 → 8, T°= 25°C). The

buffers were selected according to the requirements of the European Pharmacopoeia eighth edition (PBS pH 3, acetate buffer pH 4.5, PBS pH 5, PBS pH 6, PBS pH 7.4, boric acid buffer pH 8). Then, 500 µL samples were sampled after defined periods of time (0.5, 1, 2, 3, 4, 5, 6, 24, and 48 hours) to evaluate the GHRL degradation kinetic using a suitable HPLC/ultraviolet (UV) method[219].

1.2.3 HPLC/UV method for GHRL quantification

The HPLC method adapted from the literature[219] used a TSKgel ODS-120T 150×4.6 mm, 5 µm particle column coupled with a TSKgel ODS-120T 3.2×1.5 cm (Tosoh Bioscience, Tokyo, Japan) guard gel. The column was kept at 37°C. The mobile phase was a mixture of Milli-Q water–TFA 0.1% v:v (phase A) and acetonitrile–TFA 0.1% v:v (phase B). The mobile-phase gradient used was linear, from 12% (0 minutes) to 52% (32 minutes) in phase B. The wavelength was fixed at 210 nm, and the flow rate was set at 1 mL/min. The lower limit of quantification was 5 µg/mL. The HPLC system used was 1100 series from Agilent (Santa Clara, CA, USA). The retention times for octanoylated and desoctanoylated GHRL were 18 and 9 minutes, respectively.

1.2.4 Preparation of DSPE-PEG micelles

A GHRL solution was prepared by dissolving an appropriate amount of GHRL in ultrapure water to reach a concentration of 1 mg/mL. DSPE-PEG was dissolved in ultrapure water to produce a 6 mg/mL stock solution.

An equal volume of each stock solution was mixed together under gentle agitation to allow the production of micelles with a homogeneous distribution (final concentrations: GHRL = 0.5 mg/mL, DSPE-PEG = 3 mg/mL).

A second protocol was established with the addition of sodium chloride (NaCl) at a concentration of 0.9% w/v to decrease the critical micelle concentration (CMC) of DSPE-PEG.

1.2.5 Preparation of liposomes and HTCC-coated liposomes

The second formulation strategy involved the development of anionic, cationic and neutral liposomes which were coated with HTCC polymer.

The protocol that was used to prepare these liposomes was based on the method developed by Bangham *et al.* which involved the rehydration of a lipid film[220]. Briefly, it

was based on the dissolution of the lipid mixture in organic solvents which led to a clear solution. The organic solvents were removed using a rotary evaporator to produce a thin lipid film in the round-bottom flask. Then, an aqueous medium was poured in the flask which was heated up to a temperature higher than the lipid phase transition temperature. The association of both mixing and heating allowed the spontaneous formation of the liposomes. At the end of this rehydration step, the mixture could be exposed to a downsizing procedure (e.g. sonication or extrusion) to produce nanoliposomes characterized by a narrow size distribution.

Three lipid mixtures were selected to obtain neutral (NL), anionic (AL) or cationic (CL) liposomes (**Tab. 4**). The aim was to assess the effect of the charge on the formulation properties with GHRL. Briefly, 100 mg of lipid mixture were introduced into a 50-mL round-bottomed flask. Neutral liposomes (NL) were obtained using a mixture of neutral lipids, composed of CHOL and LS100 50/50% (w/w). Replacing 10% w/w of neutral lipids with DHDP or DOTAP allowed the formation of AL or CL, respectively. Then, 10 mL of an organic solvent mixture (dichloromethane/methanol 50/50% (v/v)) were added to obtain a final lipid concentration of 10 mg/mL. The organic phase was evaporated using a Rotavapor® R-205 rotary evaporator (Büchi, Flawil, Switzerland) at 60°C. The pressure was set at 250 mmHg for 10 minutes and at 150 mmHg for the next 10 minutes. The lipid film was then rehydrated at 30°C for 1 hour with 10 mL of PBS pH 7.4, which contained GHRL (1 mg/mL). Before extrusion, the large multilamellar vesicles (LMV) suspension was briefly sonicated by means of a VCX 500 probe sonicator (VibraCell, Sonics & Materials Inc., Newton, USA) for 30 seconds at 30% of amplitude. The sonication provided a first downsizing step. The LMV were extruded through a LiposoFast® LF-50 extruder (Avestin, Ottawa, Canada) to produce large unilamellar vesicles (LUV). The extrusion process was carried out through polycarbonate membranes characterized by porosities of 1 µm, 0.4 µm and 0.1 µm (EMD Millipore, MA, USA).

Table 4. Lipid compositions (% m/m) selected for liposomes preparation

Lipid percentages (% m/m)				
Formulations	**Lipoid® S100**	**Cholesterol**	**DHDP**	**DOTAP**
NL	50	50	0	0
CL	45	45	0	10
AL	45	45	10	0

In addition to the uncoated liposomes previously described, another formulation involving the coating of AL with HTCC (HTCC-AL) was developed. For this purpose, a suitable amount of HTCC was weighed and dispersed under magnetic stirring in PBS pH 7.4 overnight to obtain a final solution ([HTCC]= 10 mg/mL) that was translucent and homogenous. Then, 9 mL of AL (10 mg/mL) were coated with 1 mL of HTCC (10 mg/mL) which was added dropwise under magnetic stirring at 3 000 rpm to obtain a 10-fold dilution of the initial HTCC solution ($[HTCC]_{final}$=1 mg/mL). The dispersion of coated-liposomes was left for 1 hour under magnetic stirring at room temperature before being left overnight at 4°C.

1.2.6 Evaluation of size, zeta potential and encapsulation efficiency

Both Z-average and zeta potential of DSPE-PEG micelles, AL, NL, CL and HTCC-AL loaded or not with GHRL (1 mg/mL) were evaluated in triplicate at 25°C, with 1 min of equilibration time and without dilution. Evaluations were done using dynamic light scattering and electrophoretic mobility for size and zeta potential, respectively (Zetasizer Nano ZS®, Malvern Ltd., Malvern, England). Size measurements were performed in PBS pH 7.4 with semi-micro disposable cuvettes in polystyrene (Brand Gmbh + Co. Kg., Wertheim, Germany) and results were expressed in terms of Z-average (mean ± standard deviation (S.D)) and polydispersity index (PDI). Disposable folded capillary cells were used for zeta potential evaluation that were performed in PBS pH 7.4 and results were expressed in terms of mean ± S.D.

To determine the yield of encapsulation, all formulations were centrifuged at 13,500 rpm through Amicon® Ultra-15 centrifugal tubes with a 100 kDa cut off (Merck Millipore (Darmstadt, Germany)) for 30 minutes at 25°C. Prior to formulation characterization, a PBS pH 7.4 solution of raw GHRL was centrifuged to confirm the non-adsorption of the

peptide on the filter. The total amount of GHRL, namely "$GHRL_{total}$", that was incorporated in the initial formulation was determined by HPLC. Following the solubilisation of either micelles or liposomes (that was confirmed by dynamic light scattering) in the mobile phase, GHRL could be released for quantification. The encapsulation efficiency (EE) of GHRL in DSPE-PEG micelles, AL, NL and CL was determined indirectly by quantifying GHRL in the filtrate and using the following equation:

$$EE\ (\%) = \left(\frac{[GHRL_{total}]-[GHRL_{Filtrate}])}{GHRL_{total}} \times 100\right) \qquad (1)$$

The tests were performed in triplicate and percentages were expressed as mean ± standard deviation (S.D).

1.2.7 Permeation through Calu-3 monolayer

Frozen Calu-3 cells obtained from ATCC (Manassas, USA) were used at passages 15-20. The culture medium that was used was MEM NEAA with 1 mL of gentamycin (50 mg/mL), 5 mL of sodium pyruvate (100 mM), 50 mL of heat-activated foetal bovine serum, 5 mL of L-glutamine (200 mM) and 5 mL of Pen Strep (10,000 U/mL). The medium was renewed every couple of days. The cells were subcultured with a dilution factor of 1:3 from flask to flask. Cells were maintained at 37°C and 5% CO_2.
Inserts that were used to establish the air–liquid interface culture were composed of HA mixed ester cellulose membrane with a porosity of 0.45 µm and a surface of 4.2 cm^2 adapted for 6-well plates (Merck Millipore, Billerica, Massachusetts). For inoculation in inserts, Calu-3 cells from confluent T-75 flasks were detached by means of a TRYP 0.25% (w/v) solution and suspended in 12 mL of thawed culture medium. To the apical side of each insert, 2 mL of cell suspension were added to get a fully-filled 6-well plate of inserts ($5x10^5$ cells / cm^2). The basal side was filled with 2 mL of thawed MEM NEAA medium. The apical compartment was emptied 24 hours after inoculation and the basal side medium renewed to allow the growth and the polarization of the cells under the air-liquid interface.

The transepithelial electrical resistance (TEER) was followed during the cell experiments by means of an epithelial Volt/Ohm meter EVOM2® (Wold Precision

Instruments, Sarasota, USA). TEER measurements reflect the cell monolayer integrity. Values were expressed after subtracting the value of the blank insert and normalized for surface area (4.2 cm^2). For TEER routine evaluations, 2 mL of fresh medium were added on both the apical and the basal sides. Cells were allowed to equilibrate for 30 minutes prior to taking measurements. A polarized monolayer was obtained approximately 10 days after inoculation with usual TEER values in the range 300-600 $\Omega.cm^2$ for Calu-3 cells.

Before performing permeation tests, GHRL solutions were added in empty inserts to confirm that GHRL did not adhere to the insert's components. Before adding the solutions or formulations of interest into the apical compartment, the monolayer was washed twice with HBSS pH 7.4. Then, 2 mL of HBSS pH 7.4 were added to both apical and basal side. Cells were allowed equilibrating for 30 minutes. TEER was measured and HBSS pH 7.4 from the apical side was replaced with the formulation or solution of interest. Each formulation or solution was introduced in three different inserts to perform the test in triplicate. The compounds of interest were allowed to diffuse for 3 hours and the TEER was followed at specific times during the experiments (i.e. at 30, 90, 150 and 180 min) and 24 hours after the end of the test to assess the recovery of the cells. After the 3 hours of diffusion, 500 µL of apical and basal medium each were sampled and quantified.

Depending on the purpose of the tests, the following solutions / formulations were tested: GHRL solution (1 mg/mL), unacylated GHRL solution (1 mg/mL), DSPE-PEG micelles ([GHRL] = 0.5 mg/mL, [DSPE-PEG] = 3 mg/mL) caffeine solution ([CAF]=1 mg/mL), salmon calcitonin ([CAL]=1 mg/mL), HTCC-AL ([HTCC=1 mg/mL, [GHRL]=1 mg/mL, [AL]=10 mg/mL). CAF,[221] CAL[222] and GHRL[219] were quantified using suitable HPLC/UV methods.

1.2.8 Enzymatic protection after trypsin and carboxylesterase-1 exposure

Both raw GHRL in solution and GHRL-loaded (1 mg/mL) liposomes ([AL], [NL] and [CL] = 10 mg/mL) were exposed to trypsin (TRYP) solution (140 IU/mL) for 15 minutes at 37°C after dispersion using a vortex mixer (Vortex Genius 3, IKA, Staufen, Germany). Enzymatic digestion was stopped by the addition of 100 µL of TFA (10% v/v). $GHRL_{total}$ was determined in the initial liposome suspensions using HPLC. The mobile phase that contained acetonitrile allowed the solubilization of liposomes and the release of GHRL for the quantification of $GHRL_{total}$. The remaining amount of non-

degraded GHRL was determined by withdrawing 500 µL of the solution for HPLC quantification. The percentage of GHRL protected by liposomes was determined as follows:

$$\% \, GHRL_{protected} = \frac{GHRL_{non\ degraded}}{GHRL_{total}} \times 100 \qquad (2)$$

In order to evaluate the type of interaction between GHRL and AL (e.g. adsorption or incorporation), the lipid film rehydration protocol was used and GHRL (1 mg/mL) was added during the rehydration or after the rehydration step ("post-formation method"). If the rehydration method allowed GHRL to access the AL internal aqueous compartment, it would be less impacted by enzymatic digestion than AL produced by the post-formation method. Indeed, GHRL could have more difficultly accessing the AL internal aqueous compartment and only be adsorbed at the exterior of liposomes when added after AL formation. Both formulations were exposed to TRYP degradation for 15 minutes at 37°C. The remaining quantity of GHRL was determined using the HPLC/UV method.

After this, AL were exposed to a second enzyme: the human carboxylesterase isoform 1-B (124 IU/mL, PBS pH 7.4, for 15 minutes at 37°C). The effective protection of loaded GHRL was determined using the same protocol than that used for TRYP. The remaining amount of GHRL was determined by withdrawing 500 µL of the suspension for HPLC/UV analysis and using equation (2). All experiments were repeated in triplicate and expressed as the mean ± S.D.

1.2.9 Isothermal Titration Calorimetry

From this step, all experiments were performed with HTCC-AL only. In order to study the interaction between GHRL and AL, isothermal titration calorimetry (ITC) experiments were performed as previously described[223]. All measurements were performed at 25°C using a VP-ITC (MicroCal, Northampton, MA) with a sample cell volume of 1.4565 mL. Solutions were degassed in a sonic bath for 10 minutes prior use. A 300 µl-syringe was filled with AL suspension (10 mg/mL) PBS, pH 7.4 without GHRL (empty-AL). The reference cell was filled with milli-Q water. For the blank and

the sample, the measuring cell was loaded with PBS pH 7.4 and with a 1 mg/mL GHRL solution in PBS pH 7.4, respectively. The measuring cell was magnetically stirred at 300 rpm during the experiments. The titration experiments were performed by consecutive injections of 10 µL of empty-AL (10 mg/mL) into GHRL solution (1 mg/mL). Each injection lasted 14.5 seconds. A delay of 600 seconds between each injection was applied until a steady state was reached. The resulting heat flows were recorded and raw data were processed using the software provided by the manufacturer (ORIGIN 7 e Originlab, Northampton, USA).

The ITC raw data were processed according to the cumulative model previously described[224] and applied to other molecules than GHRL[223,225] to obtain the thermodynamic parameters characteristic of the interaction of GHRL/empty-AL. The thermodynamic parameters considered were: the binding coefficient (K), the variation of Gibbs Free Energy (ΔG), of enthalpy (ΔH) and of entropy (-TΔS). If the GHRL/empty-AL interaction is spontaneous, the ΔG should be negative. The titration was repeated twice and expressed as the mean value.

1.2.10 Transmission Electron Microscopy

For transmission electron microscopy (TEM) analysis, 20 µl of AL and HTCC-AL were deposited on formvar–carbon coated electron microscopy grids. Then, 1-2 µl of glutaraldehyde 25% (v/v) were added to fix the liposomes. The preparation was left overnight at 4°C. The grids were transferred onto a drop of distilled water for washing and left for 2 minutes (3 times). For contrasting and embedding, the grids were placed onto a drop of methylcellulose-uranyl acetate (ratio 9/1 m/m) mixture for 10 minutes on an ice bath. The grids were removed and the excess fluid was blotted by gently pushing the loop sideways on filter paper. A thin film was left over the section side of the grids. Observations were performed using an FEI Tecnai 10 electron microscope (Fei, Hillsboro, Oregon, USA) operating at an accelerating voltage of 100 kV. The images were analysed and processed using iTEM analysis (Olympus Soft Imaging Solution, Münster, Germany).

1.2.11 Evaluation of osmolality and determination of mucoadhesion

The osmolality was determined in triplicate by means of an Osmomat® 3000 (Gonotec, Berlin, Germany) using a volume of 50 µL of AL or HTCC-AL. The instrument used the freezing point to evaluate the osmolality.

For assessing the mucoadhesion, a colorimetric method was used to determine the residual amount of free mucins that were not precipitated due to complexation with the formulation[226]. The test involved the use of periodic acid which, thanks to its oxidizing nature, made it possible to break the covalent bond between two hydroxyl functions. This allowed releasing aldehyde functions at the level of mucins which could subsequently interact with fuchsine by reducing it and, thus, led to the appearance of the purple coloration. A defined volume of 2 mL of HTCC-AL or AL was added to 6 mL of mucin solutions (0.5 mg/mL). The preparation was left for 20 min (a period similar to the muco-ciliary clearance time[227]) at 37°C and centrifuged at 3000 g for 4 min. Then, 2 mL of supernatant were withdrawn to determine the amount of free mucin. The percentage of mucins fixed by the formulation was indirectly determined by subtracting the quantity of unfixed mucins in the supernatant from the initial quantity of mucin (0.5 mg/mL) and expressed as a percentage:

$$\% \text{ of mucins fixed} = \frac{(Q_{\text{total mucins}} - Q_{\text{mucins in supernatant}})}{Q_{\text{total mucins}}} \times 100 \qquad (3)$$

The test was performed in triplicate and results expressed as mean ± S.D.

1.2.12 Droplet Size Distribution

The size distribution of the droplets generated from nasal devices was evaluated by laser diffraction using a Spraytec® apparatus (Malvern, Worcestershire, UK). Liquid multi-dose spray pumps VP3 were kindly provided by Aptar® Pharma (Le Vaudreuil, France). The VP3 device is presented as offering a high dose accuracy (volume delivered = 93 µL per spray) even with viscosity changes that could be encountered with HTCC. The device is also suitable for suspensions and viscous formulations. The results generated with this device were compared to those collected from another standard device SP270 (Nemera, formerly known as “Rexam Pharma”, La Verpillière, France). Before each evaluation, nasal devices were manually shaken and the first five doses generated were wasted to initiate the device. The Spraytec® parameters were fixed, with a test duration of 3000 ms, a data acquisition rate of 1000 Hz and a transmittance of 96%. Measurements were performed at room temperature and expressed in terms of median volume diameter (Dv50), mean volume diameter (Dv4,3) and percentage of the volume distribution smaller than 10 µm (% < 10µm).

1.3 Results and discussion

1.3.1 Physicochemical characterization of GHRL

1.3.1.1. Evaluation of GHRL stability

As a thorough knowledge of the drug is essential during the development of new therapeutics, it was decided to perform pre-formulation studies. This is even more relevant given the relatively small number of studies involved in the physicochemical characterization of this peptide.

Due to the potential instability of the ester bond which links the acyl chain to the core of the peptide (**Fig. 17**), the very first parameter assessed was the stability of acylated GHRL under specific conditions. Moreover, it has to be noticed that this octanoyl group is essential to allow GHRL to bind to its specific receptors GHSR-1A[228]. The first five amino acid residues on the N-term side are also required for activating its signalling pathway[229].

Therefore, GHRL in solution was exposed to various temperatures for several time of contact: at 4, 25, 37 and 60°C during 24, 48 and 72 hours (**Fig. 20**). The objective was to evaluate their influence on the chemical stability of GHRL. Indeed, such information may be relevant when establishing a protocol of formulation which includes thermal process vs. time.

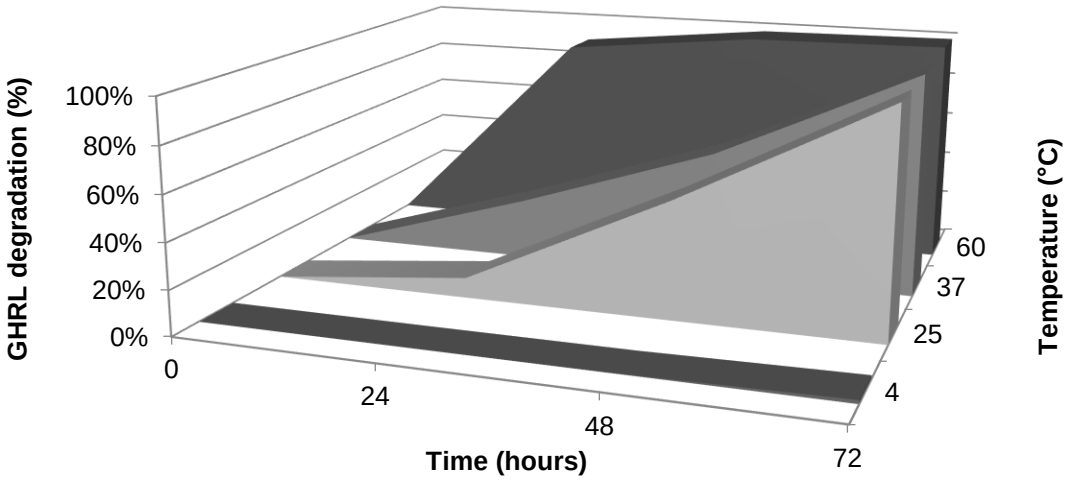

Figure 20. Degradation of acylated GHRL (%) after exposure to various temperatures ([GHRL] = 1 mg/mL, n = 3, PBS pH = 7.4)

As it can be seen on the degradation profiles, storing GHRL at 4°C allows avoiding the degradation of the peptide for at least 72h. At 25°C, the degradation of GHRL sharply increased after 24h which suggested that GHRL solutions could not be stored at ambient temperature for more than a day.

At 37°C (e.g. body temperature), 27% of GHRL were degraded after 24 hours. This degradation was higher at 60°C with 90% of GHRL degraded within a day. This highlighted the GHRL sensitivity and the challenge of working with such unstable biotherapeutics. Formulation processes involving prolonged heating should therefore be avoided. In conclusion, GHRL solutions at physiological pH should ideally be stored in refrigerated conditions (≤ 4°C).

After that, the degradation of GHRL was evaluated in function of the pH. Indeed, as liposomes are produced after rehydration of the lipid film with a buffer, the pH could greatly influence the stability of GHRL during its formulation. Therefore, GHRL was dissolved in buffers ranging from pH 3.0 to 8.0 and stored at 25°C for 24 hours (**Fig. 21**).

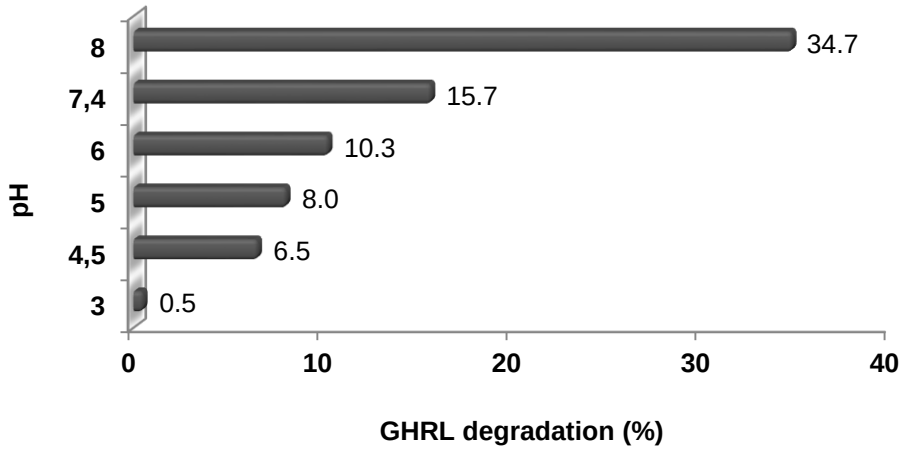

Figure 21. Degradation of acylated GHRL (%) after exposure to various pH (exposure period: 24 hours, T° = 25 °C)

It was shown that the degradation of GHRL proportionally increased with the pH. Indeed, the highest stability of the peptide was obtained at pH 3.0. This observation is similar to that of a study describing the best conditions for GHRL blood samples storage[230]. In acidic conditions, the stability of GHRL ester bond with the octanoyl group is increased and the risk of degradation by hydrolysis is greatly reduced.

In conclusion, the best conditions to store GHRL solutions are acidic pH (pH 3 - 4) at low temperature (≤ 4°C)[230]. For long-term storage (> 2 - 3 days), GHRL solutions can be frozen without degradation but repeated freeze and thaw cycles should be avoided as they induced GHRL degradations[231].

1.3.1.2. Determination of the GHRL surface charge

The charge of free GHRL was assessed as it is a very relevant parameter to take into consideration as it can influence the choice of the formulation strategy. For instance, electrostatic interactions between the drug and excipient can strongly increase the ratio of drug encapsulated in the formulation[232]. In addition, the evaluation of the zeta potential can provide a better understanding of the repulsion/attraction phenomena that can take place in a formulation. Indeed, the zeta potential is a measure of particle charge through the surrounding ions in a liquid[233]. The conventional method for measuring zeta potential is to expose the liquid sample to an electric field, and to measure the speed of movement of the particles under the effect of the electric field. The migration of a particle is directly proportional to its zeta potential and its charge.

This phenomenon is called electrophoretic mobility. When looking at GHRL's structure, the presence of three arginine and four lysine residues would theoretically afford a positive resultant charge to the peptide at physiological pH (**Fig. 17**).

The evaluation of the zeta potential of raw GHRL in PBS pH 7.4 has shown that the peptide exhibited a cationic charge of + 5.3 mV. Therefore, this may suggest that a negatively charged excipient could promote the encapsulation of the peptide in liposomes due to electrostatic interactions.

1.3.1.3. Influence of acylation on GHRL permeation

Then, the effect of the acylated chain on peptide's permeation was assessed. Indeed, it was already reported that the grafting of fatty acid chains on peptide cores (e.g. calcitonin)[234] could provide improvement in its diffusion.

Calu-3 cell line was selected to perform the permeation evaluation. Calu-3 cells are isolated from lung adenocarcinoma and differentiate in a mixed phenotype of both ciliated and mucus-secreting cells. Therefore, Calu-3 monolayer exhibits morphological similarities (i.e. mucus production, presence of cilia and tight junctions) with the nasal tissue[235]. It is important to notice that other alternatives to Calu-3 could have been considered. The first alternative was the use of animal nasal mucosa, but due to the numerous potential issues that could be encountered with such model (e.g. complex dissection of the mucosa of interest, establishment of an ethical protocol to collect the tissue from slaughterhouse, etc.), this option was rejected. Another possibility was the use of primary nasal cells. However, several limitations may be encountered with such model too with, for example, a limited number of passages or the possible microbiological contamination of the tissue. Finally, the last option was the use of another immortalized cell line, called "RPMI 2650 cells". Even if this is the only existing human nasal cell line, it is characterized by a major drawback which is the non-monolayer growth. Therefore, these cells are more frequently used for metabolic purposes than for permeation studies[236].

Calu-3 cells were grown under air-liquid interface (ALI) which means that, similarly to the respiratory tract, the cells were in contact with the culture medium on their basal side while the apical side was exposed to the external environment (**Fig. 22**). Such culture configuration allowed the polarization of the cells.

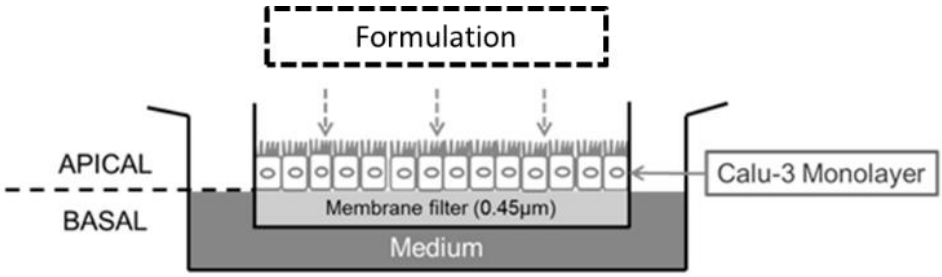

Figure 22. Illustration of the air-liquid interface for Calu-3 cell culture

GHRL permeation were compared between either its acylated or unacylated forms through Calu-3 cells. The production of desacylated GHRL was confirmed by HPLC following the peptide exposure at 60°C for 5 hours (data not shown). After spreading GHRL solutions on the apical side, the basal medium was withdrawn to quantify the amount of GHRL that diffused after 2 and 4 hours.

The desacylated form did not show any GHRL permeation through the cell layer. In contrast, the presence of the fatty acid chain has slightly increased GHRL diffusion as it was shown that 3.4% and 3.7% of GHRL were recovered in the basal medium after 2 and 4 hours, respectively (**Tab. 5**).

The effect of a peptide acylation on its permeation was attributed by other researchers to the increased interaction with lipid membranes of cells[237]. After these pre-formulation evaluations, the first trails of formulation were performed.

Table 5. Diffusion of both desacylated and acylated forms of GHRL in the basal medium after diffusion through Calu-3 cells (t=2 and 4 hours, n = 3)

Time (hours)	GHRL diffusion (%)	
	Desacylated GHRL	**Acylated GHRL**
2	0	3.4 ± 0.8
4	0	3.7 ± 0.9

1.3.2 Development of DSPE-PEG micelles

The first formulation system was based on the formation of polymeric micelles. Such nanosystems have been of great interest due to their attractive specificities, namely: biocompatibility and lower clearance rate[238]. Once in contact with an aqueous medium,

the DSPE-PEG amphiphilic structure with the polymer grafted on phospholipids allows the spontaneous arrangement in polymeric micelles[239]. Thanks to the presence of saturated acyl chains in their structure (**Fig. 23**), DSPE-PEG exhibit intense hydrophobic forces which results in a low CMC (approximately 1 x 10^{-6} M)[240,241].

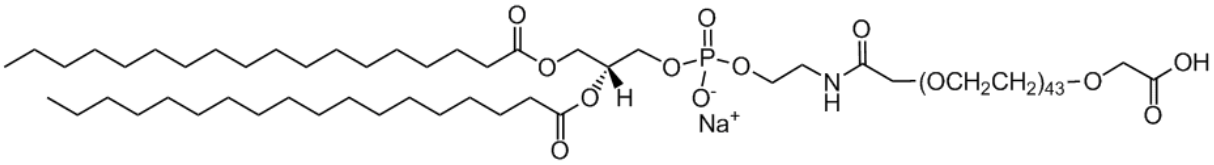

Figure 23. Chemical structure of 1,2-distearoyl-*sn*-glycero-3-phosphoethanolamine-N-[carboxy(polyethylene glycol)-2000 (www.avantilipids.com)

The internal compartment contains DSPE chains which are more hydrophobic and allow the encapsulation of lipophilic drugs. The outside layer contains the hydrophilic polymer (i.e. PEG) that provides a steric hindrance and prevents any risk of micelles aggregation. Moreover, the external PEG layer helps increasing the formulation diffusion through the nasal mucus by avoiding interactions with mucins[81]. This was confirmed by experimental evaluations reporting both higher nasal accumulation and mucopenetration with PEG-coated nanoparticles[242,243]. Therefore, DSPE-PEG micelles could be an attractive strategy to deliver GHRL as it could provide an efficient drug encapsulation coupled with an enhanced mucus penetration. The common size obtained with such polymeric micelles is usually ranged between 10 and 100 nm.

1.3.2.1. Size evaluation of DSPE-PEG micelles

At the experimental level, the first important parameter to control is the ability to produce micelles by spontaneous formation in an aqueous medium. By performing size measurement, we can first confirm that micelles have been produced and this in the size range targeted (10 - 100 nm) and with a narrow size distribution. To do this, dynamic light scattering experiments were performed (**Fig. 24**).

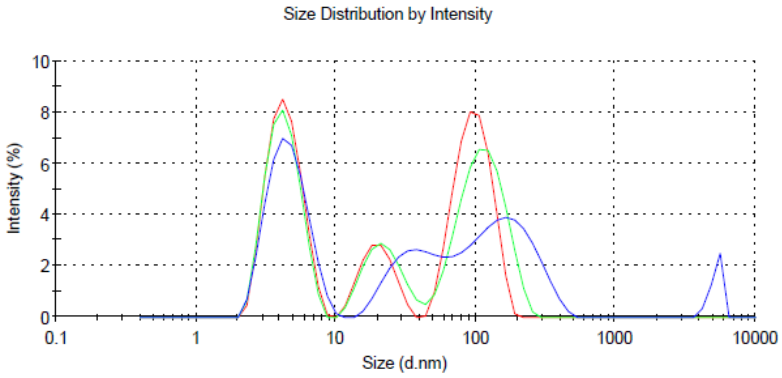

Figure 24. Size distribution expressed in intensity obtained with DSPE-PEG micelles loaded with GHRL without NaCl (individual size distribution curves, n = 3)

As it can be seen (**Fig. 24**), the use of DSPE-PEG did not allow the formation of micelles characterized by a monomodal size distribution. Indeed, the distribution was multimodal and highly dispersed (PDI = 0.409) and the repeatability between each measurement was very low. The distribution peaks at 15 and 100 nm correspond to lipid agglomerates that did not integrate into a micelle structure. It could be hypothesized that, as the CMC of DSPE-PEG was reported to be 10 times higher in water than in water containing various electrolytes (i.e. buffers with boric acid), the formation of well-structured micelles was limited. Indeed, when electrolytes are added in solution they cause the dehydration of the surfactant which decreases its solubility and therefore its CMC[244].

This is the reason why sodium chloride ([NaCl] = 0.9% w/v) was added in the second protocol. As NaCl addition could lower the CMC, it could make the micelle formation easier. Indeed, it can be seen on the size distribution (**Fig. 25**) that micelles adopted a monomodal size distribution, with a higher stability and repeatability between every measure when NaCl was added.

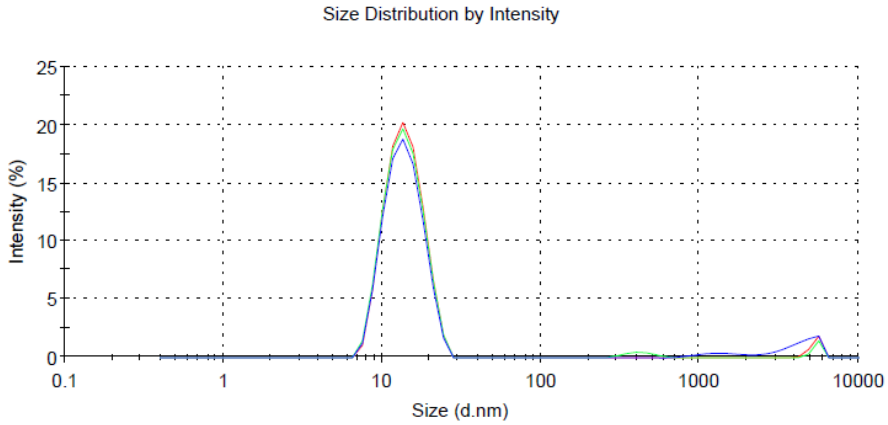

Figure 25. Size distribution expressed in intensity of DSPE-PEG micelles loaded with GHRL after NaCl addition (n = 3)

The Z-average diameter was 14.93 nm, which was in accordance with the data already published[245]. Moreover, the low polydispersity index obtained (PDI=0.277) was adapted for such nanosystems even if a PDI lower or equal to 0.2 would have be better. Indeed, this parameter represents the width of the size distribution. Due to its low value, it can be confirmed that the nanoparticles size range was properly controlled, without the presence of micelle aggregates.

1.3.2.2. Determination of the encapsulation efficiency and permeation through Calu-3 cells

The method selected for EE measurement was based on the use of ultrafiltration process. The formulation was placed on a filtration membrane which allowed free GHRL to diffuse but not DSPE-PEG micelles. Once the ultrafiltration step was completed, the filtrate was recovered for GHRL quantification. The difference between the initial amount of peptide in the whole formulation and the amount recovered in the filtrate allowed calculating the amount of GHRL retained on the filter and that incorporated in micelles.

A very efficient GHRL loading in DSPE-PEG micelles could be reached with an EE of 98%. This very high EE can be explained by the strong interactions between the DSPE-based micelles and the octanoic acid group present on GHRL peptide core.

The ability of GHRL-loaded DSPE-PEG micelles to increase cell permeation of the peptide was evaluated through Calu-3 cells. The diffusion of unformulated raw GHRL was compared to our formulation which was supposed to increase the amount of GHRL in the basal side.

Unfortunately, it appeared that the GHRL permeation was similar between GHRL solution and DSPE-PEG micelles (data not shown). DSPE-PEG did not provide any improvement regarding GHRL diffusion through the epithelial layer. Similar observation was observed in a previous study which evaluated the diffusion of coated-pegylated nanoparticles through porcine olfactory mucosa. It could be highlighted that pegylated nanoparticles deeply penetrated into the mucus but without any diffusion through the tissue[98].

Therefore, the development of DSPE-PEG micelles was aborted. Indeed, by considering the ability of the nose to rapidly clear the formulation thanks to the synergic effect of the muco-ciliary clearance and enzymatic digestion, the drug has to diffuse rapidly and efficiently through nasal epithelium. Moreover, it is usually considered that an absorption enhancing effect is needed when the drug nasally delivered is characterized by a molecular weight larger than 1000 Da. The molecular weight of GHRL being 3370 Da, it is essential to make the nasal barrier more permeable to the peptide. Without providing any permeation improvement, the potential of this formulation to be an effective treatment would already be strongly compromised.

Due to this unexpected issue, a second type of formulation had to be considered. Still considering the amphiphilic nature of GHRL and its positive net charge, negatively charged liposomes (AL) were selected to be a potential alternative strategy. Indeed, AL could involve both hydrophobic and ionic interactions with GHRL leading to a high EE. Subsequently, AL were coated with HTCC to confer additional properties to the formulation (i.e. mucoadhesion and permeation enhancing effect).

1.3.3 Development of chitosan-coated liposomes

The second liquid formulation developed was based on nanostructured lipid carriers, called liposomes. They were selected due to their effectiveness for nose-to-brain administration as well as for their protective effects against enzymatic degradation[101,103]. Moreover, such lipid-based systems exhibit low toxicity, high stability and are also able to entrap both hydrophilic and lipophilic drugs. Due to the nature of the lipids, they also have the capacity to diffuse through the BBB[246]. This property may be very interesting if a part of the formulation is not directly transferred from the nose to the brain but rather borrows the systemic pathway. In addition to these benefits, it has been decided to coat liposomes with chitosan to increase their mucoadhesion and to enhance their penetration through the mucus. Similarly to

liposomes, chitosan-based formulations have been deeply studied in the context of the nasal delivery[247–249].

The influence of the charge of the liposomes on GHRL interactions was evaluated. To this purpose, liposomes formulations exhibiting different charges (e.g. neutral, negative, and positive) were characterized in terms of size and zeta potential. Then, the EE was determined for each formulation.

1.3.3.1. Size distribution, zeta potential and encapsulation efficiency

All liposome suspensions without GHRL were in the nanosize range with z-averages of 130.2 ± 1.3 nm, 143 ± 2.2 nm and 137.3 ± 3.6 nm for AL, NL and CL, respectively (**Tab. 6**). The liposomes size distributions were characterized by a low PDI, corresponding to a narrow and monomodal size distribution. The z-average of all empty liposomes increased by 10-15 nm after loading with GHRL. This slight increase still reflected an interaction with GHRL, this could even be driven by hydrophobic interaction between the octanoyl chain of acylated GHRL and the liposome bilayer or either by electrostatic interactions between cationic GHRL and anionic liposomes.

Such scale is essential when developing nose-to-brain formulations. Indeed, it was demonstrated that fluorescently labelled nanoemulsions could reach the brain of rats after nasal administration when the Z-average diameter of the nanoemulsion was around 100 nm[250]. When nanoemulsions in a larger size range were developed (Z-average = 900 nm), the transport of nanoparticles towards the brain could not be observed. Other studies reported an efficient nose-to-brain transport with nanoparticles characterized by a maximal Z-average of 200 nm[21,95,251]. Nevertheless, these studies were performed in rodents (mainly in rats) and the morphological specificities, such as the neuronal diameter, may strongly vary from one species to another (e.g. between rats and humans). Morphological evaluation even reported an olfactory neuronal diameter of 100 – 200 nm in murine species while, in humans, this diameter was ranged between 100 and 700 nm, which suggests the possible nose-to-brain transfer of slightly larger nanoparticles[42,252].

Table 6. Z-average, PDI, zeta potential and EE as a percentage of liposome formulations, with GHRL and lipid concentrations of 1 mg/mL and 10 mg/mL, respectively (PBS pH 7.4, n = 3, mean ± S.D)

Formulations	Z-average (nm) (PDI)		Zeta potential (mV)		EE (%)
	Empty	GHRL	Empty	GHRL	GHRL
AL	130.2 ± 1.3 (0.098)	146.9 ± 2.7 (0.105)	-14.0 ± 0.7	-0.3 ± 1.2	56.1 ± 7.8
NL	143 ± 2.2 (0.105)	152.9 ± 4.8 (0.094)	+0.5 ± 0.4	+4.1 ± 1.4	21.3 ± 4.1
CL	137.3 ± 3.6 (0.082)	151 ± 3.9 (0.062)	+13.5 ± 1.5	+18.9 ± 3.1	9.8 ± 3.7

In addition to the increase of the Z-average, the zeta potential also increased when GHRL was incorporated. At pH 7.4, GHRL is positively charged as its isoelectric point is at 11.5[253]. This could explain why the highest increase was observed with AL (+13.7 mV). Indeed, a lower increase of the zeta potential was observed with the other formulations, probably due to the absence of electrostatic attraction between cationic GHRL and NL or CL. The positive evolution of the zeta potential before and after addition of GHRL to AL rather suggested that GHRL was imbricated at the surface of the lipid bilayer. Regarding the values of zeta potential for empty liposomes, an almost neutral charge (+0.5 ± 0.4 mV) could be observed for empty-NL, whereas negative (-14.0 ± 0.7 mV) and positive (+13.5 ± 1.5 mV) charges were obtained for empty-AL and empty-CL (**Tab. 6**). The modulation of the charge was made possible by replacing 10% (w/w) of neutral lipids (CHOL and Lipoid® S100) with DHDP or DOTAP (**Tab. 6**). The negative charge of DHDP is conferred by the phosphate group and was used to produce AL, while the ammonium residue afforded a positive charge to DOTAP and was incorporated into the CL (**Fig. 26**).

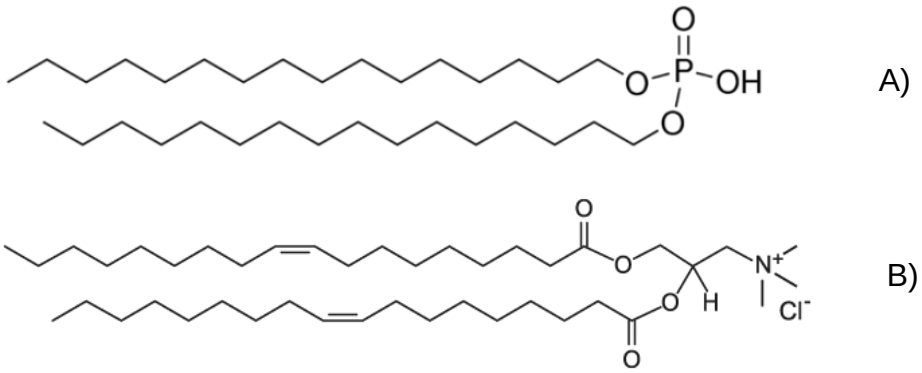

Figure 26. Chemical structures of DHDP (A) and DOTAP (B) (http://avantilipids.com)

As it is usually observed when formulating charged peptides in liposomes, both hydrophobic and electrostatic interactions are involved[254,255]. However, when evaluating the EE, it can be seen that electrostatic interactions had a non-negligible influence in the case of GHRL[256]. By providing a negative charge to AL, the percentage of GHRL loaded in AL was 5-fold higher compared to CL (**Tab. 6**). This resulted in an EE of 56.1 ± 7.8%, 21.3 ± 4.1% and 9.8 ± 3.7% for AL, NL and CL, respectively. Otherwise, when evaluating the EE's thanks to the increases of the zeta potential when GHRL was added to empty-NL and empty-CL, it could be observed that NL presented an almost doubled EE in comparison with CL (21.3 ± 4.1% versus 9.8 ± 3.7%, respectively), while the increase of the charge from NL was lower than that from CL (+3.6 mV versus +5.4 mV). The higher EE coupled with the lower increase of charge from NL suggested that a part of GHRL loaded was internalized in the structure of the liposomes. The general trend followed by the Z-average, zeta potential and EE suggested that the theoretical GHRL/AL interaction would be more pronounced than for the other formulations.

1.3.3.2. Enzymatic protection after trypsin exposure

All liposome formulations having been characterized in terms of size, zeta potential and EE, the benefits of using liposomes to protect GHRL from enzymatic degradation was evaluated. Indeed, in addition to absorption enhancement and mucoadhesion, enzymatic protection was defined as a mandatory property that should be provided by GHRL delivery system.

Table 7. All liposome formulations (AL, NL and CL) were exposed to TRYP, an endoprotease that cleaves peptide bonds between basic amino acids such as lysine or arginine and other residues. As GHRL contains seven lysine/arginine residues in its primary structure, the peptide is very sensitive to TRYP activity. Free GHRL in solution

was used as a reference due to its rapid and complete digestion by TRYP within 15 min of incubation at 37°C (data not shown). This time lapse of 15 minutes has been selected to be closer to the conventional nasal persistence time limited by the effect of mucociliary clearance.Percentage of enzymatic protection for GHRL in the presence of TRYP (140 IU/mL, 15 min, 37°C, n = 3) for the GHRL (1 mg/mL) loaded liposomes (AL, NL and CL) in PBS pH 7.4

Formulation	Enzymatic protection (%)
AL	20.6 ± 4.2
NL	10.2 ± 2.9
CL	5.6 ± 1.4

It was demonstrated that the protection afforded by the liposomes to GHRL degradation increased when their ionic charge became anionic (AL) (**Tab. 7**). This trend may be explained by higher EE (**Tab. 6**) obtained with AL in comparison with CL and NL. When the EE was increased, a lower amount of GHRL was potentially exposed for enzymatic degradation. The protection reached 20.6 ± 4.2% for AL compared to 10.2 ± 2.9% for NL and 5.6 ± 1.4% for CL. As it can be seen, TRYP led to a consequent degradation of GHRL, even when it was encapsulated into the liposomes. This can be explained by the potential adsorption of GHRL at the surface of the liposomes instead of its incorporation into the bilayered structure. As a consequence, most of the sites of cleavage of TRYP remained outside the liposomes and were free to interact with the enzyme. These results supported the fact that electrostatic attractions between AL and GHRL resulted in an increase in both loading and protection, while electrostatic repulsions with CL decreased them. With CL, GHRL was most probably located at the liposomes' surface rather than encapsulated in it which lead to higher drug degradation after TRYP exposure. Overall, it should be mentioned that the protection percentage previously discussed were underestimated. Indeed, all liposome formulations were not purified which meant that, for example, in AL formulation, 43.9% of GHRL were not encapsulated. This meant that 43.9% of GHRL were not protected and directly exposed to TRYP degradation. Therefore, the percentage of protection that was mentioned (20.6 ± 4.2%) should be compared to the EE which should result in even more satisfactory results in terms of enzyme protection.

In the nasal cavity, numerous enzymes such as the CYP450 family, flavin-containing monooxoygenase, aldehyde dehydrogenases, epoxyde hydrolase, carboxyl esterase and phase-II enzymes can be found[257]. Moreover, olfactory epithelium appears to have an intense metabolic activity[258] and it is reported that CYP-450 activity could be even higher than in the liver[22]. For instance, it is described that peptide hormones, such as insulin, could be rapidly metabolized after nasal delivery[227]. These observations usually justify the use of enzyme inhibitors in formulations used for nasal drug delivery and, more particularly, when the olfactory region is targeted. Indeed, it was demonstrated that the amounts of salmon calcitonin quantified after permeation through rat nasal mucosa were found to be higher when TRYP inhibitors were added to the formulation[259]. Therefore, it is relevant to develop a formulation that could both enhance nasal permeation and provide effective protection against enzymatic degradation, especially for biotherapeutics. In order to protect GHRL effectively, it therefore seems necessary to encapsulate it in the liposome structure rather than to graft it on the outer surface.

Therefore, the next step was the evaluation of the amount of GHRL that was effectively encapsulated inside the liposomes instead of being adsorbed at their surface. Therefore, the degradation of GHRL was evaluated after the use of the conventional protocol of rehydration of the lipid film, where GHRL was added during the formation of AL in PBS pH 7.4, but also after a second method where GHRL was allowed to diffuse in already-formed AL (i.e. the post-formation method). Both formulations were exposed to TRYP for 15 minutes at 37°C. Using the post-formation method, GHRL could only be fixed onto the outer side of the liposomes, with the octanoyl group embedded in the lipid bilayer and the peptide body exposed to the external environment. In contrast, using the rehydration method, the GHRL peptide body should access the internal aqueous cavity of the lipid structure in addition to the adsorption effect, resulting in higher protection. It can be observed that the protection obtained from the rehydration method (24.0 ± 3.7%) was clearly higher than that from the post-formation protocol (0%) (**Tab. 8**).

Table 8. Comparison of the protection between two different preparation methods for AL (film rehydration and post-formation methods)

Preparation method	**Enzymatic protection (%)**
Rehydration method (AL)	24.0 ± 3.7
Post-formation method (AL)	0

This suggested that with the rehydration method, some of the encapsulated GHRL could be incorporated inside the liposomes. On the other hand, GHRL added by post-formation cannot reach the internal aqueous cavity or the hydrophobic bi-layer and was therefore more exposed to TRYP. This configuration, as well as the need of TRYP to access the main peptide body for digestion, would explain the complete degradation of GHRL when the post-formation method was used.

1.3.3.3. Enzymatic protection to carboxylesterase-1 activity

Based on the positive results previously obtained, further experiments were essentially conducted with AL. It was decided to work with human carboxylesterase-1 (CES-1) as an additional enzyme that targets another location of the peptide. As the nasal enzymatic activity of carboxylesterase is not exactly known[260], the concentration of CES-1 was fixed when the degradation of free GHRL was observable after 15 minutes (a period of time equivalent to the mucociliary clearance[227], which could theoretically correspond to the time spent by GHRL in the nasal cavity). CES-1 is strongly present in the nasal cavity on both ciliated and non-ciliated respiratory epithelium but also in the olfactory area in Bowman's gland of the *lamina propria* and the sustentacular cells of the epithelial barrier[261]. Carboxylesterases are usually found in the cytoplasma and endoplasmic reticulum of cells in a wide variety of tissues. Carboxylesterase are involved in many reactions of activation (e.g. pro-drugs) or inactivation of acylated substrates (e.g. methylphenidate) in the body[262]. CES-1 types are responsible for the hydrolysis of both ester- and amide-bond containing drugs. They also hydrolyse long-chain fatty acid esters and thioesters such as the octanoyl group of GHRL. Since the presence of the octanoyl chain was shown to be essential to preserving the physiological activity of GHRL, it seemed necessary to demonstrate the ability of anionic liposomes to preserve the integrity of the octanoyl group of GHRL from the activity of CES-1.

It can be observed that the protection obtained with AL was 4.7-fold higher (81.6%) than with raw GHRL in solution (17.2%) (**Tab. 9**). The degradation observed from GHRL-loaded AL upon contact with CES-1 was lower than that found under TRYP exposure (79.4% with TRYP and 18.4% with CES-1).

Table 9. Enzymatic protection of GHRL in solution and GHRL-loaded AL after CES-1 exposure [CES1] = 124 UI/mL, t = 15 min, t° = 37°C, pH 7.4, n = 3, mean ± S.D)

	Protection (%)
Raw GHRL in solution	17.2 ± 4.9
GHRL-loaded AL	81.6 ± 8.9

CES-1 selectively hydrolyses the ester bond between the main peptide body and the octanoyl chain.[263] This chain is most probably inserted inside the bilayer of the liposomes, as previously hypothesized (**Fig. 27**). This configuration could make the ester bond less accessible to CES-1 due to steric hindrance, while TRYP could more easily attack the hydrophilic body and thus induce a higher degradation.

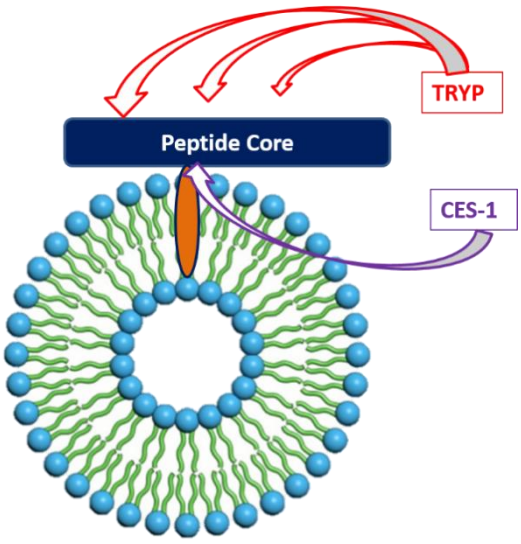

Figure 27. Enzymatic digestion mechanisms of TRYP and CES-1 on GHRL once loaded in AL

Regarding overall enzymatic degradation, AL showed very interesting results which could make the administration of this type of unstable peptide possible and compatible

with the conditions encountered in the human nasal cavity (e.g. presence of various enzymes such as aldehyde dehydrogenase, cytochrome P-450 dependent monooxygenase and carboxylesterase[258]).

1.3.3.4. Isothermal Titration Calorimetry

Isothermal titration calorimetry (ITC) has become a method of choice when interactions between two entities (e.g. drug and excipients) should be characterized. This technique is very sensitive and easy to implement. It provides the experimenter detailed information about the nature of the interaction but also about its spontaneous character. Thermodynamic parameters such as enthalpies of reaction can subsequently be determined. Moreover, the technique does not need any modification of the sample analysed (e.g. by fluorescent labelling)[264].

The measure is based on the recording of heat flows that appears when two selected molecules are put in contact. The instrument consists of two cells (a reference and a sample) that must be kept rigorously at the same temperature. AL aliquots are gradually added to GHRL in the sample cell and the heat flows at each addition are recorded by the microcalorimeter. Then, the system equilibrates to reach the initial temperature again.

As a potential GHRL/AL interaction was suggested by size and zeta potentials data, ITC has been selected to collect additional information on the binding of GHRL to empty-AL. The binding coefficients as well as the heat flow collected should be useful for a better understanding of GHRL-AL interaction.

The decrease of the exothermic signal in the ITC profile after each injection of AL (**Fig. 28**) showed that the amount of GHRL available for binding to empty-AL decreased after each addition of liposomes. This confirmed that GHRL was progressively bound onto the surface of unloaded AL.

Table 10. Binding coefficient (K), Gibbs Free Energy (ΔG), enthalpy (ΔH) and entropy (-TΔS) resulting from ITC analysis with empty-AL (10 mg/mL) and GHRL (1 mg/mL), n=2, T=26°C, PBS buffer pH 7.4, mean ± S.D)

	K (mM^{-1})	**ΔG (Kcal/mol)**	**ΔH (Kcal/mol)**	**-TΔS (Kcal/mol)**
Mean	0.875 ± 0.135	-6.4 ± 0.09	-0.09 ± 0.01	-6.315 ± 0.105

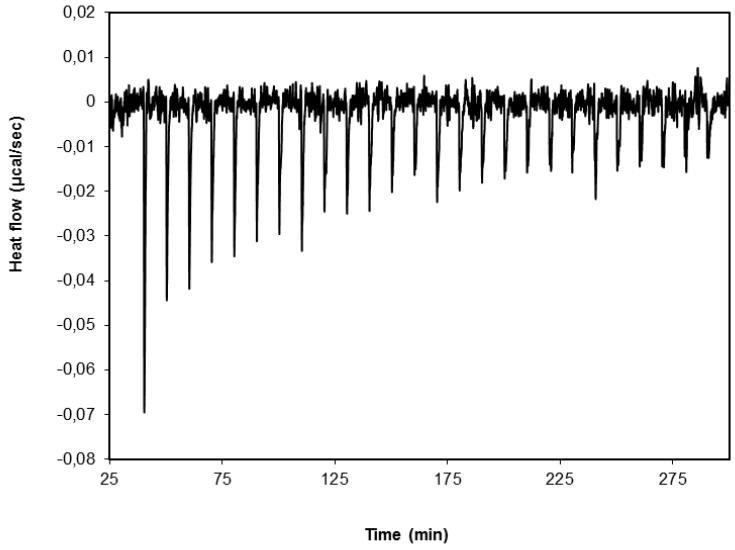

Figure 28. Heat flows observed by ITC after each addition of empty-AL (10 mg/mL) in GHRL (0.33 mg/mL) versus time (PBS pH 7.4, T = 26°C)

The negative value (**Tab. 10**) observed for the Gibbs Free Energy (ΔG) with the GHRL/ empty-AL interaction revealed the favourable and spontaneous nature of the interaction. Moreover, the absolute variation of entropy (-TΔS) was higher than the absolute variation of enthalpy (ΔH), which suggested that the interactions involved were mainly driven by hydrophobic affinities[265]. However, as it was previously observed, the charge modulation clearly impacted the encapsulation efficiency, which suggested a strong influence of the charge on the GHRL/empty-AL interaction.

The interaction between GHRL and empty-AL could take place in two different ways. A first hypothetical GHRL localization could include the body of the peptide inside of the liposomes' internal hydrophilic cavity while the octanoyl chain would be inserted into the hydrophobic liposome bilayer. In such a case, GHRL should pass through the liposome bilayer to reach the hydrophilic cavity. This passage would probably not be energetically favourable and thus not in accordance with ITC results.

The second localization would be quite similar, except that the body of GHRL would be present at the external part of the liposomal structure. In both theoretical localizations, the octanoyl fatty acid group is inserted in the lipid structure. This interaction is already described in other studies[255,256] and is shown to provide a

significant protection to the octanoyl group, which is essential for preserving the physiological activity of GHRL[266].

1.3.3.5. Characterization of liposomes coated with chitosan

It was previously shown that GHRL could interact with AL which improved the protection of the peptide. However, the residence time as well as the absorption in the nasal cavity of the liposomes also needed to be optimized. Chitosan derivatives have been well-studied for various administration routes, including intranasal administration. They offer several advantages such as mucoadhesion properties and their ability to open the tight junctions (TJ)[215]. To combine the beneficial effects of chitosan derivatives and liposomes, it was decided to coat anionic liposomes with HTCC. As it was shown in paragraph 1.3.3.1, the zeta potential of liposomes remained negative after GHRL incorporation. Therefore, it was theoretically possible to associate them to cationic chitosan. HTCC derivative was selected as it is soluble at physiological pH (pH of the nasal cavity: 6.3). The nasal administration of peptide with such formulation strategies has already shown interesting properties (also with other administration routes)[267,268].

Table 11. Comparison of the Z-average, PDI and zeta potential between empty-AL, AL and HTCC-AL ([HTCC]= 1 mg/mL, [AL]= 10 mg/mL, [GHRL]= 1 mg/mL) formulations (n = 3, mean ± S.D, T° = 25°C, PBS pH 7.4)

	Empty-AL	**AL**	**HTCC-AL**
Z-average (nm ± S.D) (PDI)	131.0 ± 3.9 (0.104)	147.3 ± 4.3 (0.119)	194.0 ± 6.1 (0.198)
Zeta potential (mV ± S.D)	-14.0 ± 1.2	-0.6 ± 0.3	+6.0 ± 0.4

The HTCC concentration range used after dilution in the AL suspensions for the coating was fixed between 1 mg/mL and 5 mg/mL[269]. Higher HTCC concentrations (>1 mg/mL) did not provide satisfactory results with a PDI larger than 0.198 (data not shown). It is usually considered that a PDI larger than 0.2 reflects a non-monomodal size distribution. The coating of AL with 1 mg/mL HTCC was then performed and showed a large increase of the Z-average (+48 nm) in comparison with uncoated AL

(**Tab. 11**). The zeta potential of cationic GHRL involved a switch from -14 mV to -0.6 mV before and after the addition of GHRL to AL, respectively. As the resultant charge remained almost neutral or slightly anionic (-0.6 mV), the coating with cationic HTCC was possible thanks to electrostatic attraction. Once AL was coated with HTCC, the resultant charge was positive (+6 mV).

The HTCC concentration of 1 mg/mL was selected for further characterization since the Z-average and PDI were satisfactory (PDI = 0.198) with a monomodal size distribution.

To visualize the morphology and confirm the size of both AL and HTCC-AL, TEM analyses were performed.

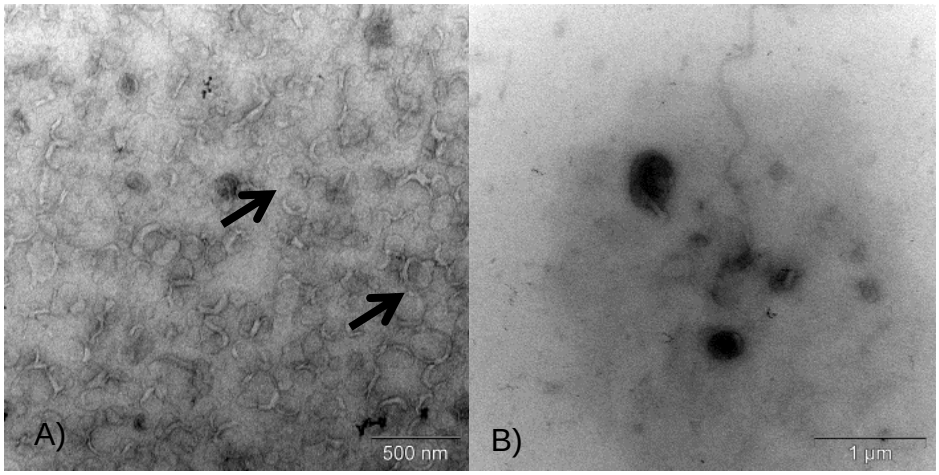

Figure 29. TEM pictures obtained with AL (A) and HTCC-AL (B)

The TEM pictures (**Fig. 29**) confirmed the “large unilamellar vesicle” structure of liposomes, with a Z-average larger than 100 nm and a single lipid bilayer. Once the liposomes were coated with HTCC, it can be seen that liposomes became black due to the polymer coated onto them. The sizes observed by TEM imagery for AL were comparable with the Z-average values obtained by dynamic light scattering, which were 147.3 ± 4.3 nm. For HTCC-AL, the size range observed on TEM pictures was a bit larger than those collected by dynamic light scattering (194 ± 6.1 nm). The experimental protocol used to prepare the samples and TEM analysis may be responsible of this gap between both size measurement techniques. The protocol imposing specific treatments to the sample (e.g. drying step), this could have an influence on the behaviour of HTCC in the coating and cause a size increase.

1.3.3.6. Permeation studies, mucoadhesion and osmolality

Chitosan derivatives are known to provide mucoadhesion as well as to allow opening the TJs. This action on TJs was assessed using the Calu-3 cell line. Calu-3 are epithelial cells isolated from lung adenocarcinoma. They may be used to evaluate both permeability and potential toxicity of nasal drug delivery sytems[248,270]. The use of lung cells to evaluate the response of nasal epithelial cells to a drug is explained by the multiple similarities between Calu-3 and nasal mucosa. Indeed, Calu-3 are characterized by mucus production, the presence of TJs and cilia. These characteristics justify the use of such cells for permeation studies of formulations intended for nasal delivery[271,272]. Specific cell culture conditions, under an air-liquid interface, induce the polarization of the cells, similarly to the physiological conditions that may be found in the respiratory tract.

The cellular transport of GHRL through the BBB has already been studied[273]. It was observed that the transport of GHRL towards the brain involved a saturable system therefore limiting the flow of GHRL entering the brain. The nose-to-brain delivery could therefore bypass this saturable transport but no data are available regarding GHRL's nose-to-brain transfer. As GHRL's transport is assumed to be paracellular, such as most of peptides[274], the addition of HTCC in the formulation could be justified by its ability to open TJs[215].

Table 12. Distribution of GHRL, calcitonin and caffeine solutions at a concentration of 1 mg/mL, with or without HTCC (1 mg/mL) and with respect to apical and basal compartments of inserts (n=3, mean ± S.D, t=3 hours, T°=37°C, HBSS pH 7.4)

Formulations	Apical (%)	Basal (%)
GHRL	100.0 ± 1.3	0
GHRL+HTCC 1 mg/mL	91.8 ± 5.5	8.2 ± 0.97
CAF	64.4 ± 3.42	35.5 ± 2.90
CAF+HTCC 1 mg/mL	66.9 ± 0.30	33.0 ±1.92

CAL	100.0 ± 6.11	0
CAL+HTCC 1 mg/mL	97.1 ± 0.06	2.9 ± 0.22

GHRL permeation was compared with that of salmon calcitonin (CAL). As it is well-known that paracellular transport of molecules is limited by their molecular weight, CAL was selected as a positive control model of peptide as it is characterized by a molecular weight close to that of GHRL (3,454.9 Da and 3,370.9 Da for CAL and GHRL, respectively) and a paracellular transport[275]. Caffeine (CAF) was also used as a positive control model of transcellular transport as it is characterized by a small molecular weight (194.19 Da)[276]. Both compounds are physiologically active in the brain.[277,278] Regardless of the molecule, the passage was evaluated with and without the addition of HTCC (1 mg/mL). The impact of HTCC on the permeation was assessed due its enhancing effect on the permeation of peptide through nasal mucosal layers[247,279]. All the compounds were dissolved in PBS buffer pH 7.4 prior uses. The degree of substitution of the HTCC was 33% to minimize potential cytotoxicity[280]. If GHRL crosses a Calu-3 monolayer using paracellular transport, the diffusion should be higher when HTCC was added (similarly to CAL).

It was demonstrated that the addition of HTCC increased the cell permeation of both CAL and GHRL up to 2.9 and 8.2%, (**Tab. 12**). In general, it is considered that peptides and proteins exhibit a low nasal permeation (1 %) due to their hydrophilic nature which made the results of cell's diffusion here rather satisfactory[163]. The higher permeation that was observed with the use of GHRL could be explained by its amphiphilic nature which could make its transfer easier than that of CAL. The GHRL diffusion (8.2 %) represented a GHRL amount of 164 µg that diffused in the Calu-3 basal compartment from the initial dose (100% = 2 mg) on the basal side. Taking into consideration the ranges of doses that are usually administered in humans by IV (2 – 7 µg/Kg), 164 µg would suit for the management of cachexia by nose-to-brain delivery.

Globally, it could be concluded that the addition of HTCC to CAL and GHRL induced a permeation increase via a paracellular transport. This observation can be supported by the evaluation of the TEER values (**Fig. 30**). These were reduced when HTCC was used, confirming the TJs' opening. Indeed, the integrity of the epithelium may be indirectly evaluated through the evaluation of the TEER. This is the electrical

resistance between the apical and basal compartments and is calculated using the following equation[281]:

$$TEER\ (\Omega * cm^2) = Resistance\ (\Omega)\ x\ Effective\ membrane\ area\ (cm^2) \quad (5)$$

This technique is non-destructive and allows measuring in real time the effect of a formulation on the cell layer. TEER was even used to confirm the reversibility of the TJ's opening and this was confirmed 24 hours after putting the formulation in contact with Calu-3 cells (e.g. 1398 ± 15 Ω.cm²). However, due to the chronic administration that would be required with such treatment in cachectic patients, the recovery of the TJ's opening should be assessed after a shorter delay (e.g. 2 hours). In contrast, CAF showed an overall cell permeation through the Calu-3 monolayer higher than those observed with CAL and GHRL due to its low molecular weight which allowed a transcellular transport. Indeed, its permeation was not influenced by the addition of HTCC (**Tab. 12**). Moreover, the CAF transport could already be saturated which could explain the absence of HTCC influence with regards to its permeation.

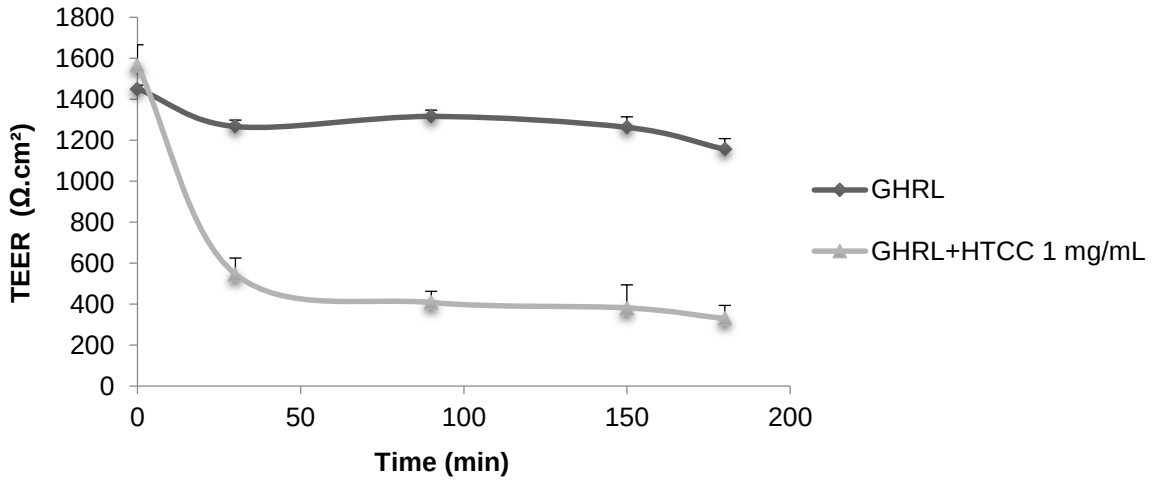

Figure 30. Evolution of TEER (expressed for inserts of 4.2 cm²) versus time for inserts containing GHRL in solution before and after HTCC addition (1 mg/mL)

The GHRL diffusion increased via a paracellular transfer being confirmed, it was decided to evaluate the potential benefit of anionic liposomes, coated with HTCC (HTCC-AL).

Table 13. Mean values of osmolality, mucoadhesion and percentage in the basal side after permeation through Calu-3 cells for both AL and HTCC-AL (pH 7.4, n = 3, mean ± S.D)

Formulations	Osmolality (mOsm/Kg ± S.D)	Mucoadhesion (% ± S.D)	Basal (% ± S.D)
AL	405 ± 4	39.8 ± 4.7	3.6 ± 0.25
HTCC-AL	409 ± 2	62.7 ± 5.6	10.8 ± 0.71
GHRL solution	-	-	0

To demonstrate the interest of coating liposomes with HTCC, the adhesion to mucins was evaluated for AL and HTCC-AL. Indeed, mucins are the most represented glycoproteins in the nasal mucus (2–5%)[282]. They contain sulphate and sialic acids, which confer a negative resultant charge on the mucus surface[283]. Moreover, they are characterized by a pKa of 2.6 which allow them to be fully ionized at physiological pH[284]. The adhesion of the formulation to mucins is essential to avoid rapid mucus clearance of the liposomes in the nasal cavity and to prolong the time of diffusion to the brain[285]. Both formulations showed the ability to complex mucins, with 39.8% and 62.7% adhesion for AL and HTCC-AL, respectively (**Tab. 13**). The coating with HTCC and the positive charge of the amino groups allowed electrostatic interactions with negative sialic acid of mucins. This led to a 22.9% increase in bioadhesion. This interaction with mucins could extend the residence time of the formulation in the nasal cavity and thus would optimize its transfer to the brain.

Before proceeding to permeation tests on Calu-3 cells, the osmolality of both coated and non-coated formulations was assessed. It is known that a liquid formulation intended for nasal delivery should be close to, or even slightly higher, than 290 mOsm/Kg and less than 500 mOsm/kg.[286] Hypertonic formulations can be used occasionally, while isotonic solutions are suited for chronic use. Hypotonic formulations should be avoided. For AL and HTCC-AL, the values obtained were quite close, at 405 and 409 mOsm/Kg, respectively (**Tab. 13**). These values respect the physiological conditions of the nasal cavity.

After this, the permeation of GHRL (1 mg/mL) in AL and in HTCC-AL was assessed. HTCC-AL (10.8%) provided a very limited improvement of permeation compared to HTCC in solution (8.2%, **Tab. 12**). Indeed, GHRL-loaded AL which were coated with HTCC seemed to enhance the transport of the peptide compared to a solution of raw HTCC and GHRL. Moreover, HTCC-AL showed enhanced permeation compared to AL (10.8 ± 0.71 versus 3.6 ± 0.25% for HTCC-AL and AL, respectively). It appears that the coating of AL with HTCC had a positive effect on their permeation in contrast with AL without coating. AL only offered a slight increase of permeation in comparison with raw GHRL in solution (3.6 ± 0.25% versus 0% for AL and GHRL in solution, respectively). This suggested that their major interest lied rather in the enzymatic protection. Finally, a 10-fold increase was obtained with HTCC-AL in comparison with raw GHRL in solution (10.8 ± 0.71% versus 0% for HTCC-AL and GHRL solution, respectively).

Therefore, this formulation offered the advantage of combining the protective effects of AL with an increase of permeability provided by HTCC.

1.3.3.7. Droplet size distribution in the aerosol

The mean diameter and the size distribution of the droplets generated from a device are predominant parameters that may influence the deposition of an aerosol in the respiratory tract[287]. As specified by both FDA and EMA guidelines, the percentage of droplets smaller than 10 µm must be minimized in nasal delivery[288,289]. Indeed, it is well established that particles with a diameter larger than 20 µm will preferably be impacted in the anterior part of the nasal cavity (where the olfactory region is located), while small particles (< 5 µm) won't be stopped in the nose[290,291]. In contrast, when particles/ droplets are characterized by a median diameter smaller than 10 µm, they can potentially continue their journey to the lower respiratory tract by circumventing the nasal cavity[292]. It has been suggested that the highest degree of deposition in the olfactory region could be achieved with particles/droplets characterized by a median diameter of around 10 µm[293]. Larger particles are also usually more quickly cleared from the nasal cavity due to mucociliary clearance[294].

Figure 31. VP3 multidose spray pump from Aptar Pharma (on the left, https://pharma.aptar.com) and SP270 nasal spray from Nemera (on the right, https://www.nemera.net)

The main parameters that will directly influence the size distribution are the physicochemical properties of the formulation (e.g. viscosity, density, surface tensions) and the design of the nasal device (e.g. orifice shape, metering chamber, volume delivered)[295]. The devices used for the generation of the liquid aerosol were the VP3 multidose spray pump from Aptar Pharma and the SP270 device from Nemera (**Fig. 31**). The aerosol properties obtained with both devices were then compared.

Table 14. Particle size data collected by laser diffraction (Spraytec®) from aerosols produced by VP3 and SP270 with both HTCC-AL and AL in PBS pH 7.4, with the following concentrations: HTCC 1 mg/mL, AL 10 mg/mL and GHRL 1 mg/mL (n = 3, mean ± S.D)

VP3 device			
Formulations	**% Volume < 10 µm**	**Dv50 (µm)**	**D(4,3) (µm)**
AL	3.2 ± 1.2	37.6 ± 5.74	40.8 ± 8.9
HTCC-AL	4.1 ± 1.40	38.47 ± 5.76	41.8 ± 7.58
SP270 device			
Formulations	**% Volume < 10 µm**	**Dv50 (µm)**	**D(4,3) (µm)**
AL	3.6 ± 2.54	40.4 ± 2.78	42.4 ± 2.80
HTCC-AL	6.9 ± 2.32	95.36 ± 9.57	96.75 ± 9.79

The VP3 pump coupled with the 144GI actuator generated only 3.2% of droplets smaller than 10 µm for AL (**Tab. 14**), which could be potentially deposited in the lower airways. This percentage represented only a small fraction of the entire droplet population and suggested a negligible loss in the lower airways. The median diameter (Dv50) was 37.6 ± 5.7 µm and the mean diameter D(4,3) was 40.8 ± 8.9 µm. When HTCC-AL dispersion was introduced in the device, the Dv50 of the droplets generated was similar to that obtained with AL (37.6 ± 8.7 µm and 38.5 ± 5.8 µm, respectively).

The droplet-size distribution was also studied with SP270 device. The median diameter Dv50 obtained with AL in this conventional device was very close to that obtained with the VP3 device. However, a significant increase in Dv50 and D(4,3) was observed for HTCC-AL from the conventional device, showing droplets more than 2-fold larger (Dv50 ranging from 40.41 ± 2.78 µm to 95.36 ± 9.57 µm with AL and HTCC-AL, respectively). The potential viscosity afforded by HTCC could be responsible for this evolution, as it was already observed in other studies[296]. The SP270 device was clearly more impacted by the viscosity variations than the VP3 device.

1.4 Conclusion

The first formulation did not provide suitable data (i.e. no permeation increase) suggesting that the nasal administration of GHRL using DSPE-PEG micelles could not be possible.

For the second liquid formulation developed, the encapsulation of GHRL in charged liposomes was assessed. By changing the liposome compositions, it was possible to modulate the ionic charge as well as to increase both drug loading and enzymatic protection (TRYP and CES-1). Electrostatic and hydrophobic interactions between GHRL and AL have been demonstrated and AL appeared to be an interesting choice of formulation for GHRL nasal delivery with brain targeting.
The coating of AL with HTCC was confirmed by the increase both size and charge, but also by morphological assessments. HTCC-AL showed a stronger adhesion to mucins than AL and the osmolality values were consistent with nasal administration.

Calu-3 experimentation showed that GHRL permeation could be increased via paracellular transport after HTCC addition. It was also underscored that AL needed to be coated with HTCC to obtain improved GHRL permeation. By combining the

beneficial effects of both AL and HTCC, it was possible to protect GHRL, to increase the bioadhesion of the liposomes and to optimize their transfer through Calu-3 cells.

The aerosol properties after actuation of the device were satisfactory with suitable size distributions.

Overall, the GHRL-loaded coated liposomes could closely match the criteria required for efficient nose-to-brain delivery. However, stability during storage of such biopharmaceutical in aqueous medium is usually quite low (e.g. due to significant hydrolysis). Moreover, the residence time of nasal liquids has been reported to be lower than nasal powders[66]. Considering these essential points, it was decided to carry on the pharmaceutical development with the production of a formulation in the form of a nasal dry powder.

2. Results part II: Development of a dry-powder formulation for the nose-to-brain delivery of GHRL

2.1 Introduction

In the previous part a liquid formulation based on GHRL-loaded HTCC-AL was developed[297]. The formulation provided promising data in terms of entrapment efficiency (56%), enzymatic protection (20.6% and 81.6% in the presence of trypsin and carboxylesterase, respectively) and permeation enhancement (10.8% through a Calu-3 monolayer).

The decision has been made to move forward to a powder form to achieve a better storage stability of the peptide (e.g. avoidance of the cold chain during shipping) as well as to avoid the use of preservatives[61]. Moreover, permeation in the nasal cavity has been described to be increased with powders as the low volume of nasal liquid available for dissolution creates a high concentration gradient that positively impacts the diffusion of a drug through the nasal membrane[63–65]. In addition, powders are characterized by a prolonged residence time in the nasal cavity and, this, even more if the formulation contains bioadhesive excipients. This thus offers more opportunity for the peptide to be transferred through the olfactory mucosa[66]. Regarding the physicochemical properties of the excipient, it has been reported that chitosan derivatives offered a higher transmucosal bioavailability of drugs when delivered as a powder[67].

On the other hand, the development of a dry-powder formulation presents some additional issues such as reproducible and homogenous drug content. Other powder-specific parameters such as particle size, density, residual moisture and electrostatic charges may strongly influence and modify the physical behavior of the powder. Nevertheless, even if liquid formulations still represent the majority of nasal medicines, the number of studies that focus on the development of nasal powders are growing up[68–70]. Up to now, most of the marketed nasal products based on the use of powders contain corticosteroids for rhinitis management and the number of studies related to nasal powders containing peptides is still very low[72,73].

This part of the work aims to develop and evaluate a powder formulation for nose-to-brain delivery that contains chitosan-coated liposomes loaded with GHRL by particle engineering using the spray drying technique. Such formulation should protect GHRL from early degradation, and increase its permeation through the olfactory mucosa due to the formulation's mucoadhesion properties as well as GHRL's long-term storage

stability. Lactose is a well-characterized matrix agent in inhalation that allows HTCC-coated liposomes dispersion once in contact with nasal fluids[298]. The spray drying method was already used to produce both nasal powders and lung inhaled powders containing liposomes[299,300].

Once the drying parameters were optimized, the physicochemical properties of the powder were evaluated. The powder was also introduced in a dry-powder device which was designed to target the olfactory region for optimal nose-to-brain delivery[301]. The aerosol that was generated from this device was deeply studied (e.g. deposition in a nasal cast, aerosol size measurements). The powder was evaluated in terms of mucoadhesion, permeability through a Calu-3 monolayer as well as drug and aerosol stability during storage.

A part of these results are published in the following article: “Salade, L., Wauthoz, N., Vermeersch, M., Amighi, K. & Goole, J. Chitosan-coated liposome dry-powder formulations loaded with ghrelin for nose-to-brain delivery. *Eur. J. Pharm. Biopharm.* **129,** 257–266 (2018)”.

2.2 Materials and methods

2.2.1 Materials

Synthetic human acylated GHRL (purity ≥ 98%) was purchased from Shanghai Science Peptide Biological Technology co., Ltd (Shanghai, China). Acetonitrile, methanol, trifluoroacetic acid (TFA), dichloromethane (all solvents were high-performance liquid chromatography (HPLC) grade), dihexadecyl phosphate (DHDP) and cholesterol (CHOL) were obtained from Sigma Aldrich (St Louis, MO, USA). Soybean lecithin “Lipoid® S100” (LS100) was purchased from Lipoid® Gmbh (Ludwigshafen, Germany). Trypsin-EDTA 0.25% w/v solution (TRYP), Hank’s balanced salt solution (HBSS), certified US origin heat-inactivated foetal bovine serum (FBS), sodium pyruvate 100 mM, L-glutamine 200 mM, penicillin (10 000 U/mL)/streptomycin (10 000 µg/mL), gentamicin 50 mg/mL and minimum essential medium containing no essential amino acids (MEM NEAA) were obtained from Thermo Fisher Scientific (Walthman, MA, USA). Calu-3 lung adenocarcinoma cells (ATCC®

HTB-55™) were purchased from ATCC (Manassas, USA). Inserts used for a Calu-3 air–liquid interface culture were composed of a mixed ester cellulose membrane with 0.45 µm porosity and 30 mm diameter adapted for 6-well plates and Amicon® Ultra-15K centrifugal tubes with a 100 kDa cut-off. These were purchased from Merck Millipore (Darmstadt, Germany). The chitosan derivative was a HTCC derivative with a MW of 92 kDa, a deacetylation degree of 80% and a substitution degree of 33% (Kitozyme, Herstal, Belgium). Lactohale® 210, which is a grade of lactose intended for inhalation, was used as a matrix agent and obtained from DFE Pharma (Goch, Germany).

2.2.2 Production of HTCC-coated liposomes for spray-drying

The protocol used for HTCC-coated liposomes production is described in paragraph 1.2.5: “Preparation of liposomes and HTCC-coated liposomes. From the initial dispersion of HTCC-coated liposomes, 1.0 g of Lactohale® 210 (DFE Pharma, Goch, Germany) was dissolved prior spray-drying in the liquid formulation to act as a matrix agent. The preparation was left for 15 minutes under magnetic stirring for complete solubilization.

2.2.3 Determination of the spray drying parameters and powder characterizations

A design of experiment (DoE) including four factors, four resolutions and two levels per parameter was established using the statistical software Minitab (*Minitab* Inc., USA). This software selected drying conditions that offered the highest yield as well as a representative fraction of particles larger than 10 µm. For each drying parameter, two levels were defined (minimum “-1” and maximum “+1”, **Tab. 15**).

Table 15. Parameters for the DoE for optimizing the spray drying conditions, with their maximum (+1) and minimum (-1) levels

Parameters	Level (-1)	Level (+1)
X1 = Inlet temperature (°C)	90	130
X2 = Feed rate (mL/min)	2.6	6.2
X3 = Spray gas flow (L/h)	283	667
X4 = Aspirator rate (m^3/h)	32	38

The spray drying was performed with a Mini Spray-Dryer B-290 (Büchi, Switzerland) equipped with a 0.7 mm diameter nozzle and a high performance cyclone. Powders were produced by spray drying 10 mL of liquid formulation containing 10% (w/v) Lactohale® 210, 0.1% (w/v) GHRL, 1% (w/v) lipid mixture and 0.1% (w/v) HTCC. The small volume (10 mL) of liquid formulation injected into the apparatus was mainly justified by the desire to limit the losses of GHRL during the development of the method. Four parameters inherent to the drying process were studied, namely: inlet temperature, feed rate, spray gas flow and aspiration rate.

The production yield (%) for the spray drying process was calculated as follows:

$$\text{Yield (\%)} = \frac{W_r}{W_i} \times 100 \qquad (6)$$

where "W_r" is the residual mass of powder collected (in milligrams) after drying and "W_i" is the mass of components contained in the initial liquid formulation injected in the spray dryer (in milligrams) through the peristaltic pump.

For each spray drying parameter, maximum and minimum values were fixed in order to set up the design of experiment (**Tab. 15)**.

2.2.4 Particle size distribution analysis and scanning electron microscopy

The particle size distributions were obtained by laser diffraction using the Aero S dry powder dispersion system (Mastersizer® 3000, Malvern Instruments, Malvern, UK). Approximately 50 mg of powder were deposited on the tray of the Aero S dry dispersion plate and the vibration rate was fixed at 100%. The powder was dispersed at a pressure of 4 bars and the refractive index was fixed at 1.35. Size distributions were reported and characterized using the median volume diameter “Dv50” that represents the diameter at which 50% of the population is comprised below this value.

The morphology of the powder particles was studied by SEM analysis using a Hitachi SU-70 ultra-high resolution microscope (Hitachi, Tokyo, Japan). The particles were coated with gold (35 mA for 4.5 min at 1 mbar under argon) before analysis.

2.2.5 Thermogravimetric analysis

Powders (15-20 mg) were studied by thermogravimetric analysis (TGA) for their residual moisture (% w/w) using a TGA Q500 (TA Instruments, New Castle, Delaware, USA). The temperature range studied was fixed between 35 and 120°C and the heat rate set at 10°C/min. The percentage of residual moisture was determined with TA Instrument Universal Analysis 2000 software by determining the weight variation (% w/w) between 35 and 120°C (n=3).

2.2.6 HPLC-UV method

The method used for GHRL quantification is described in paragraph “1.2.3 HPLC/UV method for GHRL quantification”.

2.2.7 GHRL content uniformity and stability

The GHRL content uniformity in HTCC-AL powder was determined by solubilizing 50 mg of HTCC-AL powder in 2 mL of PBS pH 7.4. The amount of GHRL in each sample was determined by HPLC and the variability was compared between five distinct samples.

The GHRL stability was compared between the HTCC-AL powder and liquid formulations. Both formulations were stored for 2, 4 and 12 weeks at 4°C and 25°C/50% relative humidity (RH). Powder samples were stored with silica desiccant in

sealed vials. At the end of the test, GHRL was quantified and the degradation percentages were compared between HTCC-AL liquid and powder formulations. HTCC-AL powder was extemporaneously dispersed in PBS pH 7.4 (50 mg/mL) for HPLC quantification. The remaining amounts of GHRL were compared to the initial GHRL quantities at the beginning of the test. The degradation percentages were expressed using the following equation:

$$\text{Degradation percentage (\%)} = \frac{(GHRL_{before} - GHRL_{after})}{GHRL_{before}} \times 100 \qquad (7)$$

Measurements were performed in triplicate (n = 3) and expressed as mean values ± SD.

2.2.8 Adsorption of mucins on HTCC-AL

A defined amount of HTCC-AL powder (50 mg) or HTCC-AL liquid formulation (2 mL) was added to 6 mL of mucin solution (0.5 mg/mL). Mucoadhesion was determined based on a colorimetric method combining periodic acid and Schiff reagent already described in paragraph “1.2.11”.

The test was performed in triplicate and expressed as mean values ± SD.

2.2.9 Characterization of the reconstituted aqueous dispersions

2.2.9.1. Size distribution, zeta potential and entrapment efficiency

GHRL-loaded coated liposomes from the initial HTCC-AL liquid formulation and the HTCC-AL liquid dispersion which were reconstituted from the HTCC-AL powder were evaluated and their size distribution, zeta potential and entrapment efficiency were compared (by moistening the powder with PBS). For the reconstituted dispersion, 50 mg of HTCC-AL powder per mL of PBS pH 7.4 was dispersed using a magnetic stirrer for 30 minutes. Both Z-average and zeta potential of both formulations were evaluated in triplicate at 25°C by dynamic light scattering and electrophoretic mobility, respectively (Zetasizer Nano ZS®, Malvern Ltd., Malvern, UK). Size distribution analysis were performed using PS semi-micro disposable cuvettes and results were expressed in terms of the Z-average (means ± SD) and polydispersity index (PDI).

Disposable folded capillary cells (DTS1070) were used for zeta potential evaluation and results were expressed as a mean ± SD (n = 3).

For entrapment efficiency assessment, both HTCC-AL liquid and reconstituted formulations were centrifuged at 13 500 rpm through Amicon® Ultra-15 centrifugal tubes with a 100 kDa cut-off membrane for 30 minutes at 25°C. Before, a GHRL solution (PBS pH 7.4) was centrifuged to confirm the non-adsorption of GHRL onto the filter membrane. The total amount of GHRL, "$GHRL_{total}$", contained in the initial HTCC-AL formulations was determined by the HPLC-UV method. The fraction of GHRL loaded into liposomes and retained on the filter was determined by quantifying the GHRL in the filtrate using the following equation:

$$\%\ GHRL_{loaded\ liposomes} = \left(\frac{[GHRL_{total}]-[GHRL_{Filtrate}]}{GHRL_{total}} \times 100\right) \qquad (8)$$

The tests were performed in triplicate and percentages were expressed as the mean ± SD.

2.2.9.2. Enzymatic protection

To evaluate the protection afforded by the liposomes to GHRL against enzymatic degradation, the HTCC-AL liquid formulation and the HTCC-AL reconstituted dispersion were exposed to TRYP solution (140 UI/mL) for 15 minutes at 37°C (Vortex Genius 3, IKA, Staufen, Germany). The reaction was stopped by the addition of 100 µL of TFA (10% v/v). "$GHRL_{total}$" in the initial formulations was determined by the HPLC-UV method. The remaining amount of intact GHRL after digestion was determined by withdrawing 500 µL for HPLC quantification. The percentage of GHRL protected by liposomes was determined as follows:

$$\%\ GHRL_{protected} = \frac{GHRL_{non\ degraded}}{GHRL_{total}} \times 100 \qquad (9)$$

2.2.9.3. Transmission electron microscopy

20 µL of HTCC-AL liquid formulation and reconstituted HTCC-AL dispersion (50 mg_{powder}/mL of PBS pH 7.4) were deposited on Formvar carbon-coated electron microscopy grids. Then, 1–2 µL glutaraldehyde 25% v/v was added to fix the liposomes. The preparation was left overnight at 4°C. Grids were transferred onto a drop of distilled water for washing and left for 2 minutes (three times). For contrasting and embedding, grids were placed onto a drop of methylcellulose-uranyl acetate (ratio 9:1 m/m) mixture for 10 minutes in an ice bath. The grids were removed and the excess fluid blotted by gently pushing the loop sideways on filter paper. A thin film was left over the section side of the grids. Observations were performed using a Tecnai 10 electron microscope (FEI, Hillsboro, OR, USA) operating at an accelerating voltage of 100 kV. Images were analyzed and processed using transmission electron microscopy (TEM) analysis (Olympus Soft Imaging Solutions, Münster, Germany).

2.2.10 Aerosol characterization from nasal device

Twenty-five milligrams of HTCC-AL powder were accurately weighed and put into a unit-dose system (UDS) nasal device. The UDS device was developed to target the olfactory region, the main area of interest for nose-to-brain transfer (kindly provided by Aptar Pharm, Le Vaudreuil, France). The aerodynamic particle size distribution emitted by the UDS device was studied by laser diffraction using a Spraytec® apparatus (Malvern Instrument, Malvern, UK). The analysis parameters were set as follows: test duration of 3 000 ms, actuation distance of 3 cm and data acquisition rate of 1 000 Hz. The volume median diameter “Dv50”, the volume mean diameter “D(4,3)” and the percentage of particles smaller than 10 µm “% < 10 µm” were recorded.

The uniformity of mass delivered from the UDS device was also determined (n = 10) by gravimetric analysis after triggering UDS devices in volumetric flasks.

To assess the potential modifications of the aerosol properties that could appear during storage, the UDS devices were stored at 25°C 50% RH for 2, 4 and 12 weeks. The particle size distribution was measured and compared to the initial distribution.

2.2.11 Aerosol deposition in a nasal cast

A nasal cast was used to evaluate the deposition profile of the HTCC-AL powder in the nasal cavity. For the nasal cast design, a nasal scan from a human Caucasian male was selected as a model (Aptar Pharma, Le Vaudreuil, France). Specific sections of the cast could be disassembled (**Fig. 32**) to recover GHRL that was impacted in each nasal region. Five sections could be analyzed, namely: the nose + nasal valves, turbinates, olfactory region, rhinopharynx and filter which captures small particles that did not deposit before.

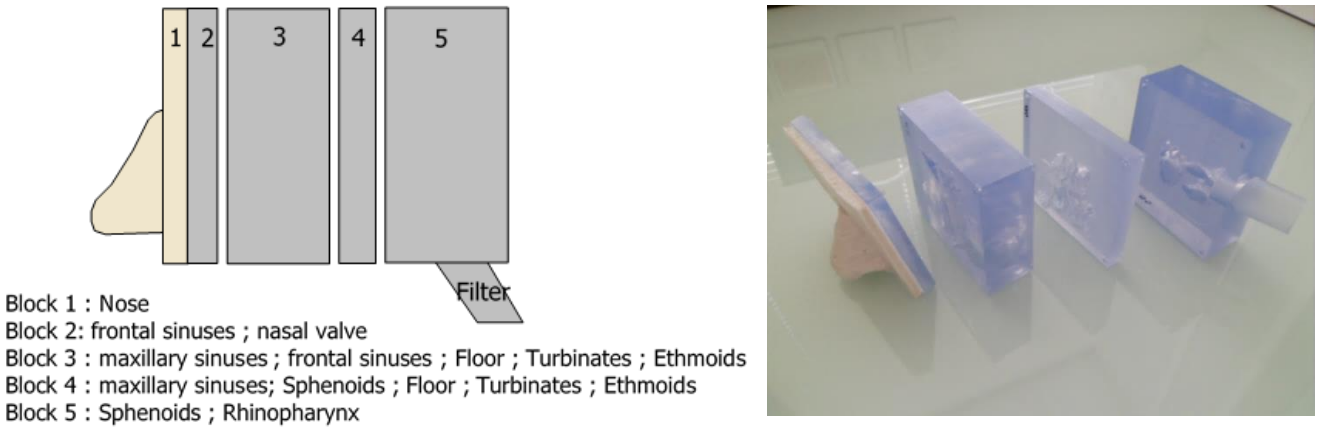

Figure 32. Illustration of the nasal cast used for the assessment of the drug distribution in the nasal cavity (Aptar© Pharma)

Prior to administration of the powder, the nasal cast was humidified with nebulized MilliQ water for 10 minutes to mimic nasal humidity. The UDS device was introduced in the nostril of the model at a depth of 10 mm and an angle of 45°. A single dose of 25 mg powder was delivered into each nostril (m_{total} = 50 mg) and each section was washed with a section-specific volume of MilliQ water for collecting GHRL. The recovery media were lyophilized by means of an Epsilon 1-6 freeze-dryer (Martin Christ GmbH, Osterode, Germany) for concentrating the samples. Lyophilized powders were solubilized in 1 mL of MilliQ water and quantified by the HPLC-UV method. Two formulations were tested. One with HTCC-AL powder containing GHRL and another with HTCC-AL powder combined with sodium fluorescein (650 µg of sodium fluorescein per 25 mg of total powder per nostril). Sodium fluorescein was added during the liposome rehydration step simultaneously with GHRL. The quantification of sodium

fluorescein was performed by HPLC-UV at 490 nm with a quantification limit of 0.1 µg/mL. This sensitivity allowed the quantification of sodium fluorescein in each section of the nasal cast. Results were compared with the powder containing only HTCC-AL powder. For GHRL quantification, three samples (n = 3) were freeze-dried and concentrated in PBS pH 7.4 (n = 1). For sodium fluorescein, measurements were performed in triplicate and expressed as mean percentages of recovery ± SD.

2.2.12 Permeation test on Calu-3 cells

Before adding HTCC-AL powder or HTCC-AL liquid formulation onto Calu-3 cells, the monolayer was washed twice with HBSS pH 7.4. Then, 2 mL of HBSS pH 7.4 were added to both apical and basal sides. Cells were left for equilibration for 30 minutes. Each liquid or powder formulation was introduced into three different inserts to perform the test in triplicate.

For the deposition of powder, UDS devices were filled with 25 mg of HTCC-AL powder, and a tip that was designed for nasal administration in rats (Aptar Pharma, Le Vaudreuil, France) was fixed onto the device (**Fig. 33**).

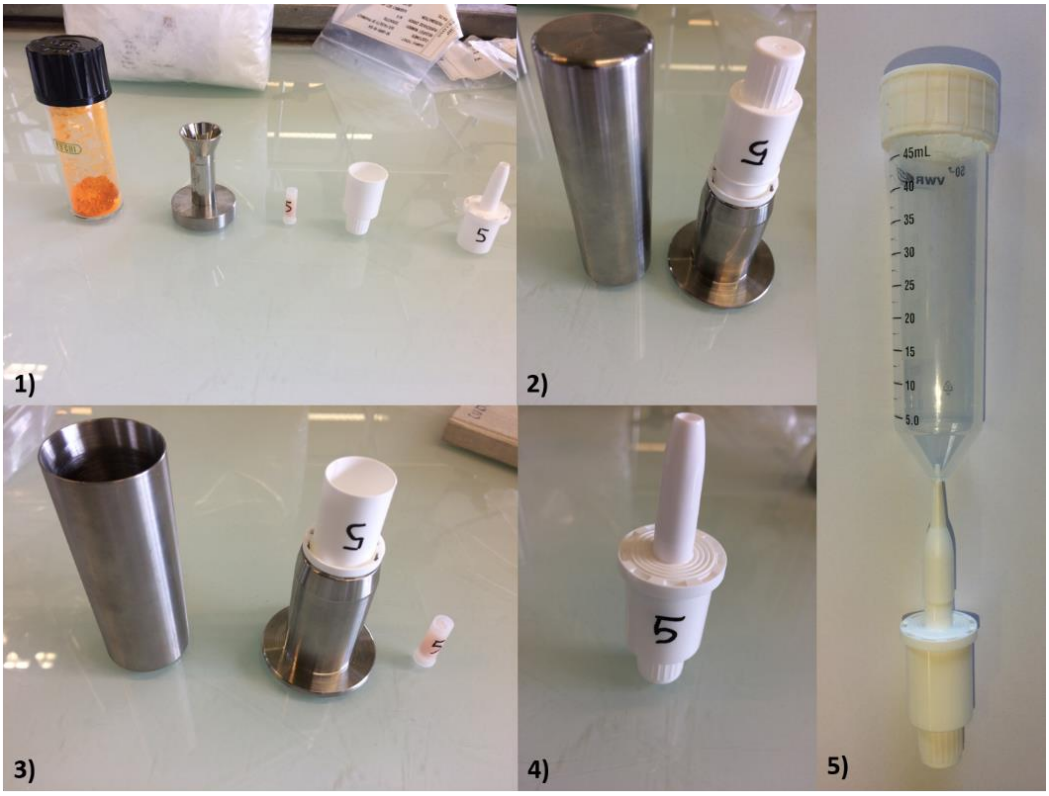

Figure 33. Assembly of the UDS device (1–4) and configuration for aerosol deposition on cell inserts with tip designed for nasal administration in rats and 50 mL-falcon tube (5)

The tip was introduced into a SuperClear™ Ultra High Performance Centrifuge Tube (VWR International, Lutterworth, Leicestershire, UK) that was pierced on the conical side. The centrifugal tube was placed vertically, with the device at the top and the cell insert in contact with the bottom. The device was triggered and the powder was impacted on the cell monolayer. A couple of doses of powder (25 mg/dose) were delivered per insert ($m_{total/insert}$ = 50 mg). The amount of powder impacted on inserts was determined by weight before and after administration.

For the instillation of HTCC-AL liquid formulations, 2 mL were introduced on the apical side of inserts using conventional micropipettes. GHRL was allowed diffusing for 3 hours. Then, 500 µL of basal medium was sampled and quantified by HPLC-UV method. The permeation was compared between HTCC-AL powder and HTCC-AL liquid formulations.

The TEER was followed at specific times during the experiments (i.e. at 0, 30, 90, 150 and 180 min) and 24 hours after the end of the test to assess the cell recovery. The

TEER was recorded using an epithelial Volt/Ohm meter EVOM2® (Wold Precision Instruments, Sarasota, USA). Data were expressed after subtracting the value of the blank insert and normalized for surface area (4.2 cm^2). For TEER daily evaluations, 2 mL of fresh medium were added on both the apical and the basal sides. Cells were left for 30 minutes prior to taking measurements. An epithelium monolayer was obtained approximately 10 days after inoculation (TEER around 1500 Ω cm^2).

2.3 Results and Discussion

2.3.1 Optimization of the spray-drying process

The liquid formulation has already been characterized, with promising results in terms of permeation enhancement, mucoadhesion and enzymatic protection[108]. This study discusses the development and the characterization of the dry powder formulation as well as the benefits provided by the dry state in comparison to the liquid state.

The powder was produced using the spray-drying technique. The general principle of the spray drying comprises the nebulization of a liquid in fine droplets which are brought into contact with a hot air stream which allows these drops to be dried. Then, the air flow passes through a cyclone which separates the dry product from the air flow. Although the spray-drying technique involves the use of relatively high temperatures, it has been preferred to freeze-drying due to its ability to produce powders with relatively spherical and amorphous particles as well as characterized by a narrow size distribution[302]. However, the temperature of the dried product is lower than the temperature of the incoming air due to significant moisture/solvent evaporation.

The spray-dried powder should contain particles larger than or equal to 10 µm to maximize the deposition in the nasal cavity as well as to avoid the deposition of small particles in the lower respiratory tract[303]. In order to properly control the particle size distribution of the spray-dried powder, the spraying gas flow must be well controlled as it directly influences the size of the droplets to be dried and, therefore, the size of the particles that are collected. Indeed, when the spraying gas flow decreases, the size of the droplets increases as well as the mean diameter of the dried particles.

In order to maximize the yield of the process, the evaluation of the influence of the feed rate can be relevant. Indeed, a high feed rate involves a risk of an incomplete drying process due to a loss of material that may stick on the walls of the spray-drier[304].

Therefore, an optimization of the drying process was required to reach the targeted granulometry as well as to increase the yield of production.

The first observation highlighted by the DoE (**Tab. 16**) was that the yield of production decrease when the Dv50 values increased. This trend could be confirmed by making a comparison between batches 2 and 3. Here, the Dv50 increased from 5.6 to 14.3µm while the yield decreased from 83.8% to 13 (w/w), respectively.

Table 16. DoE parameters followed during the spray drying process. The formulation dried was the HTCC-AL liquid formulation with GHRL 1 mg/mL, AL 10 mg/mL, HTCC 1 mg/mL and Lactohale® 210 100 mg/mL. Residual moisture (%) was determined by thermogravimetric analysis and powder particles size (Dv50) was measured by laser diffraction

Batch number	X1: Inlet temperature (°C)	X2: Feed rate (mL/min)	X3: Spraying gas flow (L-h)	X4: Drying air flow rate (m^3-h)	Dv50 (µm)	Yield (% w/w)	Residual moisture (%)
1	90	6.2	667	32	6.2	59.8	-
2	130	6.2	283	32	14.3	13	7.3
3	130	6.2	667	38	5.6	83.8	-
4	90	6.2	283	38	14.8	7.5	-
5	130	2.6	283	38	16.6	25	2.3
6	90	2.6	283	32	15.5	15.8	-
7	90	2.6	667	38	6.9	76.8	-
8	130	2.6	667	32	6.0	87.4	-

It could be observed that, when the spraying gas flow (i.e. X3) was increased from 283 L/h to 667 L/h, the size of the powder particles decreased. Indeed, when the spraying

gas flow is raised, the size of the nebulized droplets in the spray drier are lowered which lead to the production of smaller particles. Moreover, the increase of the spraying gas flow makes the drying process more efficient as the drying of such small droplets is easier to achieve. Droplets that were not fully dried could not reach the collection vessel and remained stuck on the walls of the drying chamber[305].

In order to confirm that a potential inefficient drying process was responsible of the low production yield observed, TGA experiments were performed. The TGA do not only provide information on the efficiency of the drying process, it also makes part of the characterization of a powder formulation. Indeed, the flowability of the powder may be improved by the presence of small amounts of residual moisture as water can act as a lubricant by reducing electrostatic charges. However, an excess of water (> 3% w/w) may cause the formation of liquid bridges and thus limit the correct dispersion of the powder during aerosolization[306,307].
The residual moisture also usually influences the stability of a drug in the powder (e.g. higher water content suggests a higher risk of hydrolysis[138]. A marked difference between batch 2 and batch 3 was highlighted, with residual moisture of 7.3 and 2.5% (w/w), respectively. The high percentage of residual moisture in batch 2 can explain the loss of material during the drying process and the substantially lower yield value obtained.

Another hypothesis explaining this phenomenon could be based on the transition temperature of Lipoid® S100 which is below 0°C (phase transition temperature of soybean phosphatidylcholine: -20/-30 °C)[308]. When the formulation was exposed to the heat during the spray drying (output temperature range: 50-55°C), Lipoid® S100 became softer and could stick to the walls of the atomizer, leading to a loss of product and a decrease of in the yield.

However, this hypothesis was discarded after a second trial, in which Lipoid S®100 was replaced by a hydrogenated phosphatidylcholine (Phospholipon® 90H, Lipoid, Ludwigshafen, Germany) that was characterized by a higher glass transition temperature (55°C). The loss of material in the drying apparatus was similar (data not shown), suggesting that sticking issues in the drying chamber were rather due to residual moisture. Additionally, the HTCC polymer coated onto the external side of liposomes was directly available for adhering to the walls of the apparatus. This could also contribute to the low yield of production that was observed.

In order to select the most suitable combination of spray-drying parameters, a major fraction of particles larger than 10 µm and a minimal loss during the drying process were inquired. Batch 5 (B5) showed the most suitable association, with a satisfactory yield of 25% w/w and an ability to produce dried particles with a volume median diameter larger than 10 µm (Dv50 = 16.6 µm). Batch 6 (B6) offered an interesting Dv50 (15.5 µm) but the decrease in the inlet temperature (i.e. X1) from 130°C (B5) to 90°C (B6) negatively impacted the yield of the process, which decreased from 25 to 15.8% (w/w), respectively. Indeed, when the inlet temperature was decreased, the drying of the particles was not achieved and moistened particles were trapped on the walls of the spray dryer.

Additionally, it is commonly accepted that the size of the drying chamber can sometimes be a limiting factor. Indeed, the spray dryer used in this study (B-290 Mini Spray Dryer, Büchi) is a laboratory-scale apparatus which was designed for the production of small amounts of powder. The small size of the drying chamber does not allow the production of large particles, unlike larger industrial spray dryers. With such industrial instruments, the drying chambers can be a few meters long. They thus provide a prolonged residence time, allowing very large droplets that are efficiently dried without being impacted on the walls of the apparatus[309]. Finally, B5 drying conditions were maintained for further characterizations.

Using the drying parameters corresponding to B5, the residual moisture in the dried powder was shown to be 2.3% (w/w) (**Tab. 16**), which could be considered satisfactory[310]. The residual moisture is a crucial parameter that may directly impact the physicochemical properties of a powder intended to be nasally administered. Indeed, a low water content is known to increase the stability of the drug during storage[311], while high residual moisture (> 2-5% w/w) may negatively impact the disaggregation of the powder during its aerosolization from the device[312,313]. In addition, powder flowability may be also decreased by residual water due to the presence of liquid bridges[306]. When water content is very low (< 1% w/w), electrostatic charges may appear. Increasing the water content may overcome the generation of such electrostatic charges and positively impact the flowability as water acts as a lubricant.[298]

There is a direct relation between residual moisture and drying parameters (e.g. spraying gas flow, feed rate, inlet temperature). For instance, a lower feed rate or an increase in the inlet temperature reduces the residual moisture content[310].

The characterization of spray-dried HTCC-AL powder was further continued with the analysis of the particles shape. As already described, the shape of the particles may strongly influence the aerodynamic behavior of powder for inhalation[314]. The contact surface between particles as well as the potential surface asperity can drastically modify the powder properties.

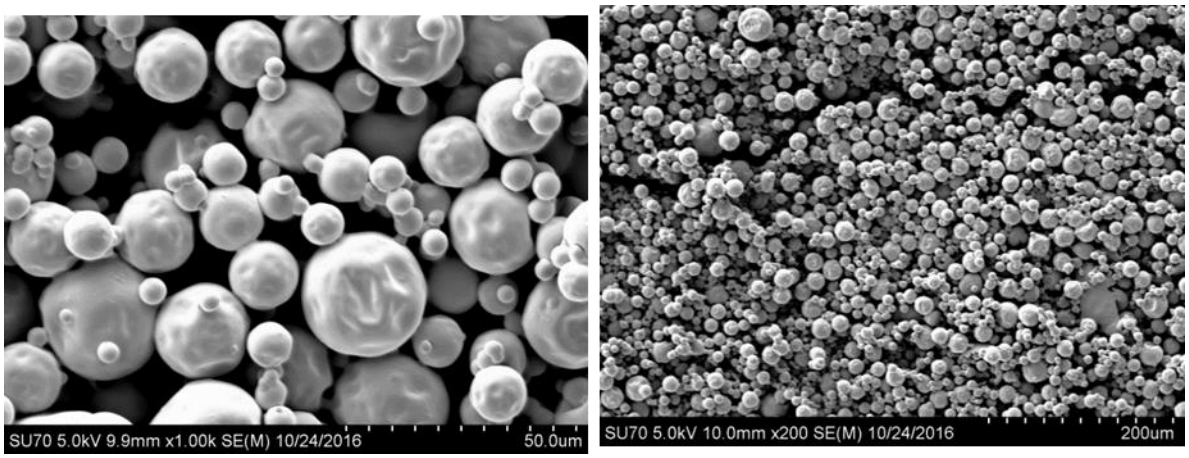

Figure 34. SEM pictures of HTCC-AL powder with magnifications of 1000x (left) and 200x (right)

A spherical shape coupled to a slight agglomeration of particles was observed on SEM pictures (**Fig. 34**). The particle surfaces were smooth and non-porous. The diameter of the particles appeared to be ranged between 10 and 40 µm. These particles of about 10 - 40 µm are thus constituted, in a major part by lactose, that is used as a carrier in order to bring the nanoparticles (HTCC-AL) into the nasal cavity. Indeed, the nasal delivery of such nanoparticles as they are and in the form of a dry powder would not be feasible. Therefore, the use of a carrier (i.e. lactose) allows the incorporation of a few nanoparticles of chitosan-coated liposomes in larger particles with the desired size range (> 10 µm). The particles spherical shape allows minimizing the interactions between the particles and usually provides a good aerodynamic profile (e.g. no agglomeration, good flowability) of the powder[315].

Different batches of HTCC-AL powders were produced using the spray-drying parameters of B5 (**Tab. 16**). It was demonstrated that the uniformity of dose of GHRL was preserved with a limited variability of 1.13 ± 0.02 mg of GHRL per g of dry powder formulation (**Tab. 17**). such amount represented a GHRL dose variability of 2.1%. Therefore, it could have been concluded that the powder produced by spray drying contained accurate and reproducible amounts of GHRL at the end of the process.

Table 17. Determination of residual moisture (% w/w, n = 3) and GHRL content uniformity ($GHRL_{amount}$ mg/ g of powder, n = 3) of HTCC-AL powder (5 different batches produced using B5 parameters). Values expressed as mean ± SD.

Parameters	Results
Residual moisture (% w/w)	2.3 ± 0.4
Content uniformity (mg/g of powder)	1.13 ± 0.02
Dose variability (%)	2.1

2.3.2 Comparison of mucoadhesion and GHRL stability between powder and liquid formulations

This section compares the ability of the formulation to adhere to mucins and the drug stability during storage for both liquid and powder formulations. As previously explained, it is of great importance to develop powder that also extends the residence time and the stability of the peptide during the nasal administration but also during the therapeutic storage. This could be achieved through the mucoadhesive properties of HTCC and the physical state of the dried formulation which may remain longer in the nose than a liquid formulation. Cationic chitosan derivatives are known to electrostatically interact with anionic charges on the mucosa surface[316]. Mucins, which are well-represented glycoproteins in the nasal mucus, are characterized by a global negative charge conferred by sialic acids and sulfate functions. The opposite charges present in mucins and chitosan derivatives induce electrostatic interactions. This phenomenon has been assessed by testing adhesion to submaxillary mucins.

It was shown that HTCC-AL in solid state fixed 89 ± 4% of mucins, which confirmed the electrostatic interactions between cationic HTCC and anionic charge of mucins at physiological pH[317]. The liquid formulation could also fix mucins but with a lowered percentage: 61 ± 4%. Therefore, the dry-powder formulation seemed to have an advantage over liquid formulations in terms of mucoadhesion.

Another potential advantage of dry powder formulation over liquid formulation is the better stability of GHRL during storage. Other studies have already mentioned the increase in stability for sensitive drugs, such as vaccines, when switching from a liquid

to a dry formulation[318]. Therefore, it was decided to compare the stability of GHRL from formulations in both physical states.

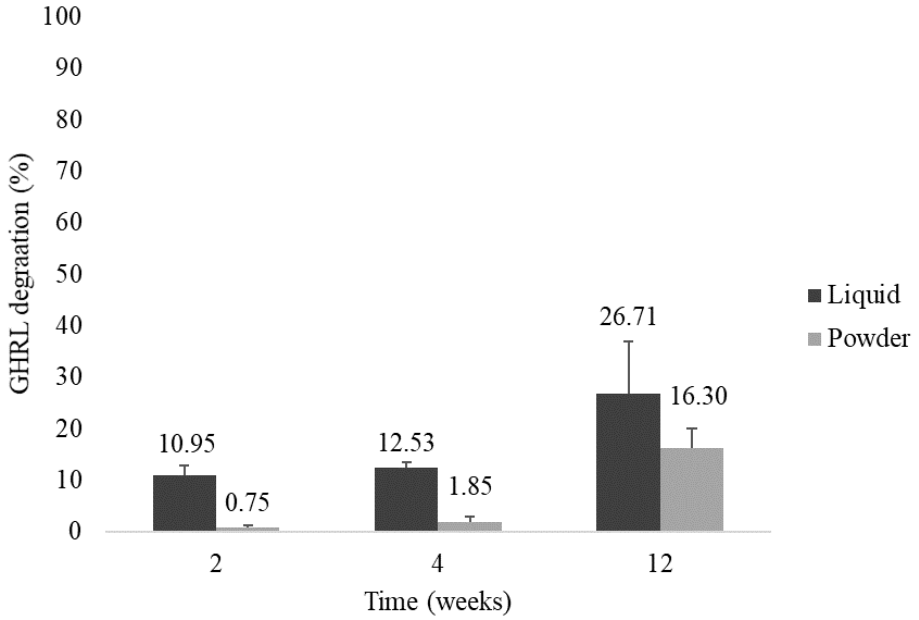

Figure 35. Comparison of the degradation percentages of GHRL for HTCC-AL liquid and powder formulations at 4°C 50% RH after 2, 4 and 12 weeks (n = 3, mean ± SD).

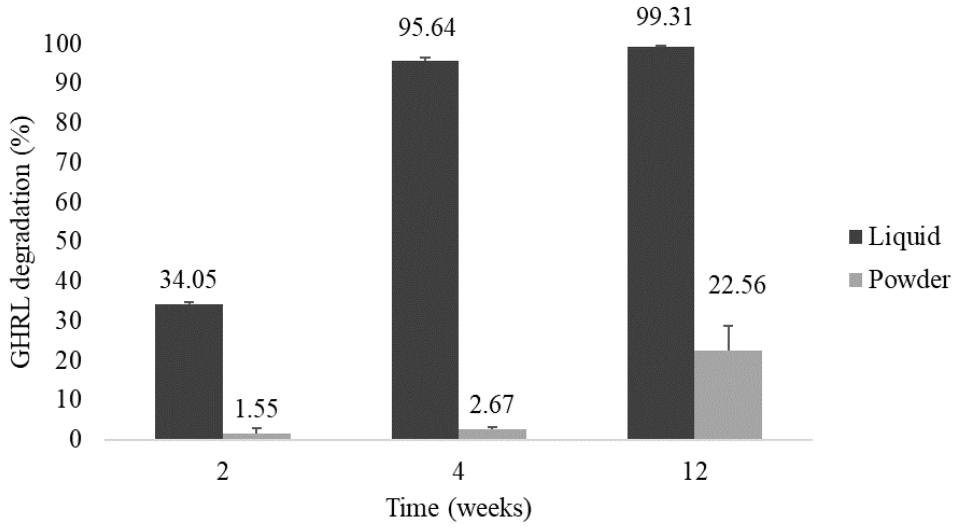

Figure 36. Comparison of the degradation percentages of GHRL for HTCC-AL liquid and dry formulations at 25°C 50% RH after 2, 4 and 12 weeks (n = 3, mean ± SD).

The benefit of the dry formulation over the liquid at 4 and 25°C can easily be visualized when comparing the degradation profiles (**Fig. 35 and 36**). At 4°C, the degradation in

the liquid formulation was more limited but the amount of GHRL degraded was higher than 10% after 4 weeks (12.53 ± 0.92%). At the same temperature, the powder form globally offered a strongest stability decreasing this way the GHRL degradation of about 10% for each incubation period versus the liquid formulation.
Moreover, at 25°C, almost all the GHRL (95.64 ± 0.85%) was degraded in the liquid formulation after one month. In contrast, the degradation of GHRL from the dry formulation was still very limited, with 2.67 ± 0.57% after 4 weeks at 25°C of GHRL degraded. A slight increase of the degradation could be observed after 12 weeks at 25°C with 22.56% of GHRL degraded in the powder.

By comparing the powder form at both temperatures (i.e. 4 and 25°C), it can be seen that an increase of 6.26% of GHRL degradation is observed when stored at 25°C versus 4°C. Therefore, the development of a dry powder dosage form for such unstable biopharmaceutics appears relevant. Moreover, by storing the dry powder in refrigerated conditions (≤ 4°C), it is thus possible to further reduce GHRL degradation.

2.3.3 Characterization of the reconstituted aqueous dispersion

As the formulation may undergo some modifications during spray drying and, as it will be moistened by the nasal fluid after instillation, it was decided to disperse the HTCC-AL powder in PBS pH 7.4 to evaluate/characterize the resultant dispersion. Differences and/or similarities with the initial liquid formulation (before spray drying) have been highlighted and discussed.

Table 18. Comparison of Z-average, Zeta potential, entrapment efficiency, enzymatic protection (TRYP) and osmolarity between HTCC-AL initial liquid formulation (GHRL 1 mg/mL, HTCC 1 mg/mL, Lipids 10 mg/mL) and HTCC-AL reconstituted dispersion in PBS pH 7.4, (composition of the liquid formulation added with lactohale® 210 at 100 mg/mL), mean ± SD, n = 3

Parameters	Before spray drying	After spray drying
Z-average (nm)	195 ± 6	263 ± 5
[PDI]	[0.082]	[0.203]
Zeta potential (mV)	+5 ± 0.8	+9 ± 1.2
Entrapment efficiency (%)	55 ± 4	64 ± 2
Enzymatic protection (TRYP, %)	20 ± 3	26 ± 2
Osmolarity (mOsm/Kg)	408 ± 2	359 ± 3

Particle size distribution analysis (**Tab. 18**) showed an increase in both Z-average and PDI for the HTCC-AL dispersion reconstituted from the spray dried powder (195 ± 6 nm and 263 ± 5 nm for the initial HTCC-AL liquid formulation and for the HTCC-AL reconstituted dispersion, respectively). It appeared that a slight structural rearrangement could take place during the drying process (e.g. lipid agglomeration). The Z-average increased and structural changes after spray drying were already observed in other studies with PEGylated liposomes[319]. In previous work, it was suggested that the presence of PEG could promote the interaction between liposomes rather than limit it. Similar hypothesis may be made with the use of HTCC. However, the size distribution remained monomodal, with a PDI around 0.2 in both cases. Nevertheless, a narrower distribution was achieved before spray drying (0.082 in the initial HTCC-AL liquid formulation versus 0.203 in the HTCC-AL reconstituted dispersion). Zeta potential was also subject to a slight increase (from +5 ± 0.8 mV to +9 ± 1.2 mV). This could be explained by the increase in size after spray-drying which implied a larger surface coated with HTCC. This proportional evolution of both Z-average and zeta potential between the initial and the reconstituted dispersion (after spray-drying) with chitosan-coated liposomes was already observed and mentioned in other studies[320].

We then wanted to confirm that, once the HTCC-AL suspension reconstituted, the formulation was still able to protect GHRL from enzymatic digestion. Even if nose-to-brain administration is considered to be able to bypass most of the first pass degradations, many types of enzymes may be found in the nasal cavities. The main enzyme families represented in the nose are: aldehyde dehydrogenases, cytochrome P-450-dependent monooxygenases, rhodanese, glutathione transferases, epoxide hydrolases, flavincontaining monooxygenases and carboxyl esterases[258]. A trypsin-like activity, associated with the degradation of salmon calcitonin, was even reported in rat nasal mucosa. Therefore, the authors concluded that the use of trypsin inhibitor allowed the nasal absorption of salmon calcitonin to be enhanced[259].

The selected enzyme (TRYP) was an endoprotease that cleaves lysine and arginine residues which represents seven potential cleavage sites (arginine and lysine residues) on the peptide chain of GHRL. The protection afforded by liposomes was similar and, even more pronounced, than that of the initial liquid formulation before spray drying (20 ± 3% and 26 ± 2% before and after spray drying, respectively). A basic GHRL solution was the reference for the degradation, with 100% of GHRL degraded after TRYP digestion (data not shown).

The higher GHRL entrapment efficiency and enzymatic protection could be explained by a close interaction of GHRL with HTCC-AL during spray drying. When the aqueous medium is evaporated, free GHRL might have to closely interact and be adsorbed onto the surface of HTCC-AL lipid structure. This could also increase the amount of GHRL loaded to HTCC-AL. Such interaction resulted in a greater amount of GHRL that could be protected from enzymatic degradation.

Another hypothesis for this increase of entrapment efficiency could be explained by the restructuring (i.e. size increase) of HTCC-AL during spray drying. Indeed, it was previously shown that the Z-average of HTCC-AL in the dispersion was higher than before the spray drying process (**Tab. 18**). It is known that the size of liposomes as well as the number of lipid bilayer can be correlated with the amount of drug loaded into liposomes[321]. This could also explain the raise in the GHRL loading for HTCC-AL. TEM analyses were performed to confirm that, despite the increase of the Z-average observed by dynamic light scattering, the liposomes preserved their LUV structure. This structure was similar to that of the initial suspension (**Fig. 37**).

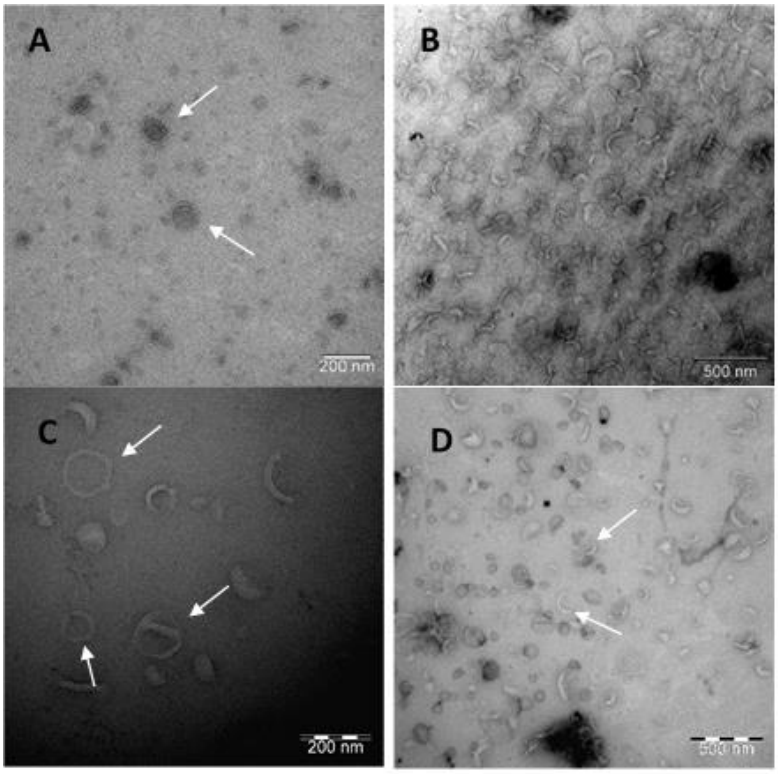

Figure 37. Transmission electron microscopy for the initial HTCC-AL liquid formulation (A-B) and for the reconstituted dispersion (C-D) (50 mg_{powder}/mL of PBS, dilution factor: 50x)

2.3.4 Powder aerosol characterization and *in vitro* nasal cast deposition

The aerosol size distribution obtained for HTCC-AL powder produced with B5 parameters is characterized by a volume median diameter “Dv 50” of 38 ± 6 µm, a volume mean diameter “D(4,3)” of 42 ± 8 µm and a percentage of particles smaller than 10 µm of 4 ± 1% (**Tab. 19**). In comparison with the size distribution measured in the raw powder (section “2.3.1 Optimization of the spray-drying process”, **Tab. 16**), a particle size increase can be observed in the aerosol (**Tab. 19**). A plausible explanation for this phenomenon would be the slight agglomeration of the powder, once loaded into the UDS device. However, the particle size distribution was not impacted during storage at 25°C/50% RH after 4 weeks in the UDS devices (data not shown). The shape of the particle size distribution curves remained unimodal and Gaussian.

The properties of the plume generated depend on both initial size of spray-dried particles and intrinsic properties of the nasal device that is used (shape of the nozzle, mechanism of aerosolization, etc.). The size of the particles in the aerosol is very important because it will determine the amount of drug deposited in the nasal cavity.

Table 19. Data collected from the particle size analysis (mean ± SD, n = 3) by laser diffraction (Malvern Spraytec, Malvern Instrument, UK): Dv50, D(4,3) and percentage of particles smaller than 10 µm (% < 10 µm), and uniformity of mass delivered from the UDS device (m_{powder} = 25 mg, mean mass (mg) ± SD, n = 10 and CV). HTCC-AL liquid formulation with GHRL 1 mg/mL, AL 10 mg/mL, HTCC 1 mg/mL and Lactohale® 210 100 mg/mL.

Parameters	Results
Dv50 µm	38 ± 6
D(4,3) µm	42 ± 8
% < 10 µm	4 ± 1
Mass delivered (mg)	24.9 ± 0.37
[CV]	[1.49%]

Regarding the nasal device, particular attention must be paid to its choice when a nose-to-brain transfer is targeted. Indeed, the device should maximize the deposition of the formulation in the olfactory region. However, the respiratory mucosa innervated by the trigeminal nerves could also be involved in nose-to-brain delivery[322]. In contrast to the olfactory pathway, the trigeminal pathway brings drugs into the cerebrospinal fluid (and not into the olfactory bulb) and would contribute in a lower manner to the nose-to-brain transfer[48].

Therefore, the criteria that were considered for the selection of the nasal device included (1) a proper impaction of the powder on the olfactory region, (2) a manual filling and (3) a suitable design to contain powder formulations. Based on these requirements, the UDS device from Aptar Pharma® was selected. This UDS device is a unit-dose dispensing system which operates via a plunger coupled with a membrane that is pierced upon activation of the device. It generates a positive pressure that expels the powder contained in the reservoir, allowing the generation of the aerosol.

The UDS device had been also described to properly deliver accurate amounts of powder. This was confirmed by a “uniformity of mass delivered” test. Indeed, the amount of emitted powder was found to be 24.9 ± 0.37 mg with HTCC-AL powder (**Tab. 19**). The repeated device actuations were characterized by a low variation in the

uniformity of the mass delivered with a coefficient of variation (CV) equal to 1.49%. Moreover, 99.6 ± 1.48% (w/w) of the loaded powder (25 mg) was expelled from the device. These results are in accordance with FDA recommendations that propose a maximum deviation of ±10% between the mean weigh and target weigh[323]. The amount of dry formulation that was loaded in the device was selected on the basis of the usual quantities of powder delivered nasally[135,324].The accuracy reached in terms of powder emitted with the UDS/HTCC-AL powder association was satisfactory in comparison with other devices. For example, only 8.27 ± 0.83 mg of beclomethasone dipropionate powder could be emitted from the initial amount (28.8 ±0.4 mg) loaded in the Puvlizer device from Teijin (Osaka, Japan)[68].
Additionally, the usual doses of octanoylated GHRL administered in clinical studies with intravenous injections by bolus or infusion are in the ranges of 0.03-10.0 µg/Kg and 0.003-1.33 µg/Kg.min, respectively[325]. Therefore, the dose of GHRL selected for the nasal administration in this work (28 µg/dose) is very close to the usual parenteral doses administered in humans and could provide satisfactory effects for potential future clinical studies.

After studying the aerosol properties, the deposition profile of the powder in an artificial nasal cavity, called “nasal cast”, was assessed. Nasal cast has become, in recent years, an inevitable step in the development of drug delivery systems for nasal administration[236]. Indeed, the particle size analyses which are usually performed by laser diffraction only represent the behavior of the aerosol in a free-volume. Indeed, without volume constraint related to nasal cavities, the spray has a large space to expand. In contrast, when administered in nasal cavities, the available volume is very limited and the spray is rapidly impacted onto the nasal walls. Therefore, a distribution study in a reproduced nasal cavity allows evaluating in a much more representative way the behavior of the aerosol during its delivery. Such nasal casts also make it possible to study the influence of physiological parameters such as the inspiratory flow of the patient or anatomical specificities on the deposition.

Medical imagery (e.g. sectioned scans[326,327], computed tomography or magnetic resonance imaging scans[328]), initially performed for the diagnosis of diverse nasal pathologies or deformations (e.g. nasal septum deviation)[329], constitute a very rich and varied databank used for the design of such artificial nasal cavities. The combination of the computed tomography scans and 3D printing allow the manufacture of complex

and biosimilar cavities[330]. In order to build the nasal cast, the raw data resulting from medical analysis are digitally converted to be compatible with 3D-printing software.

Nasal casts can provide both qualitative ((e.g. a translucent model that stains when the formulation deposits) and quantitative data, with anatomical models constructed in separable structures that allow quantification in specific areas of the nose. The model selected for our study was designed with 5 separable anatomical areas, namely: nostrils, vestibule, turbinates, olfactory region and rhinopharynx. The model was constructed on basis of a human male nasal cavity and the drug quantification was performed by dropping the distinct sections in buffer solutions. Each recovery bath was used for GHRL quantification by HPLC.

Depending on the nasal pathway that is targeted (e.g. local, systemic or nose-to-brain), the deposition of the droplets/powder should be preferentially targeted in specific areas in the nasal cavities. For instance, when a local effect or a systemic transfer is expected, the formulation should cover the largest area of the nose to maximize the surface of contact. This may be achieved by developing a formulation with a device that is able to generate small particles or droplets as they cover a large surface.

In contrast, when a nose-to-brain transfer is considered, it is mandatory to maximize the nasal deposition in a very restricted area that only represents 5.2% of the total surface of the nasal cavity, namely the olfactory mucosa[331]. It is well-known that the deposition of large particles or droplets (50-60 µm) do not occur in posterior areas of the nasal cavity and thus limits the amount of drug potentially bypassing the olfactory mucosa[134,332,333]. However, if the median diameter is too large, the formulation can be deposited at the entry of the nose and can be quickly removed by sneezing or cleaning[334].

The rhinopharynx and the filter sections, located at the back of the nasal casts, are the representative areas for the evaluation of losses of small inhalable particles. Indeed, the rhinopharynx section contains an aerosol part that circumvents the nasal cavity, while the filter section acts as a barrier to block the smallest particles (< 5 µm), which

could theoretically continue to the deeper respiratory tract.

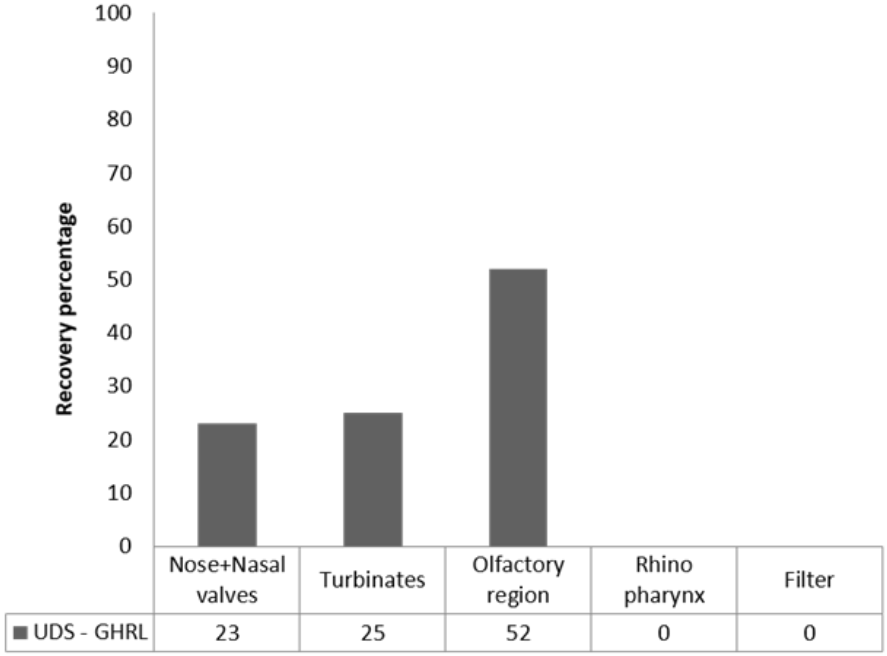

Figure 38. Recovery percentage of GHRL in various sections of the nasal cast with the UDS device and HTCC-AL powder ($m_{powder\ delivered/nostril}$ = 25 mg, $m_{GHRL\ delivered/nostril}$ = 28 µg, with an administration angle of 45° and a nostril insertion depth of 10 mm, n = 1)

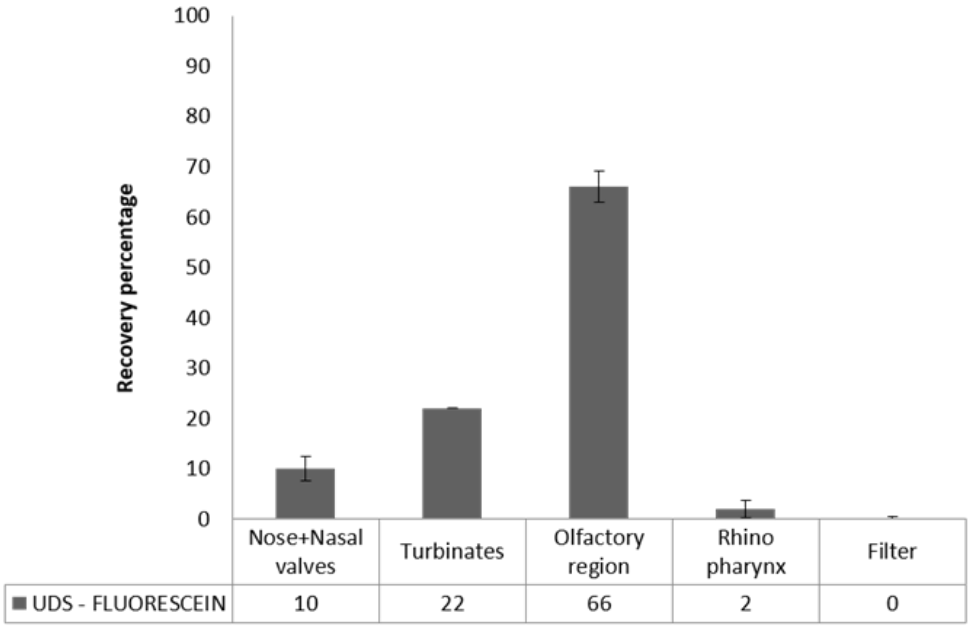

Figure 39. Recovery percentages of fluorescein in various sections of the nasal cast with UDS device and HTCC-AL powder ($m_{powder\ delivered/nostril}$ = 25 mg, $m_{total\ powder}$ = 50 mg, $m_{fluorescein/nostril}$ = 650 µg), with an administration angle of 45° and a nostril insertion depth of 10 mm, n = 3, mean ± SD)

For the deposition profile of GHRL with HTCC-AL powder (**Fig. 38**), it was necessary to combine the washing media following the deposition experiments and to concentrate them by freeze-drying to reach a sufficient concentration for quantification. It was demonstrated that 23% of GHRL were recovered in the “nose+nasal valves” section. This section concerns the deposition of largest particles which can be rapidly removed by sneezing or cleaning the nose[334]. Another 25% of GHRL was quantified in the found in the ”turbinates” section. Regarding the “rhinopharynx” and “filter” sections, they should trap the smallest particles which could potentially reach the lower parts of the respiratory tract. The absence of GHRL in both areas (i.e. rhinopharynx and filter sections) can be explained by the very low percentage of particles characterized by a mean diameter smaller than 10 µm (4 ± 1%, **Tab. 19**). The highest amount of GHRL was recovered in the olfactory region (52%). The deposition of 52% represented a total dose of GHRL of 29.1 µg on the olfactory mucosa after delivery in both nostrils. Therefore, it seemed that the combination of the UDS device and the HTCC-AL powder allowed a maximized deposition in this section.

A second deposition study was performed with HTCC-AL powder containing fluorescein as a colored molecule model for quantification. Even if it is always better to quantify the active compound directly, sodium fluorescein could be an interesting alternative for evaluating the deposition profile of nasal powders loaded with expensive drugs that are available in limited quantities. In addition, the quantification of fluorescein can be done in a much more sensitive way which allows to precisely determine the amounts of powder deposited in each section of the nasal cast. By using fluorescein, it was also possible to repeat experiments three times in order to collect more statistically representative data. Indeed, with GHRL we had to combine collection media of three experiments and proceed to freeze-drying in order to make the test quantifiable. For these reasons, the deposition of the powder with fluorescein was compared to that of GHRL. However, such comparison must be carefully controlled. Indeed, the physicochemical properties of the formulation containing the fluorescein must remain similar to that delivering the drug/peptide.

To compare GHRL and sodium fluorescein, the particles size distribution, the aerosol size distribution, uniformity of mass delivered and content uniformity were controlled and compared to the initial HTCC-AL powder formulation without fluorescein. All experimentations showed similar properties between formulations with or without

fluorescein (see section “Appendices I.”). These results could be supported by the quantification of sodium fluorescein in the different sections of the nasal cast (**Fig. 39**). It could be seen that the powder with fluorescein was similarly distributed to that of GHRL. However, it should be noticed that higher amounts (+14%) of fluorescein were found in the olfactory region compared to those of GHRL. This observation could be explained by the great difficulty in accessing the olfactory region. Indeed, since the olfactory mucosa is located after a very narrow zone and in the upper part of the nose, the variability observed in terms of deposition may be greater than in other nasal localizations.

2.3.5 Permeation study on Calu-3 cells

Prior to permeation tests, the maximal amount of powder that could be deposited on inserts from the UDS-Falcon® system was estimated. It was shown that, from the initial amount of powder (m = 25 mg), 16 ± 1.2 mg were impacted on insert membrane. This amount represents 64 ± 4.8% w/w of the loaded amount of peptide.

Regarding GHRL permeation, HTCC-AL powder showed an enhanced permeation of GHRL compared to the HTCC-AL liquid formulation before spray drying. Indeed, the amounts of GHRL that diffused through the basal compartments were 9.7 ± 0.6% and 22.8 ± 2.5% for the suspension and the powder, respectively (**Tab. 20**). Therefore, it seemed that the potential higher GHRL concentration, which was due to the dissolution of the powder in a small volume of residual liquid on the apical side, increased the diffusion through the cell monolayer.

Table 20. Percentage of GHRL in basal compartments of inserts, TEER drop between the start and the end of the experiment for both HTCC-AL liquid and powder formulations (n = 3, t = 3 hours, HBSS pH 7.4, mean ± SD). Percentage of powder emitted from the UDS-Falcon® system (n = 3, mean ± SD).

Parameters	HTCC-AL liquid	HTCC-AL powder
Basal (%)	9.7 ± 0.6	22.8 ± 2.5
TEER drop (Ω.cm²)	87 ± 3.8	97 ± 4.1
% of powder emitted	/	64 ± 4.8

It also appeared that HTCC in the dry powder form induced a slightly greater drop of the TEER value (97 ± 4.1 Ω.cm²) in comparison with the liquid form (87 ± 3.8 Ω.cm²). However, TEER values are subject to strong variations from on experiment to another and this observation should be confirmed in another permeation test with Calu-3 cells and both formulations. This suggested that HTCC would better open the tight junctions when administered as a powder form and thus provide a better permeation-enhancing effect. In another study, this superior effect of chitosan powder on the TJs opening was attributed to the mucosa water catching by the chitosan powder[335].

2.4 conclusion

In comparison with the liquid formulation, the development of the dry-powder could be considered as an attractive alternative due to the higher stability of the drug during long-term storage, its increased mucoadhesion and enhanced permeation across biological membranes. The development of such dry dosage form appeared achievable even if the drying yield remained limited. However, this issue could be easily overcome by using a spray dryer with larger drying chambers. On the other hand, the powder obtained presented convenient residual moisture as well as a suitable particle size distribution for nasal delivery. The characterization of the reconstituted dispersion highlighted a slight increase in the mean diameter of the liposomes, in entrapment efficiency and in enzymatic protection, which was probably caused by a structural rearrangement of AL or a stronger interaction between GHRL and AL. The aerosol produced from the UDS device was characterized by larger particles suitable for nasal deposition and a very limited fraction of particles smaller than 10 µm. The UDS device offered the reproducible delivery of accurate doses of powder very close to the nominal dose. This reproducibility makes possible the repeated administration of precise amounts of GHRL. Ideally, the data collected should be completed by tolerance experiments. Indeed, a chronic administration (e.g. three times a day) of a nasal powder could potentially involve an inflammatory reaction at the level of the nasal mucosa. Finally, nasal casts showed that targeted delivery in the olfactory mucosa could be achieved. The deposition in the olfactory region was maximized.

Following this detailed characterization, we have been able to prove that the development of a nasal powder containing HTCC-AL loaded with GHRL was a

promising choice. Taking into account the many positive results, this formulation appears as an excellent candidate for a future nose-to-brain treatment. However, it lacks the essential, the proof of an efficient nose-to-brain transfer once administered in a living organism. It is therefore necessary to further continue the development with *in vivo* experiment, which is the next part of the manuscript.

3. Results part III: *In vivo* characterization of chitosan-coated anionic liposome

3.1 Introduction

In order to assess the efficiency of our formulations (i.e. its ability to provide GHRL with a substantial access to the brain) as well as to evaluate the possibility to make *in vitro-in vivo* correlations, pre-clinical studies were conducted in mice.

Indeed, *in vitro* analysis were performed to reproduce a specific property/activity that could be met in the nasal cavity (e.g. enzymatic digestion or mucoadhesion), only *in vivo* evaluation can assess the behaviour of a formulation after administration (e.g. impaction, residence time, diffusion, stability). *In vivo* experiments also provided additional information that could not be collected from *in vitro* evaluations (e.g. biodistribution).

Several animal species may be used to perform *in vivo* experiments on a nose-to-brain formulation: sheep, rats, rabbits, monkeys, dogs, Guinea pigs and mice[336]. Among them, mice and rats are described to be widely used as a plethora of useful data may be easily collected from such rodents.

Both liquid and powder nasal formulations can be characterized in such animals but the nasal administration of liquids still remains easier to implement. Indeed, by using a conventional micropipette, the investigators can deposit droplets of formulation at the entry of the animal's nose. After inhalation, the formulation may enter into the nose and diffuse throughout the nasal cavity. Due to the ease and the well-known procedure of administration, only the liquid formulation was evaluated for preliminary *in vivo* studies.

Even if, to our knowledge, there is no available device that was able to specifically target the olfactory mucosa of such small animals, it was described that the administration of liquid formulations may be done when the animal was on its back to increase the probability to reach the targeted region of the nasal cavity[336].

Various techniques of medical imagery have been described for highlighting the transfer of a drug from the nose to the brain. Among them, drug radiolabelling, coupled to "Positron Emission Tomography", can provide very relevant information such as the drug transfer kinetic, the amount of drug reaching the brain or, the pathway of diffusion.

In the first preliminary *in vivo* evaluation, the purpose was to confirm that GHRL could reach the brain after intranasal administration of the liquid formulation. Meanwhile, the administration of formulated as well as of raw GHRL was performed to evaluate the improvement afforded by the formulation on GHRL transfer (i.e. thanks to the enzymatic protection and / or permeation enhancement).

As the aim of this first experiment has been focussed on a qualitative evaluation of GHRL transfer, fluorescent microscopy was selected as the technique of imagery. By combining the confocal microscopy to new fluorescent markers, it was possible to generate detailed images characterized by a high resolution. By collecting brain slices to analyse them by confocal microscopy after the sacrifice of the animal, this test would help us to assess the transport of GHRL towards the CNS.

Then, a second *in vivo* experiment which also involved nasal administration of fluorescent GHRL in mice was performed to follow the biodistribution of the peptide in living mice. The diffusion of GHRL could be observed for several hours and not only after a single diffusion period, as encountered for the first experiment.

3.2 Materials and methods

3.2.1 Materials

Alexa Fluor® 405 succinimidyl ester dye ($\lambda_{emission}$ 421 nm), Alexa Fluor® 647 isolectin GS-IB_4 conjugate ($\lambda_{emission}$ 669 nm) and DyLight 800 ($\lambda_{emission}$ 794 nm) were purchased from Thermo Fisher Scientific (Waltham, USA). 25-[N-[(7-nitro-2-1,3-benzoxadiazol-4-yl) methyl]amino]-27-norcholesterol (25-NBD-cholesterol, $\lambda_{emission}$ 523 nm) was obtained from Avanti Polar Lipids (Alabaster, USA). Dihexadecyl phosphate (DHDP) and cholesterol (CHOL) were obtained from Sigma Aldrich (St Louis, MO, USA). Synthetic human acylated GHRL (purity ≥ 98%) was purchased from Shanghai Science Peptide Biological Technology co., Ltd (Shanghai, China). Soybean lecithin "Lipoid® S100" (LS100) was purchased from Lipoid® Gmbh (Ludwigshafen, Germany). The chitosan derivative was a HTCC derivative with a MW of 92 kDa, a deacetylation degree of 80% and a substitution degree of 33% (Kitozyme, Herstal, Belgium). Ultrapure water was obtained from a Purelab-Ultra device (Elga). Isoflurane "Isoba®" was purchased from MSD (Kenilworth, USA). Pentobarbital sodium "Nembutal®" was obtained from Ceva Santé Animale (Libourne, France).

3.2.2 Alexa Fluor® 405 grafting on GHRL for CNS transport study

In order to graft Alex Fluor® 405 on the peptide, 20 mg of GHRL were solubilized in 2.0 mL of Na_2CO_3 buffer 0.1 M ([GHRL] =10 mg/mL). Then, 20 µL of a stock solution of Alexa Fluor® 405 (10 mg/mL) in anhydrous DMSO were introduced. The mixture was left for one hour, at room temperature, under magnetic stirring in the dark.

Fluorescently labelled GHRL (F405-GHRL) was separated from unlabelled GHRL by ultrafiltration (Ultracell, Merck Millipore, Darmstadt, Germany). The mixture was passed through membranes with a molecular weight cut-off of 3 kDa. The preparation was filtered until no UV absorbance corresponding to the Alexa Fluor 405® marker could be detected in the filtrate. When the filtration process was completed, the filtrate was lyophilized using an Epsilon 1−6 freeze-dryer (Martin Christ GmbH, Osterode, Germany).

By taking into consideration the absorbance of the conjugate (F405-GHRL) which was evaluated with a UV spectrophotometer (UV Nanophotometer NP80, Implen, Munich, Germany), the Alexa-Fluor 405 dye extinction coefficient ϵ value (34,000 $M^{-1}cm^{-1}$) and its absorbance at λ_{max} (401 nm), it was possible to determine the degree of labelling (DOL) after following the supplier instructions. The DOL represents the average number of dye molecules that reacted with one mole of GHRL: DOL = 0.5.

3.2.3 DyLight® 800 grafting on GHRL for biodistribution study

For GHRL labelling with DyLight® 800, 6 mg of GHRL were solubilized in 1 mL of 0.05 M borate buffer pH 8.5. Then, 250 µL of GHRL were added to 50 µg of DyLight® 800. The mixture was vortexed and left for 3 hours at 37°C. After that, unlabelled GHRL was separated from labelled GHRL (F800-GHRL) using purification resins in microcentrifuge tubes equipped with spin columns. The microcentrifuge tubes were centrifuged for 1 minute at 1000 x g. The purified F800-GHRL was then collected and stored at 4°C. The DOL was calculated in a similar way than that in the previous section (3.2.1) with the λ_{max} (777 nm), the DyLight® extinction coefficient ϵ value (270,000 $M^{-1}cm^{-1}$). The DOL was 0.2.

3.2.4 Preparation of fluorescent HTCC-coated liposomes

For the first experiment (CNS transport study), the protocol used for the preparation of HTCC-coated liposomes was slightly adapted from that previously described (see

section “1.2.5 Preparation of liposomes and HTCC-coated liposomes”). Briefly, in the lipid mixture (100 mg) composed of 45% (w/w) cholesterol, 45% (w/w) LS100 and 10% (DHDP), 1 mg of unlabelled cholesterol was replaced by fluorescent 25-NBD-cholesterol. The purpose was to follow the distribution of liposomes after nasal delivery. Another modification was made during the rehydration step of the lipid film with the 10 mL of PBS pH 7.4, which contained GHRL (1 mg/mL). In the GHRL solution, 300 µg of GHRL were substituted by F405-GHRL to follow the distribution of the drug.

The coating with HTCC was performed as previously described. The formulation process was done in a dark room. The labelled formulation showed similar size distribution and z-average that those from unlabelled liposomes (see section “Appendices II.”).

For the second experiment (biodistribution study), the protocol described in section “1.2.5 Preparation of liposomes and HTCC-coated liposomes” was strictly similar except that 300 µg of GHRL were substituted by F800-GHRL.

3.2.5 Animal care

For CNS transport study, male C57BL/6 mice aged of 6 weeks were purchased from Janvier Labs (Le Genest-Saint-Isle, France). Animals were housed in controlled and standard conditions at 22 ± 2°C, 55 ± 10 % humidity and 12 hours’ light/dark cycle. The mice received a standard pellet diet. The protocol and the experiments were validated by the “Commité d’Ethique du Bien-Etre Animal (CEBEA)” from the Faculty of Medicine (ULB) with the ethical protocol number 608N. The laboratory federal agreement number is LA 1230568.

For biodistribution experiments, female SKH1-Hr mice aged of 6 weeks were ordered from Charles River and animals were housed in the same conditions than previously described. The approved ethical protocol used for this experiment was CMMI-2011-07.

3.2.6 Nasal administration to mice

For both experiments, mice were anesthetized with inhaled isoflurane dispensed with a vaporizer (TemSega, Pessac, France). The anaesthesia induction was done by delivering an isoflurane/oxygen mixture at 4% v/v with a gas flow of 2 L/min in the

induction box. Once the mice were anesthetized, the anaesthesia was maintained using 2% v/v isoflurane at 0.4 L/min.

Each mouse received 8 times 3 µL of liquid (total volume: 24 µL). They were selected depending on the mouse's experimental group. An interval of 3 min between each administration was set up to avoid any discomfort or congestion of the nostril. The liquid was nasally delivered by means of the micro-pipet equipped with non-adhesive tips (Eppendorf, Belgium).

3.2.7 Procedure for CNS transport study

Three groups of mice were defined and compared:

1) The first group (n = 3) was the negative control: PBS (pH 7.4) was nasally administered to the mice

2) The second group (n = 4) received raw F-GHRL solution (not formulated);

3) The third group (n = 4) received the whole fluorescent formulation: F-GHRL loaded in HTCC-coated liposomes

The mice were left for 4 hours to allow the nasal liquids to diffuse. Isolectin GS-IB4 Alexa Fluor® 647 conjugate was intravenously injected 2 hours before sacrifice.

After 4 hours, the mice were sacrificed by intraperitoneal injection of Nembutal®. They were directly perfused with PBS pH 7.4 and a diluted solution of formaldehyde (4% v/v in PBS pH 7.4). The mice were dissected and the brains were isolated to be exposed for an additional 12 hours in 4% v/v of formaldehyde to fix the tissue. Brains were sliced (**Fig. 40**) with the Leica VT1000S vibratome (Wetzlar, Germany) after embedding in agarose gel.

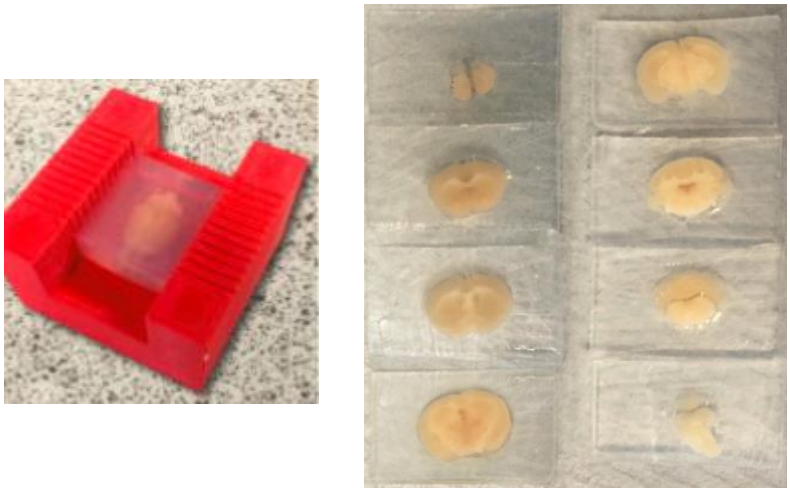

Figure 40. Example of mice brains embedding in agarose gel and 200 µm slices obtained with a vibratome[337]

When slices of 200 µm were obtained, sodium azide (0.01% w/v) diluted in PBS pH 7.4 was added to preserve the tissue until analysis.

Slices were fixed on SuperFrost™ slides (Thermo Fischer Scientific, Aalst, Belgium) in a fluorescent specific medium (Dako, Heverlee, Belgium) and covered with coverslips. The slides were observed under a Leica SP8 confocal microscope (Leica Microsystems, Wetzlar, Germany). The images were processed using ImageJ Software (National Institutes of Health, USA).

3.2.8 Procedure for biodistribution study

The experiment comprised one group of mice (n=2) that were nasally administered with F800-GHRL loaded in HTCC-coated liposomes and administrations were repeated after 1.5 hours. Images were recorded right after the administration and 0.5 hours after. The total number of administrations was 4. Images were recorded with a PhotonIMAGER Optima from Biospace Lab. (Nesles-La-Vallée, France). The excitation wavelength was fixed at 737 nm (cut-off filter 720 – 755 nm) and the emission wavelength was fixed at 797 nm (cut-off filter 780 – 815 nm). Mice were analysed from a dorsal view. At the end of the experiment (+ 5 hours), mice were sacrificed and brains were removed to be individually observed.

3.3 Results and discussion

3.3.1 CNS transport study

After the *in vitro* evaluations, it seemed relevant to confirm that the peptide could reach the brain after its nasal delivery. It should be noticed that the administration was carried out with suitable volumes for mice (20-30 µL) without involving the delivery of unrealistic volumes that could lead to biased conclusions.

The principle of fluorescent labelling of GHRL was to fix the primary amine residues present on the peptide core with a suitable marker. For instance, the GHRL peptide core contains 4 lysine residues with primary amines which were suitable candidates for the probes binding. The first fluorescent marker that was tested was N-hydroxysuccinimide fluorescein ester (NHS-fluorescein). This NHS-activated derivative had a high affinity for primary amines. However, once GHRL was labelled, this marker drastically decreased the solubility of the peptide until its precipitation. It also appeared that this marker was not bright enough to get high resolution pictures after nasal administration.

Therefore, it was decided to evaluate Alexa Fluor® derivatives. Indeed, they are amine reactive labelling compounds with high water solubility combined to brighter signal[338]. An efficient GHRL labelling could be obtained with a very sensitive conjugate.

Isolectin GS-IB4 Alexa Fluor 647 was injected to mice because this fluorescent dye had a very high affinity for brain macroglial and perivascular cells. It was a proper control to confirm that the area analysed by confocal microscopy was effectively located in the brain[248].

The area of the brain that was analysed by confocal microscopy was essentially the olfactory bulb (**Fig. 41**). Indeed, when a nose-to-brain transfer is taking place via the olfactory pathway, this is the first area of the brain where the drug can be recovered[4].

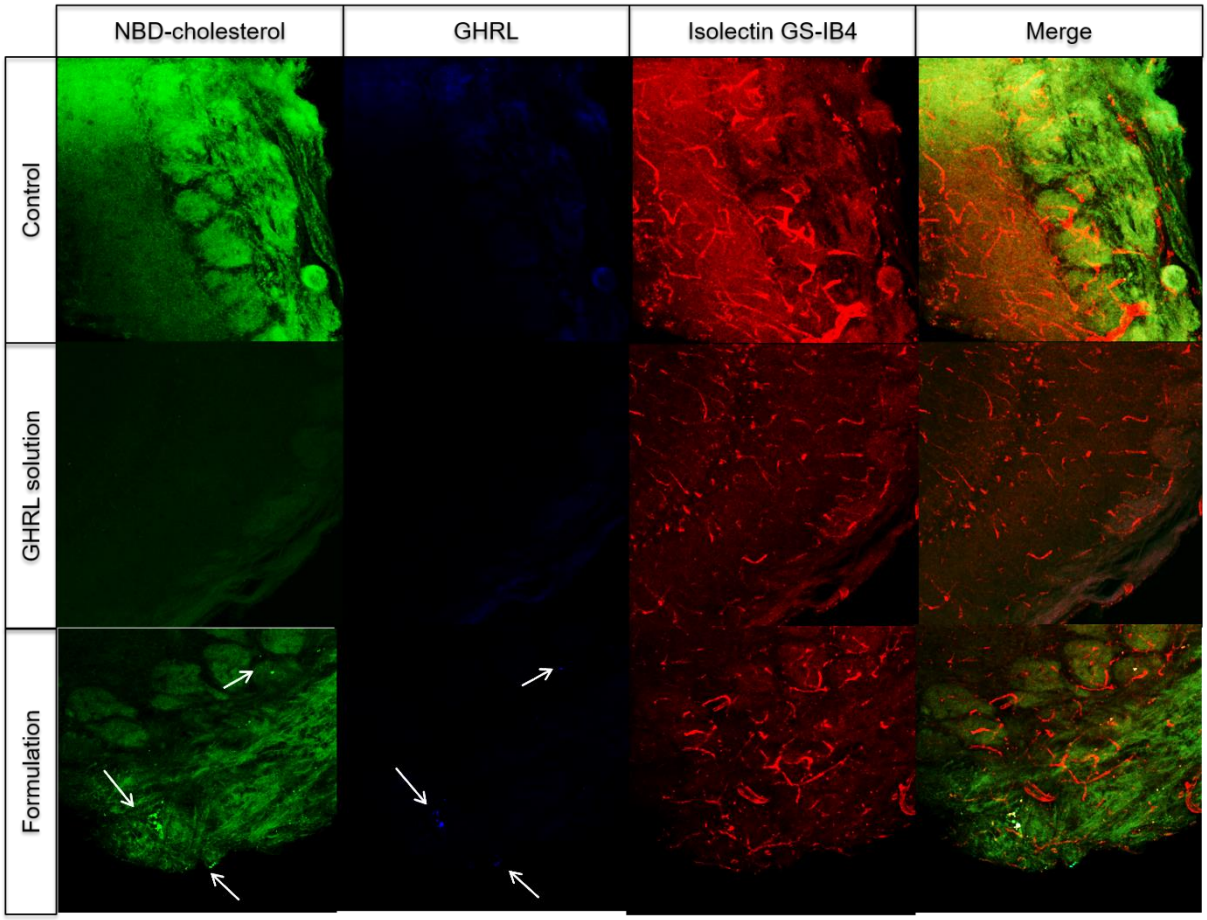

Figure 41. Pictures obtained by fluorescent confocal microscopy in the mice olfactory bulb with the control (PBS pH 7.4), the GHRL solution (mixture F405-GHRL/GHRL in PBS pH 7.4) and the formulation (mixture F405-GHRL/GHRL loaded in HTCC-AL). The diffusion period was 4 hours. Green = 25-NBD-cholesterol, blue = Alexa Fluor® 405-labelled GHRL, red = Isolectin GS-IB4 – Alex Fluor® 647 conjugate.

As it was expected, no bright fluorescence could be observed with the negative control. After the administration of F405-GHRL in solution, similar observation was made with no fluorescence in the olfactory bulb. This suggested that the nasal administration of free GHRL in solution did not allow the transfer of the peptide from the nose to the brain.

Using HTCC-coated liposomes, a slight signal could be obtained for both F405-GHRL (in blue) and liposomes (in green). Unfortunately, a low green fluorescent contamination in the NBD-cholesterol signal was encountered due to the brain cells green autofluorescence[339]. Interestingly, a co-location of both entities could be highlighted suggesting that, after 4 hours of diffusion, the peptide still remained

entrapped in the liposomes. The formulation was able to provide a nose-to-brain delivery of GHRL. However, the signal still remained limited to only a restricted number of fluorescent particles. This observation could be differently hypothesized. The main, and probably the most reasonable hypothesis, was the unsuitable kinetic of the experiment. Indeed, as it was the first *in vivo* trial, the rate of diffusion of GHRL from the nose to the brain was unknown. Therefore, in order to avoid a too early animal sacrifice, a relatively long period of diffusion (4 hours) was selected. Indeed, the diffusion time before animal sacrifice was difficult to establish as some *in vivo* experiments reported a nose-to-brain transfer only a few minutes after the nasal delivery, while other studies described a diffusion to the brain from 1 hour to several hours after the nasal administration[148,340].

However, these results have showed that the developed formulation was able to promote the diffusion of GHRL from the nose to the brain.

3.3.2 Biodistribution study

In this part, the objective was to evaluate the biodistribution of GHRL in real time after its nasal administration. Crucial information could be collected such as the residence time of the formulation in the nasal cavity as well as the rate at which it is cleaned from it or the potential accumulation of F800-GHRL in different sections of the body. As the number of meals per mice can be comprised in the range “2 – 50” per day, it was decided to proceed with repeated F800-GHRL administrations in order to reproduce the GHRL secretion peaks naturally encountered in mice organisms[341].

As it can be seen, the formulation exhibited an enhanced residence time as F800-GHRL was accumulated in the olfactory region of the nasal cavity (**Fig. 42**). However, no signal could be observed in the olfactory bulb of the brain which is located between both eyeballs (**Fig. 43**). Based on the low signal observed from the CNS transport study, it was considered that the sensitivity of the imagery technique used (i.e. fluorescence optical imaging) was not high enough to detect such small amounts of F800-GHRL that could potentially be transferred to the brain.

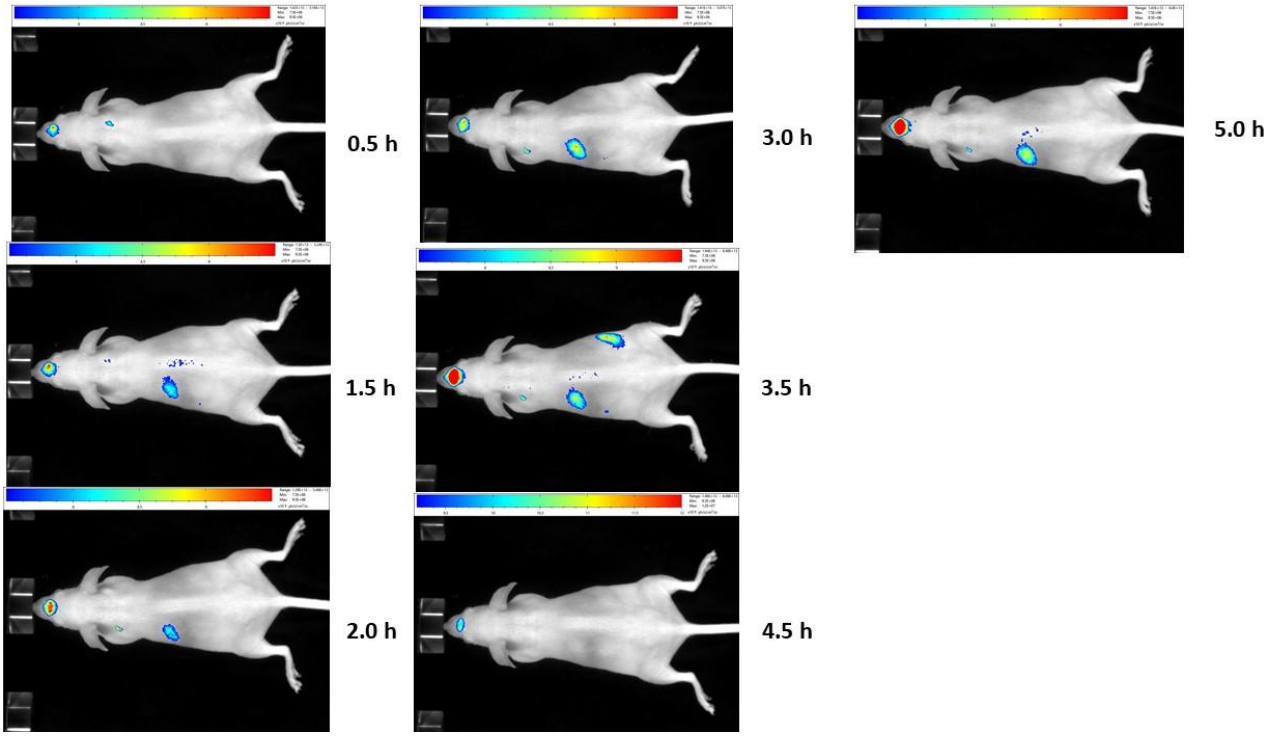

Figure 42. Fluorescent images obtained after nasal administration of F800-GHRL loaded in the HTCC-AL formulation in function of the time. Nasal administrations were performed at: t=0h, t=1.5h, t=3h, t=4.5h

It was decided to remove the brain of the mouse at the end of the experiment (t = 5h). The purpose was to analyse the brain alone without skin on the upper side that could potentially reduce the signal emitted.

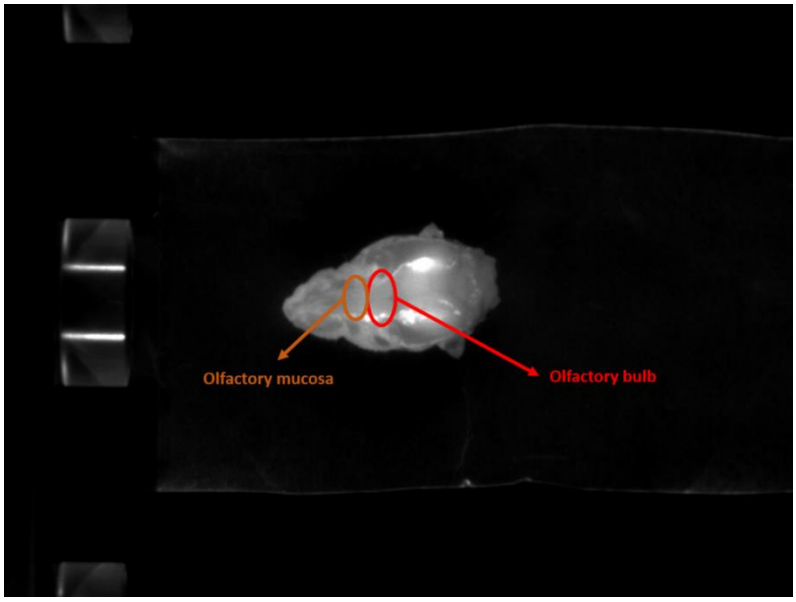

Figure 43. Localizations of the nasal olfactory mucosa and the brain olfactory bulb in mouse head

When the brain was removed, no signal could be observed. However, when the lower part of the cranial cavity was exposed for the instrument detection without the brain over it, a signal could be highlighted (**Fig. 44**). This signal was located inside the cranial cavity where the brain was located. More precisely, the signal was emitted from the cribriform plate which is the area of the brain that supports the olfactory bulb and is localized next to the nasal olfactory mucosa. This zone is called “cribriform plate” because it is a perforated bone which is traversed by olfactory nerves. This observation supported the fact that a nose-to-brain transfer was taking place. The cribriform plate being a very small area, it was possible to detect a signal as F800-GHRL was concentrated in this anatomical site. Unfortunately, after diffusion, F800-GHRL was diluted in the rest of the brain such as in the cerebrospinal fluid and could not be detected anymore.

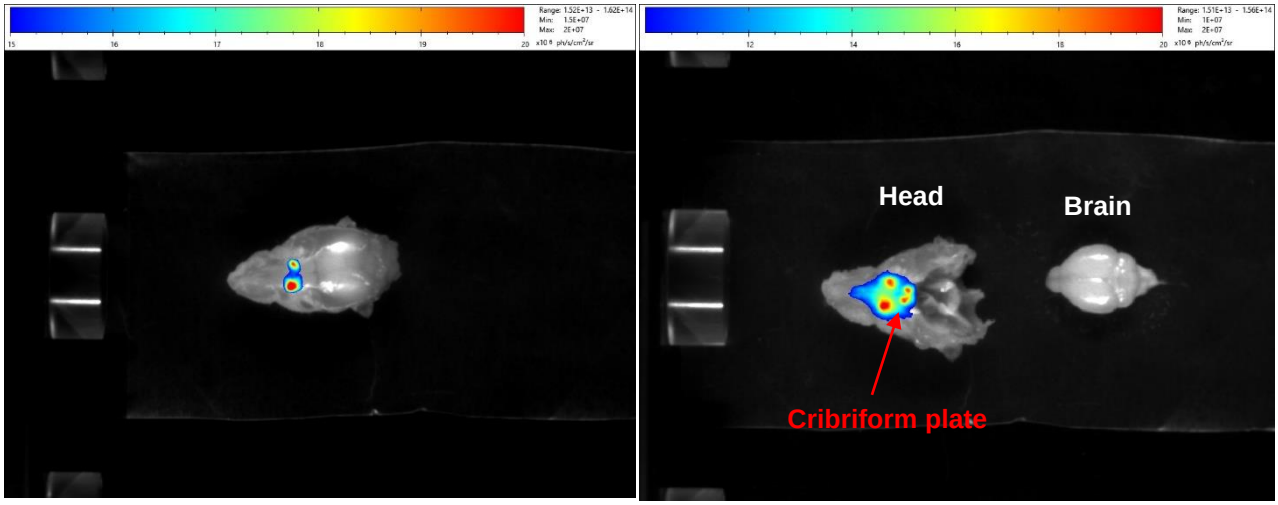

Figure 44. Images collected at the end of the experiment (t = 5h) with the whole head of the mouse (on the left) and the brain extracted from the head of the mouse with the signal emitted from the cribriform plate (on the right)

3.4 Conclusion

The CNS transport study confirmed that the HTCC-AL formulation was a mandatory vehicle to allow GHRL reaching the brain. Indeed, without formulation, no GHRL could be recovered in the olfactory bulbs. However, the F405-GHRL signal was very low.

The biodistribution study provided information regarding the residence time of the formulation in the nasal cavity. Moreover, it was shown that F800-GHRL could penetrate the cranial cavity after a nasal administration. However, further studies

should be conducted to better understand the behaviour of the formulation after its nasal administration. The powder state formulation should also be tested as it could provide higher GHRL diffusion towards the brain (based on *in* vitro results previously obtained).

For further *in vivo* studies, alternative techniques of labelling could be considered, such as the radiolabelling, in order to collect detailed quantitative results. For instance, by combining PET-Scan to radioactive isotope (e.g. Fluor-18), it could be possible to accurately quantify the amount of GHRL that could diffuse in very restricted anatomical sites (e.g. hypothalamus).

Such study should also compare both nasal and intravenous administrations of the formulation. This would help to highlight the potential higher brain transfer of the peptide after its nasal administration compared to that from the amount that reached the systemic circulation before reaching the brain.

VII. CONCLUSION AND PERSPECTIVE

Although the nasal administration has been widely used for both local and systemic delivery, the development of nose-to-brain delivery may be considered as quite recent. It is well-known that the brain is very efficiently protected by the BBB. Therefore, reaching the brain with drugs to treat neurological disorders and/or symptoms is very challenging. Bypassing the BBB from the nose-to-brain pathway would make the brain easier to access.

Moreover, the direct transfer to the central nervous system would make the administration of biomolecules more effective due to the potential lower degradation and the higher drug levels recovered in the brain. Nose-to-brain delivery would also be perfectly suitable for diseases requiring chronic administrations. Indeed, due to the non-invasiveness and the ease of administration that it affords, this route of administration may increase the compliance of patients.

Being awarded of such advantages, the interest of developing nose-to-brain delivery systems has been growing up during the last two decades as it can be observed by the tremendous increase of scientific publications (**Fig. 45**)

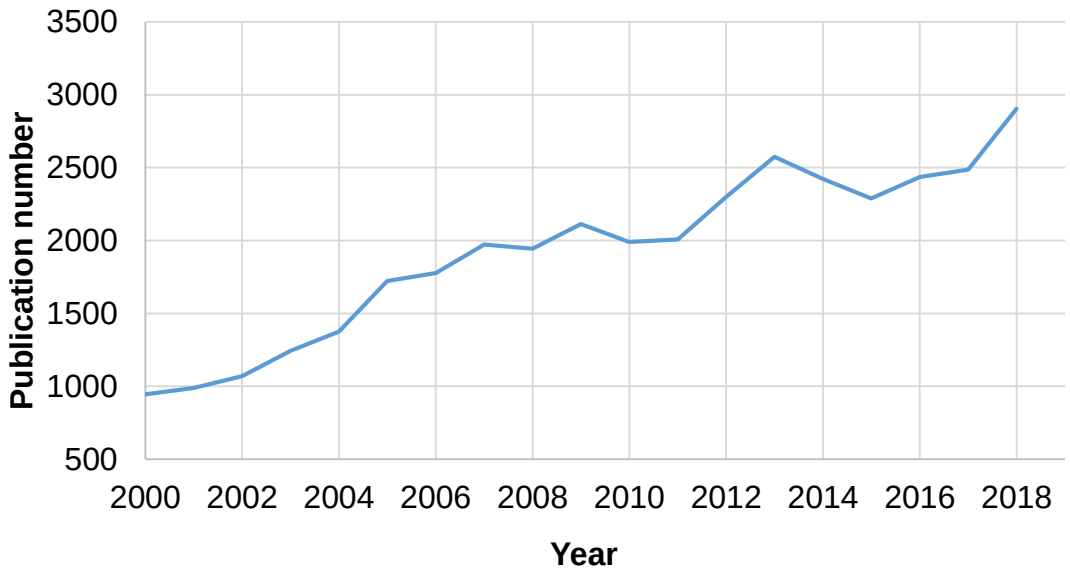

Figure 45. Evolution of the publication number addressing the nose-to-brain delivery between 2000 and 2018 (Elsevier Science Direct in February 11th 2019)

Despite the benefits previously described, the number of medicines involving the nose-to-brain pathway reaching the pharmaceutical market is still very low. This could be due to the difficulty to design adequate pre-clinical studies that really demonstrate the

superior effectiveness, or at least the efficacy, of the nose-to-brain pathway to reach the brain. In addition, there are still some gaps in proving the safety of such administration and the control/reproducibility of this transfer[342]. For instance, by making the olfactory mucosa more permeable, some undesirables pathogens or exogen's may also reach the brain. Additional issues related to the structure of the nasal cavity may also be encountered such as the limited volume of formulation that can be delivered (liquid formulation: 100 - 200 µL) or the ability to target the deposition in the olfactory mucosa. Moreover, the difficulty to standardize the deposition of the in the nasal cavity make the commercialization of such therapeutics quite difficult. One of the major factor which limits the reproducibility of such delivery is the inter-individual variability of the nasal cavity anatomy.

However, due to the growing interest that is focused on this route of administration as well as due to the new available technologies, researchers are developing experimental apparatus that make it possible to better evaluate the repeatability of the nasal deposition. It is also possible to involve anatomical modifications (e.g. nasal septum deviation) to study their effects on aerosol behaviours in the nasal cavity.

Recent studies have been focused on nasal drug distribution under the influence of the patient's inspiratory flow or on development of nasal inlet ports coupled to cascade impactors which were supposed to better mimic the respiratory tract[343,344]. The establishment of new *in vitro* methods, more representative of the nasal cavity, should lead to the marketing of much better characterized medicines which could consider the different properties of the nasal cavity.

In this work, it was proposed to develop a peptide-based nose-to-brain delivery system which could be able to afford the protection to the peptide, an increase of its permeability through the nasal mucosa and an enhanced residence time in the nasal cavity.

The first part of this work was focused on pre-formulation studies to evaluate the physico-chemical properties of the selected model peptide, Ghrelin (GHRL). This peptide appeared to be very sensitive when exposed to alkaline media and heat.

The first developed formulation was based on micelles made of phospholipids coupled with pegylated branches (DSPE-PEG 2000). The formulation has shown suitable mean diameter and size distribution as well as the high yield of encapsulation. However, although these pegylated micelles were supposed to enhance the penetration of the

formulation through the mucus, such increase was not observed during the permeation test that was conducted on Calu-3 cells monolayer. Therefore, the development of micelle-based formulations was aborted.

The second formulation was based on the use of AL coated with HTCC. By modulating the net charge of the liposomes, it was shown that the loading of GHRL was increased from anionic liposomes compared to that from cationic system. ITC measurements allowed demonstrating that such increase was due to spontaneous interaction between the anionic charge of the liposomes and the cationic charge of GHRL. Moreover, AL showed increased protection abilities when the formulation was subjected to enzymatic digestion of TRYP and CES-1. HTCC-coated AL allowed binding high amount of soluble mucins which suggested a potential prolonged residence time in the nasal cavity. The combination of the AL with chitosan also showed a significant effect on the diffusion of GHRL through cell monolayer models. This effect was probably due to the opening of tight junctions which was confirmed by TEER measurements.

Once introduced into the VP3 nasal device, the measurement of the droplets size distribution in the aerosol was assessed. It appeared that the size distribution was adequate for intranasal administration, with a very limited portion of the population smaller than 10 µm.

In the second part of the project, starting from the liquid formulation, a dry powder formulation was developed and characterized. The drying process, which was done by spray-drying, could have been optimized using a design of experiment compared to the liquid formulation, it was shown that the dry system provided higher stability during storage, increased mucoadhesion and enhanced diffusion through Calu-3 cells model.

Finally, the use of nasal cast allowed demonstrating that the targeted delivery in the olfactory area could be achieved with an adequate formulation as well as suitable nasal device.

In vivo evaluations have shown that formulating GHRL was essential to reach the olfactory bulb. However, due to the low amount of peptide that reached the brain, the signal was too low to get relevant data. The transfer from the nose towards the brain was also confirmed by the biodistribution study however the imagery technique selected was not sensitive enough to detect a signal in the brain.

Therefore, further experiments should be performed to better evaluate both kinetic and quantitative aspects. Additional experiments should be focused on the drug distribution following nasal and intravenous administrations to highlight the benefit of the nose-to-brain pathway. Ideally, the technique selected should combine high sensitivity with qualitative/quantitative data. Moreover, in case of promising results, it would be mandatory to perform similar evaluation in humans. Indeed, the anatomical structure of the nasal cavity is known to be drastically different between murine species and humans (ex: area occupied by the olfactory zone). For nose-to-brain transfer, it is quite difficult to extrapolate conclusions obtained from animals to humans.

To conclude, the formulation that was developed in this work may be a promising alternative to relief patients suffering from cachectic syndrome. Indeed, up to now, no standard treatment was developed for the management of cancer cachexia. Among the various drugs that were tested for this application (i.e appetite stimulants, progestational drugs, corticosteroids, etc), none could be considered as new therapeutic option[345]. Therefore, there is a great demand for the establishment of such new treatment. GHRL, thanks to its multiple effects on inflammation, on appetite and on various other anabolic effects, could be a promising candidate. By combining it with nose-to-brain delivery, the patients affected by cachexia could find an effective and convenient treatment.

In the near future, it could be also interesting to consider the nose-to-brain administration of anamorelin, the synthetic agonist of GHRL receptors “GHSR-1a”. Indeed, thanks to its low molecular weight (546.7 g/mol) and to its good stability , an efficient treatment could be developed. By combining these drug properties to the nose-to-brain delivery, significant anamorelin levels could be recovered in the brain, and this after involving limited amounts of drug in the nasal cavity.

VIII. BIBLIOGRAPHY

1. Gizurarson, S. The relevance of nasal physiology to the design of drug absorption studies. *Adv. Drug Deliv. Rev.* **11,** 329–347 (1993).

2. England, R. J., Homer, J. J., Knight, L. C. & Ell, S. R. Nasal pH measurement: a reliable and repeatable parameter. *Clin. Otolaryngol. Allied Sci.* **24,** 67–8 (1999).

3. Illum, L. Nasal Delivery. The Use of Animal Models to Predict Performance in Man. *J. Drug Target.* **3,** 427–442 (1996).

4. Gänger, S. & Schindowski, K. Tailoring Formulations for Intranasal Nose-to-Brain Delivery: A Review on Architecture, Physico-Chemical Characteristics and Mucociliary Clearance of the Nasal Olfactory Mucosa. *Pharmaceutics* **10,** 116 (2018).

5. Dhuria, S. V., Hanson, L. R. & Frey, W. H. Intranasal delivery to the central nervous system: Mechanisms and experimental considerations. *J. Pharm. Sci.* **99,** 1654–1673 (2010).

6. Gizurarson, S. Anatomical and histological factors affecting intranasal drug and vaccine delivery. *Curr. Drug Deliv.* **9,** 566–82 (2012).

7. Beule, A. G. Physiology and pathophysiology of respiratory mucosa of the nose and the paranasal sinuses. *GMS Curr. Top. Otorhinolaryngol. Head Neck Surg.* **9,** Doc07 (2010).

8. Cole, P. Nasal and oral airflow resistors. Site, function, and assessment. *Arch. Otolaryngol. Head. Neck Surg.* **118,** 790–3 (1992).

9. Mitra, A. K., Kwatra, D. & Vadlapudi, A. D. *Drug Delivery*. (Jones & Bartlett Learning, LLC, 2014).

10. Illum, L. Is nose-to-brain transport of drugs in man a reality? *J. Pharm. Pharmacol.* **56,** 3–17 (2004).

11. Hillery, A. M. & Park, K. *Drug Delivery: Fundamentals and Applications, Second Edition*. (CRC Press, 2016).

12. Lochhead, J. J. & Thorne, R. G. Intranasal delivery of biologics to the central nervous system. *Adv. Drug Deliv. Rev.* **64,** 614–628 (2012).

13. Jafek, B. W., Murrow, B., Michaels, R., Restrepo, D. & Linschoten, M. Biopsies of Human Olfactory Epithelium. *Chem. Senses* **27,** 623–628 (2002).

14. Morrison, E. E. & Costanzo, R. M. Morphology of the human olfactory epithelium. *J. Comp. Neurol.* **297,** 1–13 (1990).

15. Olfactory epithelium | anatomy | Britannica.com. Available at: https://www.britannica.com/science/olfactory-epithelium/media/427517/48235. (Accessed: 13th March 2019)

16. Graziadei, P. P. C. The Olfactory Mucosa of Vertebrates. in 27–58 (Springer, Berlin, Heidelberg, 1971). doi:10.1007/978-3-642-65126-7_2

17. Pardeshi, C. V. & Belgamwar, V. S. Direct nose to brain drug delivery via integrated nerve pathways bypassing the blood–brain barrier: an excellent platform for brain targeting. *Expert Opin. Drug Deliv.* **10,** 957–972 (2013).

18. Merkus, Verhoef, Schipper & Marttin. Nasal mucociliary clearance as a factor in nasal drug delivery. *Adv. Drug Deliv. Rev.* **29,** 13–38 (1998).

19. Kaliner, M., Marom, Z., Patow, C. & Shelhamer, J. Human respiratory mucus. *J. Allergy Clin. Immunol.* **73,** 318–23 (1984).

20. D'Souza, M. J. *Nanoparticulate Vaccine Delivery Systems*. (Pan Stanford Publishing, 2015).

21. Mistry, A., Stolnik, S. & Illum, L. Nanoparticles for direct nose-to-brain delivery of drugs. *Int. J. Pharm.* **379,** 146–157 (2009).

22. Sarkar, M. A. Drug metabolism in the nasal mucosa. *Pharm. Res.* **9,** 1–9 (1992).

23. Meredith, S. D., Raphael, G. D., Baraniuk, J. N., Banks, S. M. & Kaliner, M. A. The pathophysiology of rhinitis. III. The control of IgG secretion. *J. Allergy Clin. Immunol.* **84,** 920–30 (1989).

24. Swart, S. J. *et al.* Immunoglobulin concentrations in nasal secretions differ between patients with an IgE-mediated rhinopathy and a non-IgE-mediated rhinopathy. *J. Allergy Clin. Immunol.* **88,** 612–9 (1991).

25. Browning, S., Housley, D., Richards, R. & Eccles, R. The Effects of Oxymetazoline on Lysozyme Secretion from the Human Nasal Mucosa. *Acta Otolaryngol.* **117,** 851–855 (1997).

26. Cohen, N. A. Sinonasal mucociliary clearance in health and disease. *Ann. Otol. Rhinol. Laryngol. Suppl.* **196,** 20–6 (2006).

27. Stevenson, B. R., Anderson, J. M., Goodenough, D. A. & Mooseker, M. S. Tight junction structure and ZO-1 content are identical in two strains of Madin-Darby canine kidney cells which differ in transepithelial resistance. *J. Cell Biol.* **107,** 2401–8 (1988).

28. McMartin, C., Hutchinson, L. E., Hyde, R. & Peters, G. E. Analysis of structural requirements for the absorption of drugs and macromolecules from the nasal cavity. *J. Pharm. Sci.* **76,** 535–40 (1987).

29. Pires, A., Fortuna, A., Alves, G. & Falcão, A. Intranasal drug delivery: how, why and what for? *J. Pharm. Pharm. Sci.* **12,** 288–311 (2009).

30. Csaba, N., Garcia-Fuentes, M. & Alonso, M. J. Nanoparticles for nasal vaccination. *Adv. Drug Deliv. Rev.* **61,** 140–157 (2009).

31. Davis, S. S. Nasal vaccines. *Adv. Drug Deliv. Rev.* **51,** 21–42 (2001).

32. Terauchi, Y. *et al.* IgA polymerization contributes to efficient virus neutralization on human upper respiratory mucosa after intranasal inactivated influenza vaccine administration. *Hum. Vaccin. Immunother.* 00–00 (2018). doi:10.1080/21645515.2018.1438791

33. Dehghan, S., Kheiri, M. T., Abnous, K., Eskandari, M. & Tafaghodi, M. Preparation, characterization and immunological evaluation of alginate nanoparticles loaded with whole inactivated influenza virus: Dry powder formulation for nasal immunization in rabbits. *Microb. Pathog.* **115,** 74–85 (2018).

34. Bahamondez-Canas, T. F. & Cui, Z. Intranasal immunization with dry powder vaccines. *Eur. J. Pharm. Biopharm.* **122,** 167–175 (2018).

35. Thorne, R. G., Pronk, G. J., Padmanabhan, V. & Frey Ii, W. H. Delivery of insulin-like growth factor-I to the rat brain and spinal cord along olfactory and trigeminal

pathways following intranasal administration. *Neuroscience* **127,** 481–496 (2004).

36. Westin, U. E., Boström, E., Gråsjö, J., Hammarlund-Udenaes, M. & Björk, E. Direct Nose-to-Brain Transfer of Morphine After Nasal Administration to Rats. *Pharm. Res.* **23,** 565–572 (2006).

37. Giuliani, A. *et al. In vivo* nose-to-brain delivery of the hydrophilic antiviral ribavirin by microparticle agglomerates. *Drug Deliv.* **25,** 376–387 (2018).

38. Haque, S., Md, S., Sahni, J. K., Ali, J. & Baboota, S. Development and evaluation of brain targeted intranasal alginate nanoparticles for treatment of depression. *J. Psychiatr. Res.* **48,** 1–12 (2014).

39. Vyas, T. K., Shahiwala, A., Marathe, S. & Misra, A. Intranasal drug delivery for brain targeting. *Curr. Drug Deliv.* **2,** 165–75 (2005).

40. Samaridou, E. & Alonso, M. J. Nose-to-brain peptide delivery – The potential of nanotechnology. *Bioorg. Med. Chem.* **26,** 2888–2905 (2018).

41. Landis, M. S., Boyden, T. & Pegg, S. Nasal-to-CNS drug delivery: where are we now and where are we heading? An industrial perspective. *Ther. Deliv.* **3,** 195–208 (2012).

42. Morrison, E. E. & Costanzo, R. M. Morphology of olfactory epithelium in humans and other vertebrates. *Microsc. Res. Tech.* **23,** 49–61 (1992).

43. Ma, J. K. H. & Hadzija, B. *Basic physical pharmacy*. (Jones & Bartlett Learning, 2013).

44. Yeh, T.-H. *et al.* Mechanism and consequence of chitosan-mediated reversible epithelial tight junction opening. *Biomaterials* **32,** 6164–73 (2011).

45. Thorne, R. G. & Frey, W. H. Delivery of Neurotrophic Factors to the Central Nervous System. *Clin. Pharmacokinet.* **40,** 907–946 (2001).

46. Gizurarson, S., Thorvaldsson, T., Sigurdsson, P. & Gunnarsson, E. Selective delivery of insulin into the brain: Intraolfactory absorption. *Int. J. Pharm.* **140,** 77–83 (1996).

47. Gozes, I. *et al.* Neuroprotective strategy for Alzheimer disease: intranasal administration of a fatty neuropeptide. *Proc. Natl. Acad. Sci. U. S. A.* **93,** 427–32 (1996).

48. Liu, Q. *et al.* Nose-to-Brain Transport Pathways of Wheat Germ Agglutinin Conjugated PEG-PLA Nanoparticles. *Pharm. Res.* **29,** 546–558 (2012).

49. Ruigrok, M. J. R. & de Lange, E. C. M. Emerging Insights for Translational Pharmacokinetic and Pharmacokinetic-Pharmacodynamic Studies: Towards Prediction of Nose-to-Brain Transport in Humans. *AAPS J.* **17,** 493–505 (2015).

50. Illum, L. Transport of drugs from the nasal cavity to the central nervous system. *Eur. J. Pharm. Sci.* **11,** 1–18 (2000).

51. Oberdörster, G., Elder, A. & Rinderknecht, A. Nanoparticles and the brain: cause for concern?. *J. Nanosci. Nanotechnol.* **9,** 4996–5007 (2009).

52. Bourganis, V., Kammona, O., Alexopoulos, A. & Kiparissides, C. Recent advances in carrier mediated nose-to-brain delivery of pharmaceutics. *Eur. J.*

Pharm. Biopharm. **128,** 337–362 (2018).

53. Djupesland, P. G. Nasal drug delivery devices: characteristics and performance in a clinical perspective—a review. *Drug Deliv. Transl. Res.* **3,** 42–62 (2013).

54. Bhise, S. B., Yadav, A. V., Avachat, A. M. & Malayandi, R. Bioavailability of intranasal drug delivery system. **2,**

55. Kulkarni, V. S. & Shaw, C. *Essential chemistry for formulators of semisolid and liquid dosages*.

56. Tiozzo Fasiolo, L. *et al.* Opportunity and challenges of nasal powders: Drug formulation and delivery. *Eur. J. Pharm. Sci.* **113,** 2–17 (2018).

57. Yellepeddi, V. K. Stability of extemporaneously prepared preservative-free prochlorperazine nasal spray. *Am. J. Heal. Pharm.* **75,** e28–e35 (2018).

58. Kublik, H. & Vidgren, M. . Nasal delivery systems and their effect on deposition and absorption. *Adv. Drug Deliv. Rev.* **29,** 157–177 (1998).

59. Thorat, S. Formulation and Product Development of Nasal Spray: An Overview. *Sch. J. Appl. Med. Sci. Sch. J. App. Med. Sci* **4,** (2016).

60. Kushwaha, S. K. S., Keshari, R. K. & Rai, A. K. Advances in nasal trans-mucosal drug delivery. *J. Appl. Pharm. Sci.* 21–28 (2011).

61. Illum, L., Jabbal-Gill, I., Hinchcliffe, M., Fisher, A. N. & Davis, S. S. Chitosan as a novel nasal delivery system for vaccines. *Adv. Drug Deliv. Rev.* **51,** 81–96 (2001).

62. Tanaka, A. *et al.* Nasal Drug Absorption from Powder Formulations: Effect of Fluid Volume Changes on the Mucosal Surface. *Biol. Pharm. Bull.* **40,** 212–219 (2017).

63. Colombo, G. *et al.* Brain distribution of ribavirin after intranasal administration. *Antiviral Res.* **92,** 408–414 (2011).

64. Tanaka, A. *et al.* Nasal Absorption of Macromolecules from Powder Formulations and Effects of Sodium Carboxymethyl Cellulose on Their Absorption. *PLoS One* **11,** e0159150 (2016).

65. Morimoto, K. *et al.* Evaluation of gelatin microspheres for nasal and intramuscular administrations of salmon calcitonin. *Eur. J. Pharm. Sci.* **13,** 179–85 (2001).

66. Ishikawa, F. *et al.* Insoluble Powder Formulation as an Effective Nasal Drug Delivery System. *Pharm. Res.* **19,** 1097–1104 (2002).

67. Ilium, L. Chitosan and Its Use as a Pharmaceutical Excipient. *Pharm. Res.* **15,** 1326–1331 (1998).

68. Pozzoli, M. *et al.* Dry powder nasal drug delivery: challenges, opportunities and a study of the commercial Teijin Puvlizer Rhinocort device and formulation. *Drug Dev. Ind. Pharm.* **42,** 1660–1668 (2016).

69. Huang, J. *et al.* A novel dry powder influenza vaccine and intranasal delivery technology: induction of systemic and mucosal immune responses in rats. *Vaccine* **23,** 794–801 (2004).

70. Reno, F. E. *et al.* A novel nasal powder formulation of glucagon: toxicology studies in animal models. *BMC Pharmacol. Toxicol.* **16,** (2015).

71. Silberstein, S. *et al.* Early Onset of Efficacy and Consistency of Response Across Multiple Migraine Attacks From the Randomized COMPASS Study: AVP-825 Breath Powered ® Exhalation Delivery System (Sumatriptan Nasal Powder) vs Oral Sumatriptan. *Headache J. Head Face Pain* **57,** 862–876 (2017).

72. Pringels, E. *et al.* Influence of deposition and spray pattern of nasal powders on insulin bioavailability. *Int. J. Pharm.* **310,** 1–7 (2006).

73. Coucke, D. *et al.* Influence of heat treatment on spray-dried mixtures of Amioca® starch and Carbopol® 974P used as carriers for nasal drug delivery. *Int. J. Pharm.* **378,** 45–50 (2009).

74. Nagarwal, R. C. & Pandit, J. K. Phase transition system: novel oral in-situ gel. *Curr. Drug Deliv.* **5,** 282–9 (2008).

75. Galgatte, U. C., Kumbhar, A. B. & Chaudhari, P. D. Drug Delivery Development of in situ gel for nasal delivery: design, optimization, in vitro and in vivo evaluation. *Drug Deliv* **21,** 62–73 (2014).

76. Karavasili, C. & Fatouros, D. G. Smart materials: in situ gel-forming systems for nasal delivery. *Drug Discov. Today* **21,** 157–166 (2016).

77. Kouchak, M. In situ gelling systems for drug delivery. *Jundishapur J. Nat. Pharm. Prod.* **9,** e20126 (2014).

78. Paul, A., Fathima, K. M. & Nair, S. C. Intra Nasal In situ Gelling System of Lamotrigine Using Ion Activated Mucoadhesive Polymer. *Open Med. Chem. J.* **11,** 222–244 (2017).

79. Shah, R. A., Mehta, M. R., Patel, D. M. & Patel, C. N. Design and optimization of mucoadhesive nasal in situ gel containing sodium cromoglycate using factorial design. *Asian J. Pharm. Free full text Artic. from Asian J Pharm* **5,** (2014).

80. Sherafudeen, S. P. & Vasantha, P. V. Development and evaluation of in situ nasal gel formulations of loratadine. *Res. Pharm. Sci.* **10,** 466–76 (2015).

81. Sonvico, F. *et al.* Surface-Modified Nanocarriers for Nose-to-Brain Delivery: From Bioadhesion to Targeting. *Pharmaceutics* **10,** 34 (2018).

82. Merkus, F. W. H. M., Schipper, N. G. M., Hermens, W. A. J. J., Romeijn, S. G. & Verhoef, J. C. Absorption enhancers in nasal drug delivery: efficacy and safety. *J. Control. Release* **24,** 20–208 (1993).

83. Morimoto, K., Miyazaki, M. & Kakemi, M. Effects of proteolytic enzyme inhibitors on nasal absorption of salmon calcitonin in rats. *Int. J. Pharm.* **113,** 1–8 (1995).

84. Greimel, A., Bernkop-Schnürch, A., Dorly Del Curto, M. & D'Antonio, M. Transport Characteristics of a Beta Sheet Breaker Peptide Across Excised Bovine Nasal Mucosa. *Drug Dev. Ind. Pharm.* **33,** 71–77 (2007).

85. Shinichiro, H., Takatsuka, Y. & Hiroyuki, M. Mechanisms for the enhancement of the nasal absorption of insulin by surfactants. *Int. J. Pharm.* **9,** 173–184 (1981).

86. Warnken, Z. N. *et al.* Formulation and device design to increase nose to brain drug delivery. *J. Drug Deliv. Sci. Technol.* **35,** 213–222 (2016).

87. Charlton, S., Jones, N. S., Davis, S. S. & Illum, L. Distribution and clearance of bioadhesive formulations from the olfactory region in man: Effect of polymer type and nasal delivery device. *Eur. J. Pharm. Sci.* **30,** 295–302 (2007).

88. Patil, K., Yeole, P., Gaikwad, R. & Khan, S. Brain targeting studies on buspirone hydrochloride after intranasal administration of mucoadhesive formulation in rats. *J. Pharm. Pharmacol.* **61,** 669–675 (2009).

89. Harding, S. E. *Mucoadhesive interactions*. *Biochemical Society Transactions* **31,** (2003).

90. Yeh, T.-H. *et al.* Mechanism and consequence of chitosan-mediated reversible epithelial tight junction opening. *Biomaterials* **32,** 6164–6173 (2011).

91. Luppi, B., Bigucci, F., Cerchiara, T. & Zecchi, V. Chitosan-based hydrogels for nasal drug delivery: from inserts to nanoparticles. *Expert Opin. Drug Deliv.* **7,** 811–28 (2010).

92. Mourya, V. K. & Inamdar, N. N. Trimethyl chitosan and its applications in drug delivery. *J. Mater. Sci. Mater. Med.* **20,** 1057–1079 (2009).

93. Bhavna *et al.* Donepezil nanosuspension intended for nose to brain targeting: In vitro and in vivo safety evaluation. *Int. J. Biol. Macromol.* **67,** 418–425 (2014).

94. Khan, S., Patil, K., Bobade, N., Yeole, P. & Gaikwad, R. Formulation of intranasal mucoadhesive temperature-mediated *in situ* gel containing ropinirole and evaluation of brain targeting efficiency in rats. *J. Drug Target.* **18,** 223–234 (2010).

95. Bshara, H., Osman, R., Mansour, S. & El-Shamy, A. E.-H. A. Chitosan and cyclodextrin in intranasal microemulsion for improved brain buspirone hydrochloride pharmacokinetics in rats. *Carbohydr. Polym.* **99,** 297–305 (2014).

96. Wang, X., Chi, N. & Tang, X. Preparation of estradiol chitosan nanoparticles for improving nasal absorption and brain targeting. *Eur. J. Pharm. Biopharm.* **70,** 735–740 (2008).

97. Gavini, E. *et al.* Mucoadhesive microspheres for nasal administration of cyclodextrins. *J. Drug Target.* **17,** 168–179 (2009).

98. Mistry, A., Stolnik, S. & Illum, L. Nose-to-Brain Delivery: Investigation of the Transport of Nanoparticles with Different Surface Characteristics and Sizes in Excised Porcine Olfactory Epithelium. *Mol. Pharm.* **12,** 2755–2766 (2015).

99. Islam, S., Bhuiyan, M. A. R. & Islam, M. N. Chitin and Chitosan: Structure, Properties and Applications in Biomedical Engineering. *J. Polym. Environ.* **25,** 854–866 (2017).

100. Sigurdsson, H. H., Kirch, J. & Lehr, C.-M. Mucus as a barrier to lipophilic drugs. *Int. J. Pharm.* **453,** 56–64 (2013).

101. Salama, H. A., Mahmoud, A. A., Kamel, A. O., Abdel Hady, M. & Awad, G. A. S. Phospholipid based colloidal poloxamer–nanocubic vesicles for brain targeting via the nasal route. *Colloids Surfaces B Biointerfaces* **100,** 146–154 (2012).

102. Zhao, Y.-Z. *et al.* Gelatin nanostructured lipid carriers-mediated intranasal delivery of basic fibroblast growth factor enhances functional recovery in hemiparkinsonian rats. *Nanomedicine Nanotechnology, Biol. Med.* **10,** 755–764

(2014).

103. Migliore, M. M., Vyas, T. K., Campbell, R. B., Amiji, M. M. & Waszczak, B. L. Brain delivery of proteins by the intranasal route of administration: A comparison of cationic liposomes versus aqueous solution formulations. *J. Pharm. Sci.* **99,** 1745–1761 (2010).

104. Jadhav, K. R., Shaikh, I. M., Ambade, K. W. & Kadam, V. J. Applications of microemulsion based drug delivery system. *Curr. Drug Deliv.* **3,** 267–73 (2006).

105. Jogani, V. V., Shah, P. J., Mishra, P., Mishra, A. K. & Misra, A. R. Intranasal Mucoadhesive Microemulsion of Tacrine to Improve Brain Targeting. *Alzheimer Dis. Assoc. Disord.* **22,** 116–124 (2008).

106. Patel, S. *et al.* Brain targeting of risperidone-loaded solid lipid nanoparticles by intranasal route. *J. Drug Target.* **19,** 468–474 (2011).

107. Upadhyay, P., Trivedi, J., Pundarikakshudu, K. & Sheth, N. Direct and enhanced delivery of nanoliposomes of anti schizophrenic agent to the brain through nasal route. *Saudi Pharm. J.* **25,** 346–358 (2017).

108. Salade, L. *et al.* Development of coated liposomes loaded with ghrelin for nose-to-brain delivery for the treatment of cachexia. *Int. J. Nanomedicine* **12,** (2017).

109. Farkhani, S. M. *et al.* Cell penetrating peptides: Efficient vectors for delivery of nanoparticles, nanocarriers, therapeutic and diagnostic molecules. *Peptides* **57,** 78–94 (2014).

110. Rizzuti, M., Nizzardo, M., Zanetta, C., Ramirez, A. & Corti, S. Therapeutic applications of the cell-penetrating HIV-1 Tat peptide. *Drug Discov. Today* **20,** (2015).

111. Lin, T. *et al.* Nose-to-brain delivery of macromolecules mediated by cell-penetrating peptides. *Acta Pharm. Sin. B* **6,** 352–358 (2016).

112. Xia, H. *et al.* Low molecular weight protamine-functionalized nanoparticles for drug delivery to the brain after intranasal administration. *Biomaterials* **32,** 9888–9898 (2011).

113. Gao, X. *et al.* Lectin-conjugated PEG–PLA nanoparticles: Preparation and brain delivery after intranasal administration. *Biomaterials* **27,** 3482–3490 (2006).

114. Ishikawa, H. & Isayama, Y. Evidence for sialyl glycoconjugates as receptors for Bordetella bronchiseptica on swine nasal mucosa. *Infect. Immun.* **55,** 1607–9 (1987).

115. Gao, X. *et al.* Brain delivery of vasoactive intestinal peptide enhanced with the nanoparticles conjugated with wheat germ agglutinin following intranasal administration. *J. Control. Release* **121,** 156–167 (2007).

116. Broadwell, R. D., Balin, B. J. & Salcman, M. Transcytotic pathway for blood-borne protein through the blood-brain barrier. *Proc. Natl. Acad. Sci. U. S. A.* **85,** 632–6 (1988).

117. Thorne, R. G., Emory, C. R., Ala, T. A. & Frey, W. H. Quantitative analysis of the olfactory pathway for drug delivery to the brain. *Brain Res.* **692,** 278–82 (1995).

118. Wen, Z. *et al.* Odorranalectin-conjugated nanoparticles: Preparation, brain delivery and pharmacodynamic study on Parkinson's disease following

intranasal administration. *J. Control. Release* **151,** 131–138 (2011).

119. Xi, J. *et al.* Design and Testing of Electric-Guided Delivery of Charged Particles to the Olfactory Region: Experimental and Numerical Studies. *Curr. Drug Deliv.* **13,** 265–274 (2016).

120. Xi, J. & Si, X. A. Numerical Simulation and Experimental Testing to Improve Olfactory Drug Delivery with Electric Field Guidance of Charged Particles. in *Advanced Technology for Delivering Therapeutics* (InTech, 2017). doi:10.5772/65858

121. Penttilä, M., Poulsen, P., Hollingworth, K. & Holmström, M. Dose-related efficacy and tolerability of fluticasone propionate nasal drops 400 microg once daily and twice daily in the treatment of bilateral nasal polyposis: a placebo-controlled randomized study in adult patients. *Clin. Exp. Allergy* **30,** 94–102 (2000).

122. Keith, P., Nieminen, J., Hollingworth, K. & Dolovich, J. Efficacy and tolerability of fluticasone propionate nasal drops 400 microgram once daily compared with placebo for the treatment of bilateral polyposis in adults. *Clin. Exp. Allergy* **30,** 1460–8 (2000).

123. Djupesland, P. G. Nasal drug delivery devices: characteristics and performance in a clinical perspective-a review. *Drug Deliv. Transl. Res.* **3,** 42–62 (2013).

124. Harris, A. S., Nilsson, I. M., Wagner, Z. G. & Alkner, U. Intranasal administration of peptides: nasal deposition, biological response, and absorption of desmopressin. *J. Pharm. Sci.* **75,** 1085–8 (1986).

125. Trows, S., Wuchner, K., Spycher, R. & Steckel, H. Analytical challenges and regulatory requirements for nasal drug products in europe and the u.s. *Pharmaceutics* **6,** 195–219 (2014).

126. Belshe, R. B. *et al.* Live Attenuated versus Inactivated Influenza Vaccine in Infants and Young Children. *N. Engl. J. Med.* **356,** 685–696 (2007).

127. Mygind, N. & Vesterhauge, S. Aerosol distribution in the nose. *Rhinology* **16,** 79–88 (1978).

128. Gabrio, B. J., Stein, S. W. & Velasquez, D. J. A new method to evaluate plume characteristics of hydrofluoroalkane and chlorofluorocarbon metered dose inhalers. *Int. J. Pharm.* **186,** 3–12 (1999).

129. NEWHOUSE, M. Advantages of Pressurized Canister Metered Dose Inhalers. *J. Aerosol Med.* **4,** 139–150 (1991).

130. Obaidi, M. *et al.* Improved pharmacokinetics of sumatriptan with Breath Powered™ nasal delivery of sumatriptan powder. *Headache* **53,** 1323–33 (2013).

131. Tepper, S. J. & Johnstone, M. R. Breath-powered sumatriptan dry nasal powder: an intranasal medication delivery system for acute treatment of migraine. *Med. Devices Evid. Res.* **Volume 11,** 147–156 (2018).

132. Foo, M. Y., Cheng, Y.-S., Su, W.-C. & Donovan, M. D. The Influence of Spray Properties on Intranasal Deposition. *J. Aerosol Med.* **20,** 495–508 (2007).

133. Hardy, J. G., Lee, S. W. & Wilson, C. G. Intranasal drug delivery by spray and drops. *J. Pharm. Pharmacol.* **37,** 294–7 (1985).

134. Cheng, Y. S. *et al.* Characterization of Nasal Spray Pumps and Deposition Pattern in a Replica of the Human Nasal Airway. *J. Aerosol Med.* **14,** 267–280 (2001).

135. Djupesland, P. G. & Skretting, A. Nasal Deposition and Clearance in Man: Comparison of a Bidirectional Powder Device and a Traditional Liquid Spray Pump. *J. Aerosol Med. Pulm. Drug Deliv.* **25,** 280–289 (2012).

136. Craft, S. *et al.* Intranasal insulin therapy for Alzheimer disease and amnestic mild cognitive impairment: a pilot clinical trial. *Arch. Neurol.* **69,** 29–38 (2012).

137. Hoekman, J., Brunelle, A., Hite, M., Kim, P. & Fuller, C. *SPECT Imaging of Direct Nose-to-Brain Transfer of MAG-3 in Man*.

138. Salade, L., Wauthoz, N., Vermeersch, M., Amighi, K. & Goole, J. Chitosan-coated liposome dry-powder formulations loaded with ghrelin for nose-to-brain delivery. *Eur. J. Pharm. Biopharm.* **129,** 257–266 (2018).

139. Aderibigbe, B. A. In Situ-Based Gels for Nose to Brain Delivery for the Treatment of Neurological Diseases. *Pharmaceutics* **10,** (2018).

140. Hardy, J. & Selkoe, D. J. The amyloid hypothesis of Alzheimer's disease: progress and problems on the road to therapeutics. *Science* **297,** 353–6 (2002).

141. Banks, W. A. Drug delivery to the brain in Alzheimer's disease: consideration of the blood-brain barrier. *Adv. Drug Deliv. Rev.* **64,** 629–39 (2012).

142. Sood, S., Jain, K. & Gowthamarajan, K. Intranasal therapeutic strategies for management of Alzheimer's disease. *J. Drug Target.* **22,** 279–294 (2014).

143. Wong, L. R. & Ho, P. C. Role of serum albumin as a nanoparticulate carrier for nose-to-brain delivery of R-flurbiprofen: implications for the treatment of Alzheimer's disease. *J. Pharm. Pharmacol.* **70,** 59–69 (2018).

144. Stützle, M., Flamm, J., Carle, S. & Schindowski, K. Nose-to-Brain delivery of insulin for Alzheimer's disease. *ADMET DMPK* **3,** 190–202 (2015).

145. Schiöth, H. B., Frey, W. H., Brooks, S. J. & Benedict, C. Insulin to treat Alzheimer's disease: just follow your nose? *Expert Rev. Clin. Pharmacol.* **5,** 17–20 (2012).

146. Reger, M. A. *et al.* Intranasal insulin improves cognition and modulates -amyloid in early AD. *Neurology* **70,** 440–448 (2008).

147. Craft, S. *et al.* Effects of Regular and Long-Acting Insulin on Cognition and Alzheimer's Disease Biomarkers: A Pilot Clinical Trial. *J. Alzheimer's Dis.* **57,** 1325–1334 (2017).

148. Kamei, N. *et al.* Effect of an Enhanced Nose-to-Brain Delivery of Insulin on Mild and Progressive Memory Loss in the Senescence-Accelerated Mouse. *Mol. Pharm.* **14,** 916–927 (2017).

149. Cole, N. B. & Murphy, D. D. The Cell Biology of α Synuclein. *NeuroMolecular Med.* **1,** 95–110 (2002).

150. Md, S. *et al.* Bromocriptine loaded chitosan nanoparticles intended for direct nose to brain delivery: Pharmacodynamic, Pharmacokinetic and Scintigraphy study in mice model. *Eur. J. Pharm. Sci.* **48,** 393–405 (2013).

151. Jafarieh, O. *et al.* Design, characterization, and evaluation of intranasal delivery of ropinirole-loaded mucoadhesive nanoparticles for brain targeting. *Drug Dev. Ind. Pharm.* **41,** 1674–1681 (2015).

152. Mittal, D. *et al.* Brain targeted nanoparticulate drug delivery system of rasagiline via intranasal route. *Drug Deliv.* **23,** 130–139 (2016).

153. Raj, R., Wairkar, S., Sridhar, V. & Gaud, R. Pramipexole dihydrochloride loaded chitosan nanoparticles for nose to brain delivery: Development, characterization and in vivo anti-Parkinson activity. *Int. J. Biol. Macromol.* **109,** 27–35 (2018).

154. Hashizume, R. *et al.* New therapeutic approach for brain tumors: Intranasal delivery of telomerase inhibitor GRN163. *Neuro. Oncol.* **10,** 112–20 (2008).

155. Hendricks, B. K., Cohen-Gadol, A. A. & Miller, J. C. Novel delivery methods bypassing the blood-brain and blood-tumor barriers. *Neurosurg. Focus* **38,** E10 (2015).

156. Van Woensel, M. *et al.* Sensitization of glioblastoma tumor micro-environment to chemo- and immunotherapy by Galectin-1 intranasal knock-down strategy. *Sci. Rep.* **7,** 1217 (2017).

157. Mittal, D. *et al.* Insights into direct nose to brain delivery: current status and future perspective. *Drug Deliv.* (2014).

158. Alam, M. I. *et al.* Intranasal administration of nanostructured lipid carriers containing CNS acting drug: Pharmacodynamic studies and estimation in blood and brain. *J. Psychiatr. Res.* **46,** 1133–1138 (2012).

159. Vyas, T. K., Babbar, A. K., Sharma, R. K., Singh, S. & Misra, A. Preliminary brain-targeting studies on intranasal mucoadhesive microemulsions of sumatriptan. *AAPS PharmSciTech* **7,** E49–E57 (2006).

160. Patel, M. R., Patel, R. B., Bhatt, K. K., Patel, B. G. & Gaikwad, R. V. Paliperidone microemulsion for nose-to-brain targeted drug delivery system: pharmacodynamic and pharmacokinetic evaluation. *Drug Deliv.* **23,** 346–354 (2016).

161. Thorne, R. G., Emory, C. R., Ala, T. A. & Frey, W. H. Quantitative analysis of the olfactory pathway for drug delivery to the brain. *Brain Res.* **692,** 278–282 (1995).

162. Born, J. *et al.* Sniffing neuropeptides: a transnasal approach to the human brain. *Nat. Neurosci.* **5,** 514–516 (2002).

163. Ozsoy, Y., Gungor, S. & Cevher, E. Nasal Delivery of High Molecular Weight Drugs. *Molecules* **14,** 3754–3779 (2009).

164. Wu, H., Hu, K. & Jiang, X. From nose to brain: understanding transport capacity and transport rate of drugs. *Expert Opin. Drug Deliv.* **5,** 1159–1168 (2008).

165. Cuschieri, A. Enzyme histochemistry of the olfactory mucosa and vomeronasal organ in the mouse. *J. Anat.* **118,** 477–89 (1974).

166. Heni, M. *et al.* Central Insulin Administration Improves Whole-Body Insulin Sensitivity via Hypothalamus and Parasympathetic Outputs in Men. *Diabetes* **63,** 4083–4088 (2014).

167. Hölscher, C. First clinical data of the neuroprotective effects of nasal insulin application in patients with Alzheimer's disease. *Alzheimer's Dement.* **10,** S33–

S37 (2014).

168. Dictionary, A. H. *The American Heritage Medical Dictionary*. (Houghton Mifflin Company, 2011).

169. Evans, W. J. *et al.* Cachexia: a new definition. *Clin. Nutr.* **27,** 793–9 (2008).

170. von Haehling, S. & Anker, S. D. Prevalence, incidence and clinical impact of cachexia: facts and numbers-update 2014. *J. Cachexia. Sarcopenia Muscle* **5,** 261–3 (2014).

171. Delano, M. J. & Moldawer, L. L. The Origins of Cachexia in Acute and Chronic Inflammatory Diseases*. *Nutr. Clin. Pract.* **21,** 68–81 (2006).

172. Wolf, I. *et al.* Adiponectin, ghrelin, and leptin in cancer cachexia in breast and colon cancer patients. *Cancer* **106,** 966–973 (2006).

173. Suzuki, H., Asakawa, A., Amitani, H., Nakamura, N. & Inui, A. Cancer cachexia--pathophysiology and management. *J. Gastroenterol.* **48,** 574–94 (2013).

174. Argilés, J. M. *et al.* The cachexia score (CASCO): a new tool for staging cachectic cancer patients. *J. Cachexia. Sarcopenia Muscle* **2,** 87–93 (2011).

175. Fearon, K. *et al.* Definition and classification of cancer cachexia: an international consensus. *Lancet Oncol.* **12,** 489–495 (2011).

176. Bachmann, J. *et al.* Cachexia Worsens Prognosis in Patients with Resectable Pancreatic Cancer. *J. Gastrointest. Surg.* **12,** 1193–1201 (2008).

177. Inui, A. Feeding and body-weight regulation by hypothalamic neuropeptides--mediation of the actions of leptin. *Trends Neurosci.* **22,** 62–7 (1999).

178. Friedman, J. M. & Halaas, J. L. Leptin and the regulation of body weight in mammals. *Nature* **395,** 763–770 (1998).

179. Fujitsuka, N. *et al.* Potentiation of ghrelin signaling attenuates cancer anorexia-cachexia and prolongs survival. *Transl. Psychiatry* **1,** e23 (2011).

180. Benso, A. & S. Karger (Firm). *The ghrelin system*. (Karger, 2013).

181. Kojima, M. *et al.* Ghrelin is a growth-hormone-releasing acylated peptide from stomach. *Nature* **402,** 656–660 (1999).

182. St-Pierre, D. H., Wang, L. & Tache, Y. Ghrelin: A Novel Player in the Gut-Brain Regulation of Growth Hormone and Energy Balance. *Physiology* **18,** 242–246 (2003).

183. Delporte, C. & Christine. Structure and Physiological Actions of Ghrelin. *Scientifica (Cairo).* **2013,** 25 (2013).

184. Kanamoto, N. *et al.* Substantial Production of Ghrelin by a Human Medullary Thyroid Carcinoma Cell Line. *The Journal of Clinical Endocrinology & Metabolism* (2011).

185. Wu, J. T. & Kral, J. G. Ghrelin: integrative neuroendocrine peptide in health and disease. *Ann. Surg.* **239,** 464–74 (2004).

186. Drazen, D. L., Vahl, T. P., D'Alessio, D. A., Seeley, R. J. & Woods, S. C. Effects of a Fixed Meal Pattern on Ghrelin Secretion: Evidence for a Learned Response Independent of Nutrient Status. *Endocrinology* **147,** 23–30 (2006).

187. Cummings, D. E. *et al.* Plasma Ghrelin Levels after Diet-Induced Weight Loss or Gastric Bypass Surgery. *N. Engl. J. Med.* **346,** 1623–1630 (2002).

188. Albarrán-Zeckler, R. G. & Smith, R. G. The ghrelin receptors (GHS-R1a and GHS-R1b). *Endocr. Dev.* **25,** 5–15 (2013).

189. DeBoer, M. D. Emergence of ghrelin as a treatment for cachexia syndromes. *Nutrition* **24,** 806–814 (2008).

190. Akamizu, T. *et al.* Pharmacokinetics, safety, and endocrine and appetite effects of ghrelin administration in young healthy subjects. *Eur. J. Endocrinol.* **150,** 447–55 (2004).

191. Molfino, A., Gioia, G. & Muscaritoli, M. The hunger hormone ghrelin in cachexia. *Expert Opin. Biol. Ther.* **13,** 465–468 (2013).

192. Chen, V. P. *et al.* Plasma butyrylcholinesterase regulates ghrelin to control aggression. *Proc. Natl. Acad. Sci. U. S. A.* **112,** 2251–6 (2015).

193. Mattox, T. W. Cancer Cachexia: Cause, Diagnosis, and Treatment. *Nutr. Clin. Pract.* **32,** 599–606 (2017).

194. Aoyagi, T., Terracina, K. P., Raza, A., Matsubara, H. & Takabe, K. Cancer cachexia, mechanism and treatment. *World J. Gastrointest. Oncol.* **7,** 17–29 (2015).

195. Currow, D. *et al.* ROMANA 3: a phase 3 safety extension study of anamorelin in advanced non-small-cell lung cancer (NSCLC) patients with cachexia. *Ann. Oncol.* **28,** 1949–1956 (2017).

196. Zhang, H. & Garcia, J. M. Anamorelin hydrochloride for the treatment of cancer-anorexia-cachexia in NSCLC. *Expert Opin. Pharmacother.* **16,** 1245–1253 (2015).

197. Meunier, F., Prentice, H. G. & Ringdén, O. Liposomal amphotericin B (AmBisome): safety data from a phase II/III clinical trial. *J. Antimicrob. Chemother.* **28 Suppl B,** 83–91 (1991).

198. Gramatikoff, K. Liposomes. (1999).

199. Meure, L. A., Foster, N. R. & Dehghani, F. Conventional and dense gas techniques for the production of liposomes: a review. *AAPS PharmSciTech* **9,** 798–809 (2008).

200. Nag, O. K. & Awasthi, V. Surface engineering of liposomes for stealth behavior. *Pharmaceutics* **5,** 542–69 (2013).

201. Chen, M., Deng, Q., Li, X.-R. & Liu, Y. [The hypocalcemia effect of salmon calcitonin ultra-flexible liposomes after intranasal administration in rats]. *Yao Xue Xue Bao* **42,** 681–6 (2007).

202. Jain, A. K., Chalasani, K. B., Khar, R. K., Ahmed, F. J. & Diwan, P. V. Muco-adhesive multivesicular liposomes as an effective carrier for transmucosal insulin delivery. *J. Drug Target.* **15,** 417–427 (2007).

203. Rodrigues, S., Dionísio, M., López, C. R. & Grenha, A. Biocompatibility of chitosan carriers with application in drug delivery. *J. Funct. Biomater.* **3,** 615–41 (2012).

204. Chaturvedi, M., Kumar, M. & Pathak, K. A review on mucoadhesive polymer used in nasal drug delivery system. *J. Adv. Pharm. Technol. Res.* **2,** 215–22 (2011).

205. Alhalaweh, A., Andersson, S. & Velaga, S. P. Preparation of zolmitriptan–chitosan microparticles by spray drying for nasal delivery. *Eur. J. Pharm. Sci.* **38,** 206–214 (2009).

206. Anker, S. D. & von Haehling, S. Efforts begin to sprout: publications in JCSM on cachexia, sarcopenia and muscle wasting receive attention. *J. Cachexia. Sarcopenia Muscle* **5,** 171–176 (2014).

207. Argilés, J. M., Busquets, S., Stemmler, B. & López-Soriano, F. J. Cancer cachexia: understanding the molecular basis. *Nat. Rev. Cancer* **14,** 754–762 (2014).

208. Moeller, E. H., Holst, B., Nielsen, L. H., Pedersen, P. S. & Østergaard, J. Stability, liposome interaction, and in vivo pharmacology of ghrelin in liposomal suspensions. *Int. J. Pharm.* **390,** 13–18 (2010).

209. Graf, S. & Garcia, J. Anamorelin hydrochloride in the treatment of cancer anorexia–cachexia syndrome: design, development, and potential place in therapy. *Drug Des. Devel. Ther.* **Volume 11,** 2325–2331 (2017).

210. Garin, M. C., Burns, C. M., Kaul, S. & Cappola, A. R. The Human Experience With Ghrelin Administration. *J. Clin. Endocrinol. Metab.* **98,** 1826–1837 (2013).

211. Azegami, T. *et al.* Nanogel-based nasal ghrelin vaccine prevents obesity. *Mucosal Immunol.* (2017). doi:10.1038/mi.2016.137

212. Zollers, B., Rhodes, L. & Heinen, E. Capromorelin oral solution (ENTYCE®) increases food consumption and body weight when administered for 4 consecutive days to healthy adult Beagle dogs in a randomized, masked, placebo controlled study. *BMC Vet. Res.* **13,** 10 (2017).

213. Temel, J. S. *et al.* Anamorelin in patients with non-small-cell lung cancer and cachexia (ROMANA 1 and ROMANA 2): results from two randomised, double-blind, phase 3 trials. *Lancet Oncol.* **17,** 519–531 (2016).

214. Muralidharan, P. *et al.* Inhalable PEGylated Phospholipid Nanocarriers and PEGylated Therapeutics for Respiratory Delivery as Aerosolized Colloidal Dispersions and Dry Powder Inhalers. *Pharmaceutics* **6,** 333–353 (2014).

215. Casettari, L. & Illum, L. Chitosan in nasal delivery systems for therapeutic drugs. *J. Control. Release* **190,** 189–200 (2014).

216. Lee, H. & Pastor, R. W. Coarse-grained model for PEGylated lipids: effect of PEGylation on the size and shape of self-assembled structures. *J. Phys. Chem. B* **115,** 7830–7 (2011).

217. Alsarra, I. A., Hamed, A. Y. & Alanazi, F. K. Acyclovir Liposomes for Intranasal Systemic Delivery: Development and Pharmacokinetics Evaluation. *Drug Deliv.* **15,** 313–321 (2008).

218. Rosiere, R. Development of dry powder formulations for inhalation based on nanomedicine for targeted lung cancer therapy. (2016).

219. Staes, E., Rozet, E., Učakar, B., Hubert, P. & Préat, V. Validation of a method

for the quantitation of ghrelin and unacylated ghrelin by HPLC. *J. Pharm. Biomed. Anal.* **51,** 633–639 (2010).

220. Bangham, A. D. PROPERTIES AND USES OF LIPID VESICLES: AN OVERVIEW. *Ann. N. Y. Acad. Sci.* **308,** 2–7 (1978).

221. Erickson, J. Determination of the concentration of caffeine , theobromine , and gallic acid in commercial tea samples. *Concordia Coll. J. Anal. Chem.* **2,** 31–35 (2011).

222. Shah, R. B., Siddiqui, A., Shah, G. & Khan, M. A. A validated HPLC assay for simultaneous analysis of salmon calcitonin and duck ovomucoid. *Pharmazie* **58,** 620–2 (2003).

223. Nsimba Zakanda, F. *et al.* Interaction of hexadecylbetainate chloride with biological relevant lipids. *Langmuir* **28,** 3524–33 (2012).

224. Heerklotz, H. & Seelig, J. Titration calorimetry of surfactant-membrane partitioning and membrane solubilization. *Biochim. Biophys. Acta* **1508,** 69–85 (2000).

225. Razafindralambo, H., Dufour, S., Paquot, M. & Deleu, M. Thermodynamic studies of the binding interactions of surfactin analogues to lipid vesicles. *J. Therm. Anal. Calorim.* **95,** 817–821 (2009).

226. Mantle, M. & Allen, A. A colorimetric assay for glycoproteins based on the periodic acid/Schiff stain [proceedings]. *Biochem. Soc. Trans.* **6,** 607–9 (1978).

227. Tamilvanan, S. Pharmaceutical Manufacturing Handbook. *Pharmaceutical Manufacturing Handbook: Production and Processes* 1327–1366 (2008). doi:10.1002/9780470259818

228. De Vriese, C. *et al.* Ghrelin degradation by serum and tissue homogenates: identification of the cleavage sites. *Endocrinology* **145,** 4997–5005 (2004).

229. Satou, M., Nakamura, Y., Ando, H. & Sugimoto, H. Understanding the functional significance of ghrelin processing and degradation. *Peptides* **32,** 2183–2190 (2011).

230. Hosoda, H. & Kangawa, K. Standard sample collections for blood ghrelin measurements. *Methods Enzymol.* **514,** 113–26 (2012).

231. Bielohuby, M., Popp, S. & Bidlingmaier, M. A guide for measurement of circulating metabolic hormones in rodents: Pitfalls during the pre-analytical phase. *Mol. Metab.* **1,** 47–60 (2012).

232. Pillay, V., Choonara, Y. E. & Kumar, P. *Frontiers in biomaterials. Volume 2, Unfolding the biopolymer landscape.* (Bentham Science Publishers, 2016).

233. Kaszuba, M., Corbett, J., Mcneil, F. & Jones, A. High-concentration zeta potential measurements using light-scattering techniques. *Trans. R. Soc. A* **368,** 4439–4451 (2010).

234. Trier, S. *et al.* Acylation of salmon calcitonin modulates in vitro intestinal peptide flux through membrane permeability enhancement. *Eur. J. Pharm. Biopharm.* **96,** 329–337 (2015).

235. Witschi, C. & Mrsny, R. J. In vitro evaluation of microparticles and polymer gels for use as nasal platforms for protein delivery. *Pharm. Res.* **16,** 382–90 (1999).

236. Salade, L., Wauthoz, N., Goole, J. & Amighi, K. How to characterize a nasal product. The state of the art of in vitro and ex vivo specific methods. *Int. J. Pharm.* **561,** 47–65 (2019).

237. Trier, S., Linderoth, L., Bjerregaard, S., Andresen, T. L. & Rahbek, U. L. Acylation of Glucagon-Like Peptide-2: Interaction with Lipid Membranes and In Vitro Intestinal Permeability. *PLoS One* **9,** e109939 (2014).

238. Mourya, V. K., Inamdar, N., Nawale, R. & Kulthe, S. *Polymeric Micelles: General Considerations and their Applications*. *Indian Journal of Pharmaceutical Education and Research* **45,** (2011).

239. Yang, Q., Moulder K, R., Cohen, M. S., Cai, S. & Forrest, L. M. Cabozantinib Loaded DSPE-PEG2000 Micelles as Delivery System: Formulation, Characterization and Cytotoxicity Evaluation. *BAOJ Pharm. Sci.* **1,** (2015).

240. Ashok, B., Arleth, L., Hjelm, R. P., Rubinstein, I. & Önyüksel, H. In vitro characterization of PEGylated phospholipid micelles for improved drug solubilization: Effects of PEG chain length and PC incorporation. *J. Pharm. Sci.* **93,** 2476–2487 (2004).

241. Uster, P. S. *et al.* Insertion of poly(ethylene glycol) derivatized phospholipid into pre-formed liposomes results in prolonged in vivo circulation time. *FEBS Lett.* **386,** 243–6 (1996).

242. Vila, A., Gill, H., McCallion, O. & Alonso, M. J. Transport of PLA-PEG particles across the nasal mucosa: effect of particle size and PEG coating density. *J. Control. Release* **98,** 231–244 (2004).

243. Schuster, B. S., Suk, J. S., Woodworth, G. F. & Hanes, J. Nanoparticle diffusion in respiratory mucus from humans without lung disease. *Biomaterials* **34,** 3439–3446 (2013).

244. Malik, W. U. & Saleem, S. M. *Effect of Additives on the Critical Micelle Concentration of Some Polyethoxylated Nonionic Detergents*.

245. Vuković, L. *et al.* Structure and dynamics of highly PEG-ylated sterically stabilized micelles in aqueous media. *J. Am. Chem. Soc.* **133,** 13481–8 (2011).

246. Vieira, D. B. & Gamarra, L. F. Getting into the brain: liposome-based strategies for effective drug delivery across the blood-brain barrier. *Int. J. Nanomedicine* **11,** 5381–5414 (2016).

247. Illum, L., Farraj, N. F. & Davis, S. S. Chitosan as a Novel Nasal Delivery System for Peptide Drugs. *Pharm. Res.* **11,** 1186–1189 (1994).

248. Van Woensel, M. *et al.* Development of siRNA-loaded chitosan nanoparticles targeting Galectin-1 for the treatment of glioblastoma multiforme via intranasal administration. *J. Control. Release* **227,** 71–81 (2016).

249. Filipović-Grcić, J., Skalko-Basnet, N. & Jalsenjak, I. Mucoadhesive chitosan-coated liposomes: characteristics and stability. *J. Microencapsul.* **18,** 3–12 (2008).

250. Ahmad, E. *et al.* Evidence of nose-to-brain delivery of nanoemulsions: cargoes but not vehicles. *Nanoscale* **9,** 1174–1183 (2017).

251. Kozlovskaya, L., Abou-Kaoud, M. & Stepensky, D. Quantitative analysis of drug

delivery to the brain via nasal route. *J. Control. Release* **189,** 133–140 (2014).

252. de Lorenzo, A. J. Electron Microscopy of the Olfactory and Gustatory Pathways. *Ann. Otol. Rhinol. Laryngol.* **69,** 410–420 (1960).

253. Min, C. *et al.* The antimicrobial activity of the appetite peptide hormone ghrelin. *Peptides* **36,** 151–6 (2012).

254. Seelig, J. Thermodynamics of lipid–peptide interactions. *Biochim. Biophys. Acta - Biomembr.* **1666,** 40–50 (2004).

255. Staes, E. *et al.* Acylated and unacylated ghrelin binding to membranes and to ghrelin receptor: towards a better understanding of the underlying mechanisms. *Biochim. Biophys. Acta* **1798,** 2102–13 (2010).

256. Østergaard, J. & Moeller, E. H. Ghrelin-liposome interactions: characterization of liposomal formulations of an acylated 28-amino acid peptide using CE. *Electrophoresis* **31,** 339–45 (2010).

257. *Molecular Neurobiology of the Olfactory System: Molecular, Membranous, and Cytological Studies*. **11,** (Springer Science & Business Media, 2013).

258. Dahl, A. R. & Hadley, W. M. Nasal cavity enzymes involved in xenobiotic metabolism: effects on the toxicity of inhalants. *Crit. Rev. Toxicol.* **21,** 345–72 (1991).

259. Morimoto, K., Miyazaki, M. & Kakemi, M. Effects of proteolytic enzyme inhibitors on nasal absorption of salmon calcitonin in rats. *Int. J. Pharm.* **113,** 1–8 (1995).

260. Lewis, J. L., Nikula, K. J., Novak, R. & Dahl, A. R. Comparative localization of carboxylesterase in F344 rat, Beagle dog, and human nasal tissue. *Anat. Rec.* **239,** 55–64 (1994).

261. Bogdanffy, M. & Taylor, M. Kinetics of nasal carboxylesterase-mediated metabolism of vinyl acetate. *Drug Metab. Dispos.* **21,** 1107–1111 (1993).

262. Laizure, S. C., Herring, V., Hu, Z., Witbrodt, K. & Parker, R. B. The role of human carboxylesterases in drug metabolism: have we overlooked their importance? *Pharmacotherapy* **33,** 210–22 (2013).

263. Taylor, M. S., Hwang, Y., Hsiao, P.-Y., Boeke, J. D. & Cole, P. A. Ghrelin O-acyltransferase assays and inhibition. *Methods Enzymol.* **514,** 205–28 (2012).

264. Salim, N. N. & Feig, A. L. Isothermal titration calorimetry of RNA. *Methods* **47,** 198–205 (2009).

265. Chodera, J. D. & Mobley, D. L. Entropy-enthalpy compensation: role and ramifications in biomolecular ligand recognition and design. *Annu. Rev. Biophys.* **42,** 121–42 (2013).

266. Hosoda, H. *et al.* Optimum collection and storage conditions for ghrelin measurements: octanoyl modification of ghrelin is rapidly hydrolyzed to desacyl ghrelin in blood samples. *Clin. Chem.* **50,** 1077–80 (2004).

267. Channarong, S., Chaicumpa, W., Sinchaipanid, N. & Mitrevej, A. Development and evaluation of chitosan-coated liposomes for oral DNA vaccine: the improvement of Peyer's patch targeting using a polyplex-loaded liposomes. *AAPS PharmSciTech* **12,** 192–200 (2011).

268. Mady, M. M. & Darwish, M. M. Effect of chitosan coating on the characteristics of DPPC liposomes. *J. Adv. Res.* **1,** 187–191 (2010).

269. Guo, J., Ping, Q., Jiang, G., Huang, L. & Tong, Y. Chitosan-coated liposomes: characterization and interaction with leuprolide. *Int. J. Pharm.* **260,** 167–73 (2003).

270. Wen, Z. *et al.* Brain targeting and toxicity study of odorranalectin-conjugated nanoparticles following intranasal administration. *Drug Deliv.* **18,** 555–61 (2011).

271. Amoako-Tuffour, M., Yeung, P. & Agu, R. *Permeation of losartan across human respiratory epithelium: An in vitro study with Calu-3 cells*. *Acta Pharmaceutica* **59,** 395 (2009).

272. Yang, T., Hussain, A., Paulson, J., Abbruscato, T. J. & Ahsan, F. Cyclodextrins in nasal delivery of low-molecular-weight heparins: in vivo and in vitro studies. *Pharm. Res.* **21,** 1127–36 (2004).

273. Banks, W. A., Tschöp, M., Robinson, S. M. & Heiman, M. L. Extent and Direction of Ghrelin Transport Across the Blood-Brain Barrier Is Determined by Its Unique Primary Structure. *J. Pharmacol. Exp. Ther.* **302,** 822–827 (2002).

274. Ungell, A. L., Andreasson, A., Lundin, K. & Utter, L. Effects of enzymatic inhibition and increased paracellular shunting on transport of vasopressin analogues in the rat. *J. Pharm. Sci.* **81,** 640–5 (1992).

275. Torres-Lugo, M., García, M., Record, R. & Peppas, N. A. pH-Sensitive Hydrogels as Gastrointestinal Tract Absorption Enhancers: Transport Mechanisms of Salmon Calcitonin and Other Model Molecules Using the Caco-2 Cell Model. *Biotechnol. Prog.* **18,** 612–616 (2002).

276. Prueksaritanont, T. *et al.* In Vitro and In Vivo Evaluations of Intestinal Barriers for the Zwitterion L-767,679 and Its Carboxyl Ester Prodrug L-775,318: Roles of Efflux and Metabolism. *Drug Metab. Dispos.* **26,** 520–527 (1998).

277. Ribeiro, J. A. & Sebastião, A. M. Caffeine and adenosine. *J. Alzheimers. Dis.* **20 Suppl 1,** S3-15 (2010).

278. Becskei, C., Riediger, T., Zünd, D., Wookey, P. & Lutz, T. A. Immunohistochemical mapping of calcitonin receptors in the adult rat brain. *Brain Res.* **1030,** 221–33 (2004).

279. Prego, C., Torres, D. & Alonso, M. J. Chitosan nanocapsules: a new carrier for nasal peptide delivery. *J. Drug Deliv. Sci. Technol.* **16,** 331–337 (2006).

280. Huang, M., Khor, E. & Lim, L.-Y. Uptake and Cytotoxicity of Chitosan Molecules and Nanoparticles: Effects of Molecular Weight and Degree of Deacetylation. *Pharm. Res.* **21,** 344–353 (2004).

281. EVOM2: Instruction Manual. *Word Precis. Instruments*

282. Carlstedt, I., Lindgren, H., Sheehan, J. K., Ulmsten, U. & Wingerup, L. Isolation and characterization of human cervical-mucus glycoproteins. *Biochem. J.* **211,** 13–22 (1983).

283. Khutoryanskiy, V. V. Advances in Mucoadhesion and Mucoadhesive Polymers. *Macromol. Biosci.* **11,** 748–764 (2011).

284. Leitner, V. M., Marschütz, M. K. & Bernkop-Schnürch, A. Mucoadhesive and

cohesive properties of poly(acrylic acid)-cysteine conjugates with regard to their molecular mass. *Eur. J. Pharm. Sci.* **18,** 89–96 (2003).

285. Naik, A. & Nair, H. Formulation and evaluation of thermosensitive biogels for nose to brain delivery of doxepin. *Biome* **2014,** (2014).

286. Surber, C., Elsner, P., Farage, M. A. & S. Karger (Firm). *Topical applications and the mucosa*. (Karger, 2011).

287. Se, C. M. K., Inthavong, K. & Tu, J. UNSTEADY PARTICLE DEPOSITION IN A HUMAN NASAL CAVITY.

288. Fda & Cder. *Guidance for Industry Bioavailability and Bioequivalence Studies for Nasal Aerosols and Nasal Sprays for Local Action*. (2003).

289. Agency, E. M. Guideline on the Pharmaceutical Quality of Inhalation and Nasal Products. 1–27 (2006).

290. El-Sherbiny, I. M., El-Baz, N. M. & Yacoub, M. H. Inhaled nano- and microparticles for drug delivery. *Glob. Cardiol. Sci. Pract.* **2015,** 2 (2015).

291. Shi, H., Kleinstreuer, C. & Zhang, Z. Modeling of inertial particle transport and deposition in human nasal cavities with wall roughness. *J. Aerosol Sci.* **38,** 398–419 (2007).

292. Suman, J. D., Laube, B. L. & Dalby, R. Comparison of nasal deposition and clearance of aerosol generated by nebulizer and an aqueous spray pump. *Pharm. Res.* **16,** 1648–52 (1999).

293. Schroeter, J. D., Tewksbury, E. W., Wong, B. A. & Kimbell, J. S. Experimental Measurements and Computational Predictions of Regional Particle Deposition in a Sectional Nasal Model. *J. Aerosol Med. Pulm. Drug Deliv.* **28,** 20–29 (2015).

294. Harris, A. S., Svensson, E., Wagner, Z. G., Lethagen, S. & Nilsson, I. M. Effect of Viscosity on Particle Size, Deposition, and Clearance of Nasal Delivery Systems Containing Desmopressin. *J. Pharm. Sci.* **77,** 405–408 (1988).

295. Dayal, P. *et al.* Evaluation of different parameters that affect droplet-size distribution from nasal sprays using the Malvern Spraytec®. *J. Pharm. Sci.* **93,** 1725–1742 (2004).

296. Pennington, J., Pandey, P., Tat, H., Willson, J. & Donovan, B. Spray Pattern and Droplet Size Analyses for High-Shear Viscosity Determination of Aqueous Suspension Corticosteroid Nasal Sprays. *Drug Dev. Ind. Pharm.* **34,** 923–929 (2008).

297. Salade, L. *et al.* Development of coated liposomes loaded with ghrelin for nose-to-brain delivery for the treatment of cachexia. *Int. J. Nanomedicine* **12,** 8531–8543 (2017).

298. Pilcer, G., Wauthoz, N. & Amighi, K. Lactose characteristics and the generation of the aerosol. *Adv. Drug Deliv. Rev.* **64,** 233–256 (2012).

299. Rathananand, M. *et al.* Preparation of mucoadhesive microspheres for nasal delivery by spray drying. *Indian J. Pharm. Sci.* **69,** 651 (2007).

300. Chougule, M., Padhi, B. & Misra, A. Development of spray dried liposomal dry powder inhaler of Dapsone. *AAPS PharmSciTech* **9,** 47–53 (2008).

301. van Woensel, M. *et al.* Formulations for Intranasal Delivery of Pharmacological Agents to Combat Brain Disease: A New Opportunity to Tackle GBM? *Cancers (Basel).* **5,** 1020–48 (2013).

302. Broadhead, J., Edmond Rouan, S. K. & Rhodes, C. T. The spray drying of pharmaceuticals. *Drug Dev. Ind. Pharm.* **18,** 1169–1206 (1992).

303. Gardenhire, D. S. & Rau, J. L. *Rau's respiratory care pharmacology*.

304. Bilancetti, L., Poncelet, D., Loisel, C., Mazzitelli, S. & Nastruzzi, C. A statistical approach to optimize the spray drying of starch particles: application to dry powder coating. *AAPS PharmSciTech* **11,** 1257–67 (2010).

305. Kaye, R. S., Purewal, T. S. & Alpar, O. H. Development and testing of particulate formulations for the nasal delivery of antibodies. *J. Control. Release* **135,** 127–135 (2009).

306. Crouter, A. & Briens, L. The effect of moisture on the flowability of pharmaceutical excipients. *AAPS PharmSciTech* **15,** 65–74 (2014).

307. Kanojia, G. *et al.* A Design of Experiment approach to predict product and process parameters for a spray dried influenza vaccine. *Int. J. Pharm.* **511,** 1098–1111 (2016).

308. Li, J. *et al.* A review on phospholipids and their main applications in drug delivery systems. *Asian J. Pharm. Sci.* **10,** 81–98 (2015).

309. Keshani, S., Wan Daud, W., Nourouzi, M., Namvar, F. & Ghasemi, M. *Spray drying: An overview on wall deposition, process and modeling*. *Journal of Food Engineering* **146,** (2015).

310. Maa, Y. F. *et al.* Effect of spray drying and subsequent processing conditions on residual moisture content and physical/biochemical stability of protein inhalation powders. *Pharm. Res.* **15,** 768–75 (1998).

311. Jiang, G. *et al.* Anthrax vaccine powder formulations for nasal mucosal delivery. *J. Pharm. Sci.* **95,** 80–96 (2006).

312. Maggi, L. Influence of the moisture on the performance of a new dry powder inhaler. *Int. J. Pharm.* **177,** 83–91 (1999).

313. Emery, E., Oliver, J., Pugsley, T., Sharma, J. & Zhou, J. Flowability of moist pharmaceutical powders. *Powder Technol.* **189,** 409–415 (2009).

314. Saiful Hassan, M. & Wai Man Lau, R. Effect of Particle Shape on Dry Particle Inhalation: Study of Flowability, Aerosolization, and Deposition Properties. (2009). doi:10.1208/s12249-009-9313-3

315. Li, X., Vogt, F. G., Hayes, D. & Mansour, H. M. Design, Characterization, and Aerosol Dispersion Performance Modeling of Advanced Co-Spray Dried Antibiotics with Mannitol as Respirable Microparticles/Nanoparticles for Targeted Pulmonary Delivery as Dry Powder Inhalers. *J. Pharm. Sci.* **103,** 2937–2949 (2014).

316. Kockisch, S., Rees, G. D., Young, S. A., Tsibouklis, J. & Smart, J. D. Polymeric Microspheres for Drug Delivery to the Oral Cavity: An In Vitro Evaluation of Mucoadhesive Potential. *J. Pharm. Sci.* **92,** 1614–1623 (2003).

317. Capra, R. H., Baruzzi, A. M., Quinzani, L. M. & Strumia, M. C. Rheological,

dielectric and diffusion analysis of mucin/carbopol matrices used in amperometric biosensors. *Sensors Actuators B Chem.* **124,** 466–476 (2007).

318. Wang, S. H., Kirwan, S. M., Abraham, S. N., Staats, H. F. & Hickey, A. J. Stable dry powder formulation for nasal delivery of anthrax vaccine. *J. Pharm. Sci.* **101,** 31–47 (2012).

319. Wessman, P., Edwards, K. & Mahlin, D. Structural effects caused by spray- and freeze-drying of liposomes and bilayer disks. *J. Pharm. Sci.* **99,** 2032–2048 (2010).

320. Gültekin-Özgüven, M., Karadağ, A., Duman, Ş., Özkal, B. & Özçelik, B. Fortification of dark chocolate with spray dried black mulberry (Morus nigra) waste extract encapsulated in chitosan-coated liposomes and bioaccessability studies. *Food Chem.* **201,** 205–212 (2016).

321. Akbarzadeh, A. *et al.* Liposome: classification, preparation, and applications. *Nanoscale Res. Lett.* **8,** 102 (2013).

322. Johnson, N. J., Hanson, L. R. & Frey Ii, W. H. Trigeminal pathways deliver a low molecular weight drug from the nose to the brain and orofacial structures. doi:10.1021/mp100029t

323. Grobuschek, N. *et al.* Mass uniformity of nasal sprays. *Sci. Pharm. 2003, Vol. 71, Pages 151-164* **71,** 151–164 (2003).

324. Luthringer, R. *et al.* Rapid absorption of sumatriptan powder and effects on glyceryl trinitrate model of headache following intranasal delivery using a novel bi-directional device. *J. Pharm. Pharmacol.* **61,** 1219–1228 (2009).

325. Garin, M. C., Burns, C. M., Kaul, S. & Cappola, A. R. Clinical review: The human experience with ghrelin administration. *J. Clin. Endocrinol. Metab.* **98,** 1826–37 (2013).

326. Hörschler, I., Meinke, M. & Schröder, W. Numerical simulation of the flow field in a model of the nasal cavity. *Comput. Fluids* **32,** 39–45 (2003).

327. Yu, G., Zhang, Z. & Lessmann, R. Fluid Flow and Particle Diffusion in the Human Upper Respiratory System. *Aerosol Sci. Technol.* **28,** 146–158 (1998).

328. Subramaniam, R. P., Richardson, R. B., Morgan, K. T., Kimbell, J. S. & Guilmette, R. A. COMPUTATIONAL FLUID DYNAMICS SIMULATIONS OF INSPIRATORY AIRFLOW IN THE HUMAN NOSE AND NASOPHARYNX. *Inhal. Toxicol.* **10,** 91–120 (1998).

329. Lin, J. K., Wheatley, F. C., Handwerker, J., Harris, N. J. & Wong, B. J. F. Analyzing nasal septal deviations to develop a new classification system: a computed tomography study using MATLAB and OsiriX. *JAMA Facial Plast. Surg.* **16,** 183–7 (2014).

330. Hughes, R., Watterson, J., Dickens, C., Ward, D. & Banaszek, A. Development of a nasal cast model to test medicinal nasal devices. *Proc. Inst. Mech. Eng. Part H J. Eng. Med.* **222,** 1013–1022 (2008).

331. Xi, J., Kim, J., Si, X. A., Corley, R. A. & Zhou, Y. Modeling of inertial deposition in scaled models of rat and human nasal airways: Towards in vitro regional dosimetry in small animals. *J. Aerosol Sci.* **99,** 78–93 (2016).

332. Kundoor, V. & Dalby, R. N. Effect of Formulation- and Administration-Related Variables on Deposition Pattern of Nasal Spray Pumps Evaluated Using a Nasal Cast. *Pharm. Res.* **28,** 1895–1904 (2011).

333. Guo, Y., Laube, B. & Dalby, R. The Effect of Formulation Variables and Breathing Patterns on the Site of Nasal Deposition in an Anatomically Correct Model. *Pharm. Res.* **22,** 1871–1878 (2005).

334. Scherließ, R. Comparison of in vitro methods to determine nasal versus lung deposition of a protein formulation.

335. Dyer, A. M. *et al.* Nasal delivery of insulin using novel chitosan based formulations: a comparative study in two animal models between simple chitosan formulations and chitosan nanoparticles. *Pharm. Res.* **19,** 998–1008 (2002).

336. Erdő, F., Bors, L. A., Farkas, D., Bajza, Á. & Gizurarson, S. Evaluation of intranasal delivery route of drug administration for brain targeting. *Brain Res. Bull.* **143,** 155–170 (2018).

337. Tyson, A. L., Hilton, S. T. & Andreae, L. C. Rapid, simple and inexpensive production of custom 3D printed equipment for large-volume fluorescence microscopy. *Int. J. Pharm.* **494,** 651–656 (2015).

338. Hughes, L. D., Rawle, R. J. & Boxer, S. G. Choose Your Label Wisely: Water-Soluble Fluorophores Often Interact with Lipid Bilayers. doi:10.1371/journal.pone.0087649

339. Spitzer, N., Sammons, G. S. & Price, E. M. Autofluorescent cells in rat brain can be convincing impostors in green fluorescent reporter studies. *J. Neurosci. Methods* **197,** 48–55 (2011).

340. Vaka, S. R. K., Sammeta, S. M., Day, L. B. & Murthy, S. N. Delivery of nerve growth factor to brain via intranasal administration and enhancement of brain uptake. *J. Pharm. Sci.* **98,** 3640–6 (2009).

341. Rowland, N. E. *Comparative Medicine Food or Fluid Restriction in Common Laboratory Animals: Balancing Welfare Considerations with Scientific Inquiry*. (2007).

342. Agrawal, M. *et al.* Nose-to-brain drug delivery: An update on clinical challenges and progress towards approval of anti-Alzheimer drugs. *J. Control. Release* **281,** 139–177 (2018).

343. Williams, G., Blatchford, C. & Mitchell, J. P. Evaluation of Nasal Inlet Ports Having Simplified Geometry for the Pharmacopeial Assessment of Mass Fraction of Dose Likely to Penetrate Beyond the Nasopharynx: a Preliminary Investigation. *AAPS PharmSciTech* **19,** 3723–3733 (2018).

344. Moraga-Espinoza, D., Warnken, Z., Moore, A., Williams, R. O. & Smyth, H. D. C. A modified USP induction port to characterize nasal spray plume geometry and predict turbinate deposition under flow. *Int. J. Pharm.* **548,** 305–313 (2018).

345. Khatib, M. N. *et al.* Ghrelin for the management of cachexia associated with cancer. *Cochrane Database Syst. Rev.* (2018). doi:10.1002/14651858.CD012229.pub2

IX.APPENDICES

I. Characterization of the dry powder formulation (HTCC-AL) loaded with sodium fluorescein

Size measurement (raw powder), Dv 50 (µm)	18.2 ± 1.3
Size measurement (aerosol, UDS device), Dv 50 (µm)	35 ± 4
Uniformity of mass delivered (mg)	24.9 ± 0.33

II. Characterization of HTCC-AL liquid suspension containing Alex-fluor® 405 labelled GHRL

Z-average (nm)	198 ± 4.7
Zeta potential (mV)	7.4 ± 0.9